AWARD NUMBER: W81XWH-14-1-0619

TITLE: Spinal Cord Swelling and Alterations in Hydrostatic Pressure After Acute Injury

PRINCIPAL INVESTIGATOR: Dr. Brian K. Kwon

CONTRACTING ORGANIZATION: University of British Columbia, ICORD
Vancouver, BC, Canada, V5Z 1M9

REPORT DATE: October 2017

TYPE OF REPORT: Annual

PREPARED FOR: U.S. Army Medical Research and Materiel Command
Fort Detrick, Maryland 21702-5012

# REPORT DOCUMENTATION PAGE

*Form Approved*
*OMB No. 0704-0188*



| 1. REPORT DATE | 2. REPORT TYPE | 3. DATES COVERED |
|---|---|---|
| October 2017 | Annual | 30Sep2016 - 29Sep2017 |

**4. TITLE AND SUBTITLE**

Spinal Cord Swelling and Alterations in Hydrostatic Pressure After Acute Injury

**5a. CONTRACT NUMBER**

**5b. GRANT NUMBER**
W181XWH-14-1-0619

**5c. PROGRAM ELEMENT NUMBER**

**6. AUTHOR(S)**

Dr. Brian K. Kwon

E-Mail: brian.kwon@ubc.ca

**5d. PROJECT NUMBER**

**5e. TASK NUMBER**

**5f. WORK UNIT NUMBER**

**7. PERFORMING ORGANIZATION NAME(S) AND ADDRESS(ES)**

University of British Columbia, ICORD
Blusson Spinal Cord Centre
818 west 10th ave
Vancouver, BC, Canada

**8. PERFORMING ORGANIZATION REPORT NUMBER**

**9. SPONSORING / MONITORING AGENCY NAME(S) AND ADDRESS(ES)**

U.S. Army Medical Research and Materiel Command
Fort Detrick, Maryland 21702-5012

**10. SPONSOR/MONITOR'S ACRONYM(S)**

**11. SPONSOR/MONITOR'S REPORT NUMBER(S)**

**12. DISTRIBUTION / AVAILABILITY STATEMENT**

Approved for Public Release; Distribution Unlimited

**13. SUPPLEMENTARY NOTES**

## 14. ABSTRACT

In year 3 of our grant, we conducted a series of experiments evaluating the effects of duraplasty on intraparenchymal spinal cord oxygenation, blood flow, and pressure, downstream metabolic response, behavioral recovery as well as histological changes. We ended up repeating our 12-week behavioral recovery study because an earlier study that we performed showed a tremendous (and frankly, amazing) improvement in locomotor function in the duraplasty-treated animals. In our repeat experiment, we unfortunately did not see an improvement with duraplasty, although the injury severity that was generated in this last experiment was unexpectedly much more severe. While it may be that at a lesser injury severity, the duraplasty may have had a beneficial effect, we can conclude from our last experiment that with an extremely severe injury, a significant neuroprotective effect is not afforded by surgical duraplasty. Ultrasound imaging, and Somatosensory-evoked potentials (SSEP) data evaluation, and evaluation of our PRx data is still on-going and by using all these data, we shall be able to draw more definite conclusions on the impact of surgically opening the dura and expanding the subarachnoid space with a duraplasty.

## 15. SUBJECT TERMS

Spinal Cord Swelling, Hydrostatic Pressure, Duraplasty, Spinal Cord Injury, Pressure Reactivity Index

| 16. SECURITY CLASSIFICATION OF: | | | 17. LIMITATION OF ABSTRACT | 18. NUMBER OF PAGES | 19a. NAME OF RESPONSIBLE PERSON |
|---|---|---|---|---|---|
| a. REPORT | b. ABSTRACT | c. THIS PAGE | | | USAMRMC |
| Unclassified | Unclassified | Unclassified | Unclassified | 76 | 19b. TELEPHONE NUMBER *(include area code)* |

## TABLE OF CONTENTS

# 1 INTRODUCTION

After acute spinal cord injury (SCI) the spinal cord is frequently found to have swollen dramatically, particularly after it has been surgically decompressed. In traumatic brain injury (TBI), brain swelling and increases in intraparenchymal pressure are routinely considered in both the surgical and hemodynamic management of such patients. However, this swelling has largely been neglected in SCI, despite being consistently observed. Even after surgical decompression, such swelling may result in the cord being subjected to significant pressure, either due to constriction by the pia mater, the dura mater, or both. The physiologic consequences of this are poorly understood, and many fundamental questions remain about its impact on intraparenchymal pressure, spinal cord perfusion, and downstream metabolic responses. Determining the physiologic/biologic consequences of this swelling and how they can be mitigated to reduce secondary injury will guide the optimal clinical management of acute SCI. As an example of how swelling, increased intraparenchymal pressure, and its effects on perfusion are factored into clinical decision-making, TBI investigators have established the Pressure Reactivity Index (PRx) to identify where autoregulation remains intact and to guide optimal perfusion support based on that. The PRx has not been investigated in SCI, but given that the cord also swells and has impaired autoregulation, it is likely applicable here as well. This promising approach opens the possibility that we could individualize and optimize the hemodynamic support of acute SCI patients in order to support perfusion without exacerbating deleterious increases in intraparenchymal pressure.

# 2 KEYWORDS

- Spinal Cord Swelling
- Hydrostatic Pressure
- Spinal Cord Injury
- Pressure Reactivity Index
- Porcine model of SCI

# 3 ACCOMPLISHEMENTS

## 3.1 Protocol and Activity Status

- **Human Use Regulatory Protocols**

*No human subjects research will be performed to complete the Statement of Work*

- **Use of Human Cadavers for RDT&E, Education or Training**

*No RDT&E, education or training activities involving human cadavers will be performed to complete the Statement of Work*

- **Animal Use Regulatory Protocols**

  **Total Protocols:** 1 animal use research protocol will be required to complete the Statement of Work

- **Protocol:** 1 of 1
- **Protocol [ACURO Assigned Number]:** SC130008
- Title: **SCI in pigs** [IACUC protocol number A13-0013]
- **Target required for statistical significance**: n=6/group
- **Target approved for statistical significance**: n=6/group
- **Submitted to and Approved by:** Bryan K. Ketzenberger, DVM, DACLAM
- **Status: approved** 26-MARCH-2015

## 3.2 Approved Statement of Work

The approved statement of work is described below. A Gantt chart is provided in Table 1 for reference (see page 5).

| **Specific Aim 1:** Evaluate if compression by the surrounding dura produces increased intraparenchymal pressure within the injured, swollen cord. | **Months** | **Site** |
|---|---|---|
| Subtask 1: Submit documents for ACURO approval | 1-3 | UBC |
| *Milestone(s) Achieved: Obtain ACURO approval* | 3 | |
| Subtask 2: Characterize the CSF pressure changes for 7-days after SCI and decompression | 3-13 | UBC |
| Subtask 3: Characterize the cord intraparenchymal pressure changes for 7-days with probes positioned in close proximity of the epicenter and a more distal segment (control) | 3-13 | UBC |
| *Milestone(s) Achieved: Characterization of spatial and temporal hydrostatic pressure changes in the epidural space and spinal cord after SCI and decompression* (without dural decompression) | 10-15 | |

| **Specific Aim 2: To evaluate if dural compression contribute to progressive deficit in blood perfusion and contribute to the pathophysiology of secondary damage after traumatic SCI** | **Months** | **Site** |
|---|---|---|
| Subtask 1: Characterize the metabolic and spinal cord blood flow (SCBF) changes for 7-days with probes positioned in close proximity of the epicenter and a more distal segment (control) | 6-18 | UBC |
| Subtask 2: Determine the effects of surgically opening the dura and expanding the subarachnoid space with a duraplasty will alter intraparenchymal spinal cord pressure, SCBF, and metabolic responses | 6-18 | UBC |
| Subtask 3: Examine the histopathological changes in the harvested spinal cord at the 7-day time point | 12-18 | UBC |
| *Milestone(s) Achieved: Definition of any relation between changes in systemic pressure and SCBF when the spinal cord is decompressed with or without opening of the overlying dura*. | 18-24 | |

| **Specific Aim 3: Evaluate behavioral recovery for a total of 12 weeks following SCI with or without duraplasty** | **Months** | **Site** |
|---|---|---|
| Subtask 1: Assess hindlimb motor function during overground ambulation (PTIBS) | 12-32 | UBC |
| Subtask 2: Neurophysiologic monitoring with transcranial motor-evoked potentials | 12-32 | UBC |
| *Milestone(s) Achieved: Definition of any relationship between functional recovery after spinal cord decompression with or without dural decompression; preparation of manuscript* | 32-36 | |

| **Specific Aim 4: Evaluate if a moving correlation index exists between mean arterial blood pressure and CSF/cord pressure (pressure reactivity index; PRx)** | **Months** | **Site** |
|---|---|---|
| Subtask 1: Determine the temporal profile of spinal cord autoregulation following SCI during the first 7-days after SCI | 21-30 | UBC |
| Subtask 2: identify any variables - blood pressure, spinal cord perfusion, intraparenchymal pressure, or CSF pressure - associated with impairment or preservation of PRx | 21-30 | UBC |

| | | |
|---|---|---|
| *Milestone(s) Achieved: Quantification of any relation between arterial blood pressure or spinal cord perfusion and CSF pressure; preparation of 1-2 peer reviewed papers* | 30-36 | UBC |

**Table 1. Approved statement of work (Gantt Chart)**

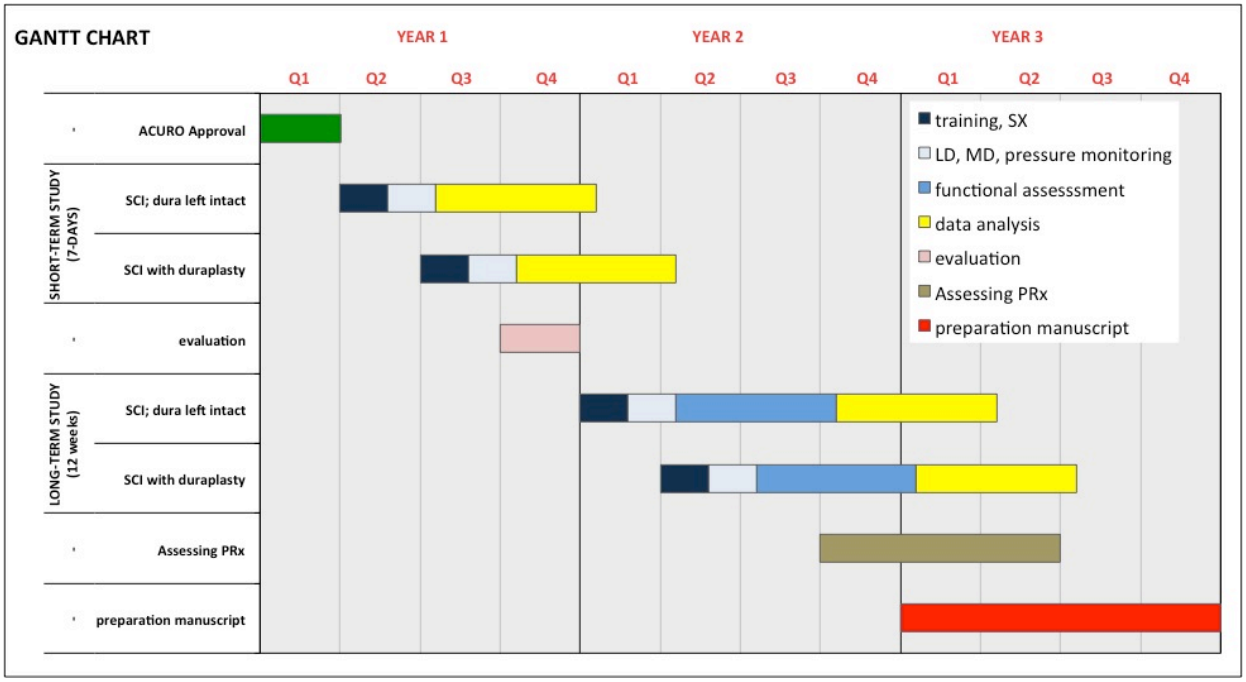

## 3.3 Current Progress on Statement of Work

A Gantt chart of the current work is provided in Table 2 for reference (page 7). The months in the approved statement of work do not necessarily match with the Gantt chart, since the Gantt chart reflects actual work completed in each year.

### Aim 1: Evaluate if compression by the surrounding dura produces increased intraparenchymal pressure within the injured, swollen cord.

- **Task 1:** Submit documents for ACURO approval

  ***Completed.*** *ACURO approval was granted 26-MARCH-2015.*

- **Task 2:** Characterize the CSF pressure changes for 7-days after SCI and decompression

  ***Completed.***

- **Task 3:** Characterize the cord intraparenchymal pressure changes for 7-days with probes positioned in close proximity of the epicenter and a more distal segment (control)

  ***Completed.*** A manuscript has been published in Journal of neurotrauma (ID NEU-2017-5034) entitled *"Changes in Pressure, Hemodynamics and Metabolism Within the Spinal Cord During the First 7-days After Injury Using a Porcine Model",* J Neurotrauma. 2017 Sep 14. doi: 10.1089/neu.2017.5034

### Aim 2: To evaluate if dural compression contribute to progressive deficit in blood perfusion and contribute to the pathophysiology of secondary damage after traumatic SCI (7-day evaluation)

- **Task 1:** Characterize the metabolic and spinal cord blood flow (SCBF) changes for 7-days with probes positioned in close proximity of the epicenter and a more distal segment (control)

  ***Completed.*** A manuscript has been published in Journal of neurotrauma (ID NEU-2017-5034) entitled *"Changes in Pressure, Hemodynamics and Metabolism Within the Spinal Cord During the First 7-days After Injury Using a Porcine Model",* J Neurotrauma. 2017 Sep 14. doi: 10.1089/neu.2017.5034

- **Task 2**: Determine the effects of surgically opening the dura and expanding the subarachnoid space with a duraplasty will alter intraparenchymal spinal cord pressure, SCBF, and metabolic responses

***Completed.*** *Data being analyzed currently for manuscript preparation.*

- **Task 3**: Examine the histopathological changes in the harvested spinal cord at the 7-day time point

  ***Completed.*** *Data being analyzed currently for manuscript preparation.*

### Aim 3: Evaluate behavioral recovery for a total of 12 weeks following SCI with or without duraplasty

- **Task 1:** Assess hindlimb motor function during overground ambulation (PTIBS)

  ***Completed.*** *Data being analyzed currently for manuscript preparation.*

- **Task 2:** Neurophysiologic monitoring with transcranial motor-evoked potentials

  ***Completed.*** A manuscript is in preparation entitled *"Sensorimotor Plasticity after Spinal Cord Injury: A Longitudinal Translational Study".* To be submitted to Science Translational Medicine.

### Aim 4. Evaluate if a moving correlation index exists between mean arterial blood pressure and CSF/cord pressure (pressure reactivity index; PRx)

- **Task 1:** Determine the temporal profile of spinal cord autoregulation following SCI during the first 7-days after SCI

  ***In progress.***

- **Task 2:** identify any variables - blood pressure, spinal cord perfusion, intraparenchymal pressure, or CSF pressure - associated with impairment or preservation of PRx

  ***In progress.***

**Table 2: Gantt chart of current work.** The Gantt chart reflects actual work completed. Therefore, months in the approved statement of work do not necessarily match with the Gantt chart, since the Gantt chart reflects actual work completed in each year.

| **Specific Aim 1+2:** *7-day Evaluation of Duraplasty evaluation* 1a. Dura intact (n=6) 1b. Duraplasty (n=6) | **YEAR 1** | | | | **YEAR 2** | | | | **YEAR 3** | | | |
|---|---|---|---|---|---|---|---|---|---|---|---|---|
| **Task:** | **Q1** | **Q2** | **Q3** | **Q4** | **Q1** | **Q2** | **Q3** | **Q4** | **Q1** | **Q2** | **Q3** | **Q4** |
| 1. ACURO Approval | | | | | | | | | | | | |
| 2. Animal training / Surgery | | | | | | | | | | | | |
| 3. Spinal cord monitoring of pressure, oxygenation, SCBF and microdiaysis | | | | | | | | | | | | |
| 4. Histologic assessments | | | | | | | | | | | | |
| 5. Data Analysis / Dissemination | | | | | | | | | | | | |
| | | | | | | | | | | | | |
| **Specific Aim 3:** *12-week Evaluation of Duraplasty* 1a. Dura intact (n=6) 1b. Duraplasty (n=6) | **YEAR 1** | | | | **YEAR 2** | | | | **YEAR 3** | | | |
| **Task:** | **Q1** | **Q2** | **Q3** | **Q4** | **Q1** | **Q2** | **Q3** | **Q4** | **Q1** | **Q2** | **Q3** | **Q4** |
| 1. Animal training / Surgery | | | | | | | | | | | | |
| 2. Behavioral / functional assessments | | | | | | | | | | | | |
| 3. Histologic assessments | | | | | | | | | | | | |
| 4. Data Analysis / Dissemination | | | | | | | | | | | | |
| | | | | | | | | | | | | |
| **Specific Aim 4:** *Evaluate if a moving correlation index exists between mean arterial blood pressure and CSF/cord pressure (pressure reactivity index; PRx)* | **YEAR 1** | | | | **YEAR 2** | | | | **YEAR 3** | | | |
| **Task** | **Q1** | **Q2** | **Q3** | **Q4** | **Q1** | **Q2** | **Q3** | **Q4** | **Q1** | **Q2** | **Q3** | **Q4** |
| 1. Determine the temporal profile of spinal cord autoregulation following SCI during the first 7-days after SCI | | | | | | | | | | | | |
| **2.** Identify any variables - blood pressure, spinal cord perfusion, intraparenchymal pressure, or CSF pressure - associated with impairment or preservation of PRx | | | | | | | | | | | | |

# 4 OVERALL PROJECT SUMMARY

Human SCI is typically caused by a combination of high velocity contusion followed by sustained mechanical compression. Relieving this 'extrinsic' mechanical compression in a timely manner intuitively would seem to be neuroprotective and result in improved neurologic function. However, the cord itself then undergoes considerable post-decompression swelling as demonstrated in SCI-patients. The spinal cord may ultimately swell to the point where it compresses against the dura, resulting in increased intraspinal pressure at the injury site as demonstrated by Papadopoulos and colleagues (2004). Such swelling and rise in the pressure within the spinal cord has also been observed in our porcine model of SCI (Figure 1 & 2). This suggests that we can utilize this model to investigate what is happening within the spinal cord during this swelling. When the cord swells against the dura, there may be an increase in pressure and reduction in spinal cord perfusion (as suggested by Papadopoulos et al.) **Our research question is: would it be beneficial to decompress the spinal cord by opening the dura and enlarging the subarachnoid space?** (as shown in Figure 3)

**Figure 1: The swollen cord expands against the dura within hours after decompression.** Prior to injury, the subarachnoid space is clearly seen between the spinal cord and dura. After SCI and within 10 min of decompression, residual deformation of the cord is observed. As inflammatory responses in the cord ensue, and the swelling cord fills the subarachnoid space, the cord pushes up against the dura within 5 hours of decompression (Jones et al., 2012).

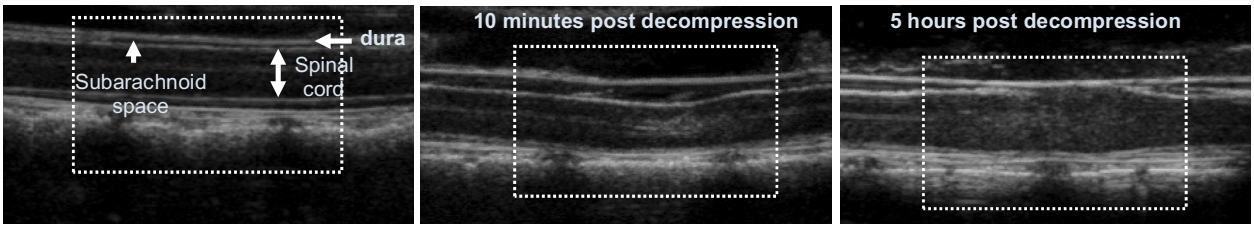


**Figure 2: Monitoring of hydrostatic spinal cord pressure in acute SCI using a porcine model. (A)** Surgical set-up to measure hydrostatic pressure within the spinal cord for 7 days. Three probes for monitoring oxygenation and blood flow, hydrostatic pressure and microdialysis were inserted through the dura and into the spinal cord 1.2 and 3.2 cm caudal to the injury. The recording wires from each probe were brought out of the surgical field, tunnelled through the skin and collected along the back of the animal. **(B)** At the injury site (1.2-cm) contusion injury followed by compression (grey shading) resulted in high intraparenchymal pressure. Following decompression intraparenchymal spinal cord pressure drops, after which it rises again remaining high for days, which suggests considerable post-SCI swelling. Such increases in cord pressure were also observed as far as 3.2-cm away from the trauma site.

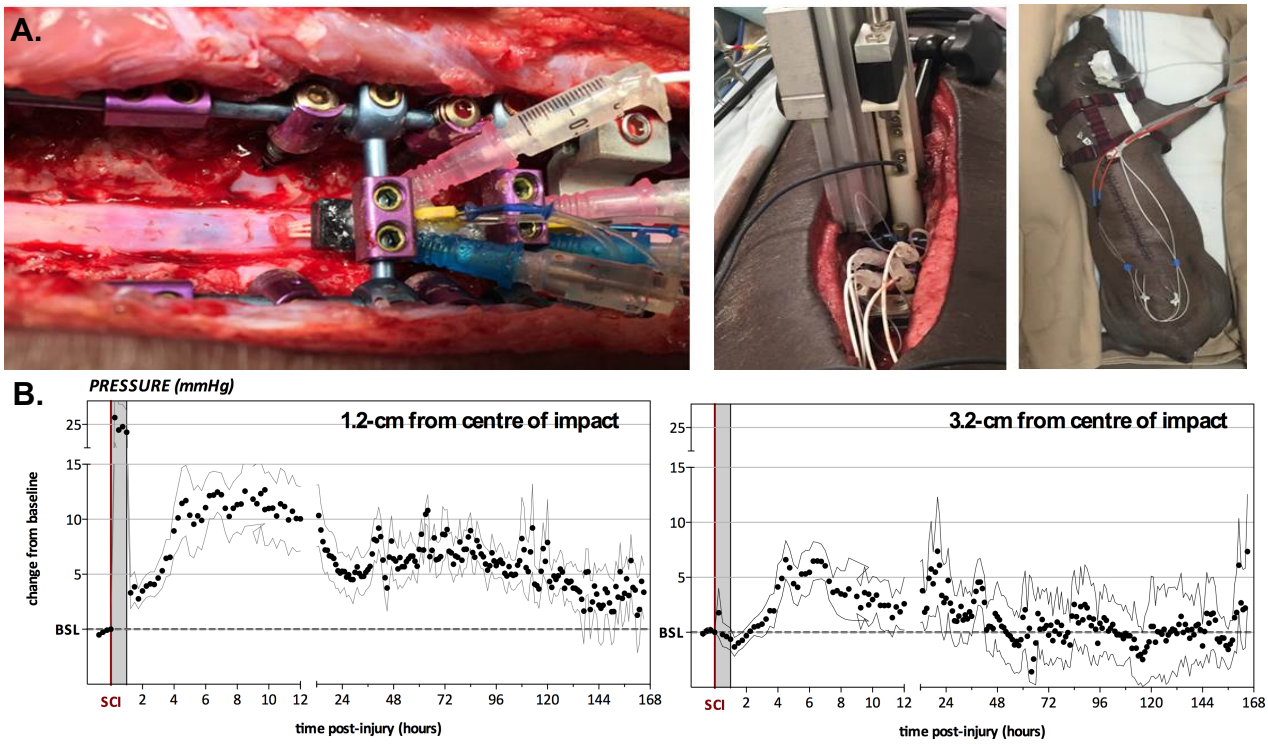


**Figure 3: Understanding the effect of relieving spinal pressure after SCI through duraplasty. (A)** Following a T10 dorsal spinal contusion injury and **(B)** C6-T13 transverse dural incision, a 10x1 cm artificial dural graft (Medtronic, US) was sutured to the remaining dura mater and sealed with fibrin glue. Control animals received an identical spinal cord contusion, however without expansile duraplasty.

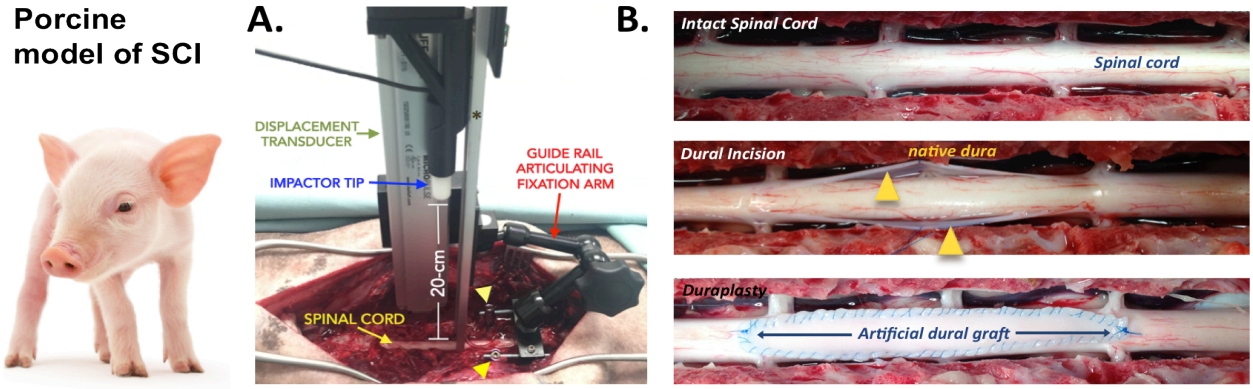

## 4.1 Results

**Aim 2, Task 2:** Evaluating the effects of surgically opening the dura and expanding the subarachnoid space with a duraplasty on metabolic responses.

We finalized and reported on the metabolite responses data over a 7-day period with or without duraplasty surgery. Eight female Yucatan pigs, weighing 29-34 kg, were used. The animals were randomly divided into two groups (n=4 per group); the first group underwent contusion/compression SCI followed by duraplasty surgery and the second group comprised the SCI controls (no duraplasty).

### Method:

In order to be able to measure metabolic responses by inserting probes, in these experiments we performed the duraplasty procedure before the probe insertion and before the actual weight drop spinal cord contusion. Moreover, we tried to create the same injury severity between animals that have an artificial dura (duraplasty) overlaying the cord versus the native dura by withdrawing the underlying CSF and laying a piece of the artificial dural graft material (Dura-Matrix, Medtronic, Minneapolis, MN) on the intact dura in the non-duraplasty animals before the drop. Microdialysis probes were inserted into the spinal cord proximal (0.2 cm) and distal (2.2 cm) to the impact site. Lactate, pyruvate, glutamate, glucose, and glycerol levels were measured with an Iscusflex Microdialysis Analyzer (CMA, Stockholm, Sweden), using the manufacturer's reagents and standard protocols. A decrease in energy-related metabolites glucose and pyruvate and an increase in the lactate-pyruvate ratio reflects the degree of ischemia in the cord following injury. Increased glycerol levels reflect a more pronounced SCI-induced breakdown of cellular membranes as a downstream result of injury and free radical release. Extracellular glutamate mediates excitotoxicity and cell death after SCI.

**Table 1.** lists of surgeries performed as part of Aim 2:

| SX date | Group | ID# | Name | Species | Injury details | Force (kdyn) | Weight (kg) |
|---|---|---|---|---|---|---|---|
| 2016-08-23 | Control | 8371 | Badminton | Yucatan | **Contusion:** 50gr/20cm **Compression:** 150gr/5min | 3227.00 | 33.0 |
| 2016-09-06 | Control | 8372 | Diving | Yucatan | | 2154.00 | 34.0 |
| 2016-09-21 | Control | 8437 | Gymnastics | Yucatan | | 2538.00 | 32.0 |
| 2016-09-27 | Control | 8400 | Heptathlon | Yucatan | | 2539.00 | 34.0 |

| SX date | Group | ID# | Name | Species | Injury details | Force (kdyn) | Weight (kg) |
|---|---|---|---|---|---|---|---|
| 2016-08-25 | Duraplasty | 8436 | Croquet | Yucatan | **Contusion:** 50gr/20cm **Compression:** 150gr/5min | 2058.00 | 29.0 |
| 2016-09-11 | Duraplasty | 8376 | Enduro | Yucatan | | 2116.00 | 34.5 |
| 2016-09-19 | Duraplasty | 8443 | Frisbee | Yucatan | | 2043.00 | 34.0 |
| 2016-09-29 | Duraplasty | 8464 | Ironman | Yucatan | | 2304.00 | 34.0 |

## Results:

Data thus far show that although pyruvate and lactate are higher in duraplasty group; there are no clear differences in L/P ratio between two groups close to the injury site. Also, no visible differences for glutamate and glycerol at 0.2 cm from injury was observed. Interestingly, higher glucose was observed in duraplasty group over 6-hours post-injury compared to control group (**Figure 4**). Further away from the injury site (at 2.2 cm) no clear difference was observed in metabolic response between two groups (**Figure 5**).

**Figure 4:** A comparison of the difference from baseline of metabolic response at 0.2cm from the middle of the injury sites, between duraplasty (filled circles) and non-duraplasty control (open circles) animals. The percentage change (%Δ) is calculated using an average of 30 minutes of baseline before SCI.

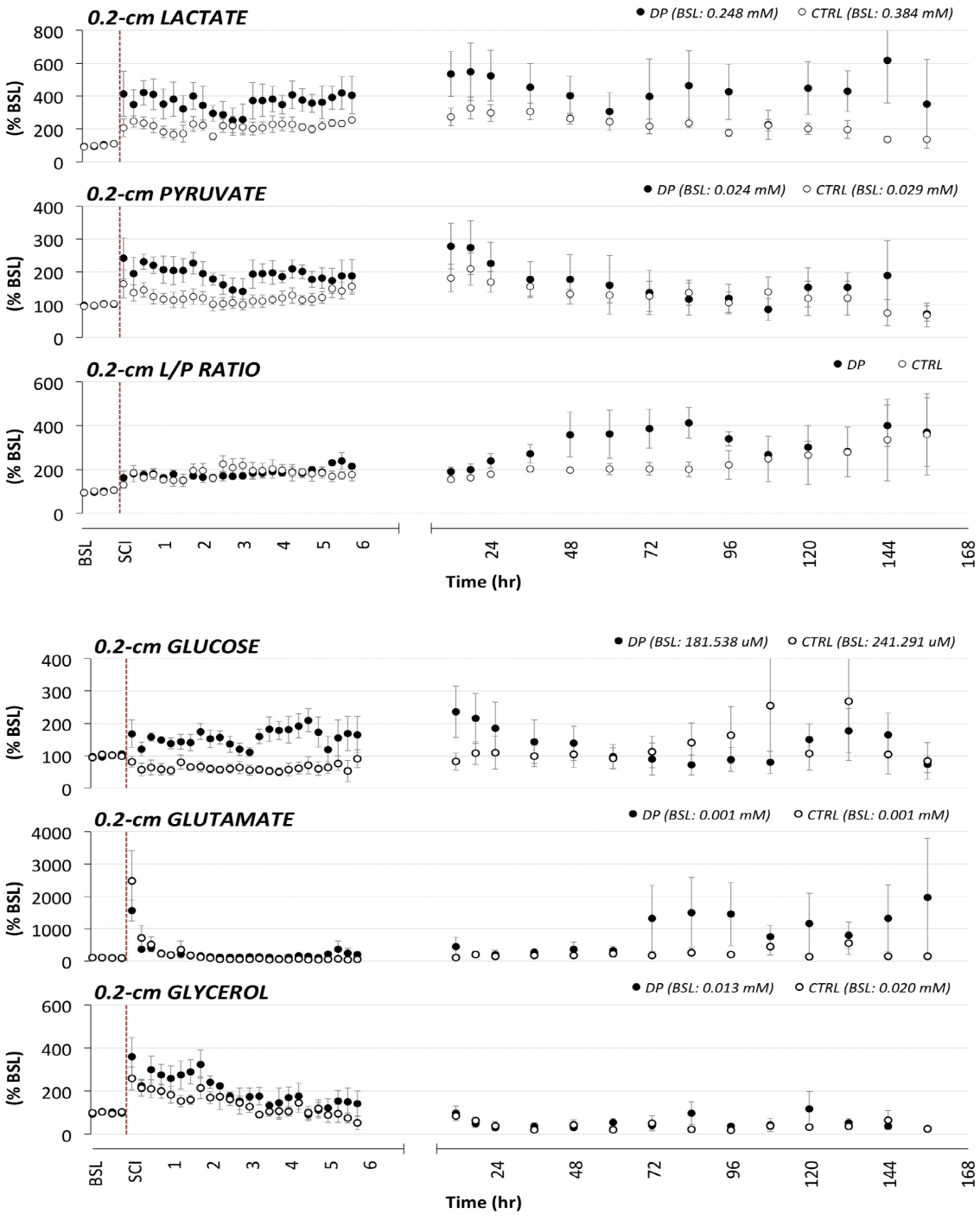

**Figure 5:** A comparison of the difference from baseline of metabolic response at 2.2cm from the middle of the injury sites, between duraplasty (filled circles) and non-duraplasty control (open circles) animals. The percentage change (%Δ) is calculated using an average of 30 minutes of baseline before SCI.

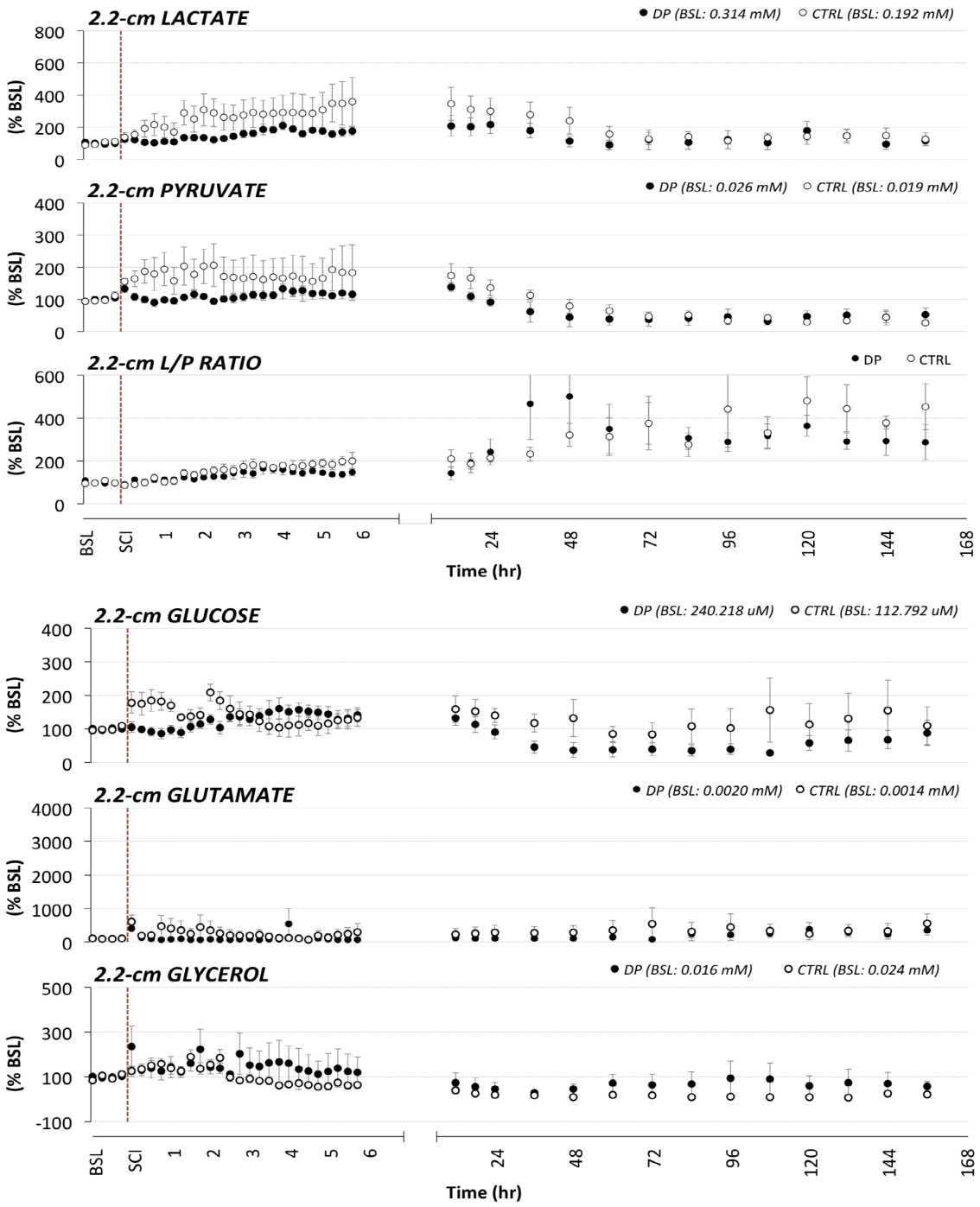

**Aim 3, task 1:** Evaluation of behavioral recovery and cord histology for a total of 12 weeks following SCI with or without duraplasty.

In Year 3 as part of **Aim 2**, besides reporting on the spinal cord microdialysis data over a 7-day period with or without duraplasty surgery, we also assessed behavioral and histological analysis of the spinal cord over a 12-week period.

## Methods:

Behavioral analysis was assessed weekly using the PTIBS (Porcine Thoracic Behavior Scale) up to 12 weeks after SCI. Then the spinal cords were harvested, processed for cryoprotection, cut in segment and frozen. The 20 µm cross-section of the frozen segments were mounted on the slides and stained in Eriochrome Cyanine R, which allows recognition of spared and damaged tissue. The spared white matter and spared grey matter were calculated with the ZEN software in each cord for the distance of 1.5 cm rostrally and caudally from the epicenter. Spared gray matter and spared white matter area data were divided by total spinal cord area at each slice to acquire a percentage value for each. Percent total spared spinal cord tissue area was calculated by adding percent white matter spared and percent gray matter spared values. Note: animal 8443 sustained a fracture through the T12 endplate during first week of recovery. The animal did survive the experiment, but because of the potential role of the displacement of the fracture, we excluded the animal from the histological analysis.

**Table 2.** lists of surgeries performed as part of Aim 3:

| SX date | Group | ID# | Name | Species | Injury details | Force (kdyn) | Weight (kg) |
|---|---|---|---|---|---|---|---|
| 2016-08-23 | Control | 8371 | Badminton | Yucatan | **Contusion:** 50gr/20cm **Compression:** 150gr/5min | 3227.00 | 33.0 |
| 2016-09-06 | Control | 8372 | Diving | Yucatan | | 2154.00 | 34.0 |
| 2016-09-21 | Control | 8437 | Gymnastics | Yucatan | | 2538.00 | 32.0 |
| 2016-09-27 | Control | 8400 | Heptathlon | Yucatan | | 2539.00 | 34.0 |
| | | | | | **Average** | **2614.5** | **33.3** |
| | | | | | **SEM** | **223.4** | **0.5** |

| SX date | Group | ID# | Name | Species | Injury details | Force (kdyn) | Weight (kg) |
|---|---|---|---|---|---|---|---|
| 2016-08-25 | Duraplasty | 8436 | Croquet | Yucatan | **Contusion:** 50gr/20cm **Compression:** 150gr/5min | 2058.00 | 29.0 |
| 2016-09-11 | Duraplasty | 8376 | Enduro | Yucatan | | 2116.00 | 34.5 |
| 2016-09-19 | Duraplasty | 8443 | Frisbee | Yucatan | | 2043.00 | 34.0 |
| 2016-09-29 | Duraplasty | 8464 | Ironman | Yucatan | | 2304.00 | 34.0 |
| | | | | | **Average** | **2130.3** | **32.9** |
| | | | | | **SEM** | **60.0** | **1.3** |

**Figure 6:** Behavioral recovery after SCI with or without duraplasty surgery as assessed with the Porcine Thoracic Behavior Scale. The duraplasty group reached on average a score of 5-6 by week 5 and was capable of some hindlimb stepping, while the control animals typically reached lower PTIBS scores (2-3), which correspond to hindlimb weight bearing extensions.

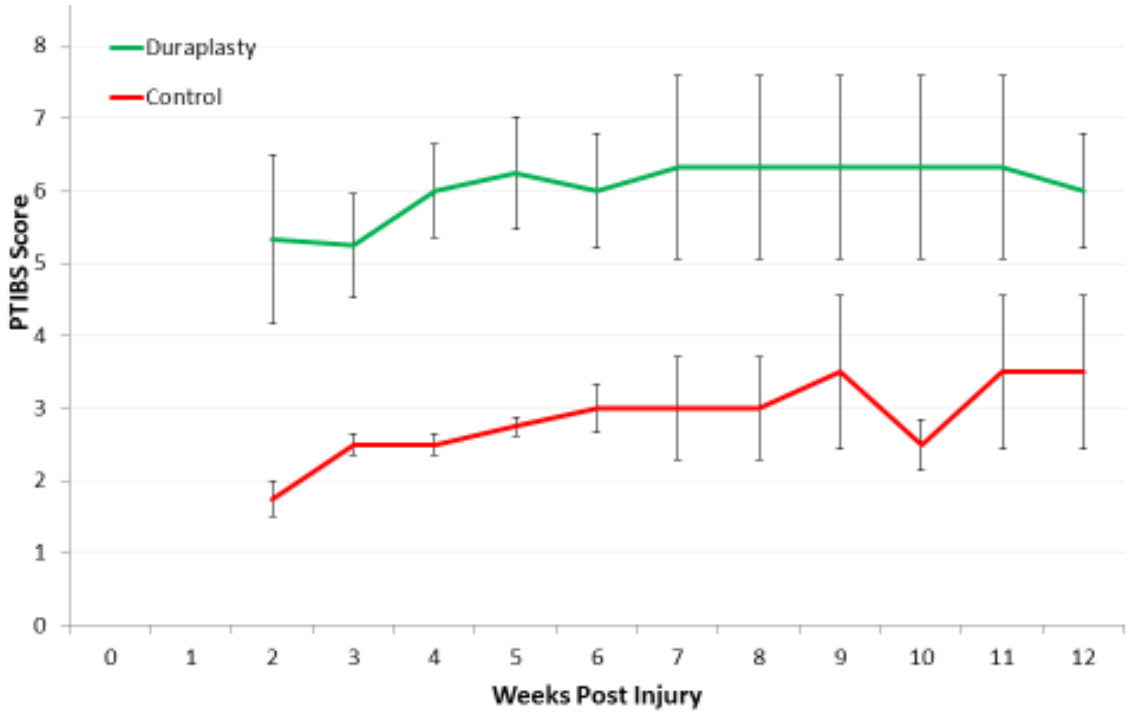

**Figure 7:** Percent spared white and grey matter of the spinal cords in the duraplasty and the control group. Duraplasty group appears to have a greater percentage of spared white matter rostral and caudal to the epicenter of injury. The epicenter is at the 0-mm position. The asterisks indicate that the difference at this point is significant with $p<0.05$.

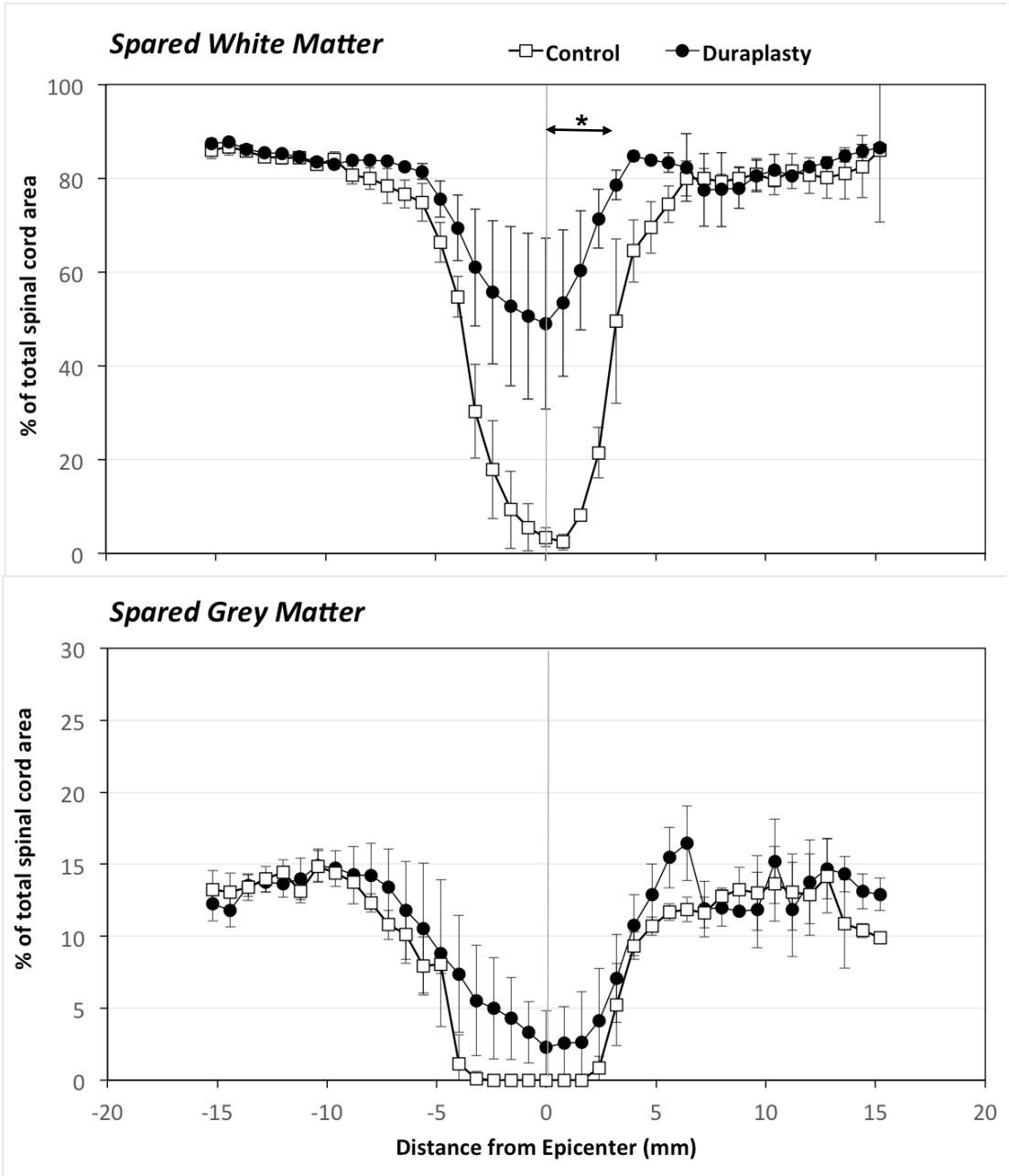

## Results:

Our data suggested a notable improvement in functional recovery after duraplasty surgery with a notable difference in PTIBS score between the groups (**Figure 6**). Moreover % spared white matter of the spinal cord in the duraplasty group was greater compared to the control animals (**Figure 7**). Significant difference between groups was reached up to 4 mm caudal to the epicenter ("0.0" mm). No obvious differences for spared grey matter were observed between the groups.

During **year 2**, we found it very challenging to equilibrate the severity of mechanical injury. To try to control this, as mentioned in **Aim 2, Task 2,** the duraplasty procedure was performed before probe insertion and weight drop and the accumulated underlying CSF within subarachnoid space around the injury site in both the control and the duraplasty animals was aspirated just before dropping the impactor on the cord. After finding significant different injury severity between the two groups, we repeated the experiment and this time we also laid a piece of the artificial dural graft material (Dura-Matrix, Medtronic, Minneapolis, MN) on the intact dura in the non-duraplasty animals. This we felt would result in the same 'cushioning' effect. However, even this time, the duraplasty group demonstrated lower SCI force values (**Table 2**) and identical 20-cm weight drop SCI caused a slightly lower impact force for the duraplasty group compared to the control animals (although not statistical different). We concluded that the difference in PTIBS between the groups could be due to a difference in impact severity. Therefore, in **year 3** of our funding, we scheduled additional duraplasty surgeries (**Table 3**) and for this set of experiments, we decided not to measure spinal cord blood flow, oxygenation, pressure and the microdialysis and cancel the probe insertion. This way, the duraplasty surgery could be done after the impact, and the impact forces would be more equivalent between these two groups (as both groups receive an impact on intact dura and spinal cord). Furthermore, our engineers made an adjustment to the impactor setup to create a more consistent and accurate weight drop.

**Table 3**. lists of surgeries performed as part of Aim 3:

| SX date | Group | ID# | Name | Species | Injury details | Force (kdyn) | Weight (kg) |
|---|---|---|---|---|---|---|---|
| 2017-04-18 | Control | 8998 | Minigolf | Yucatan | **Contusion:** 50gr/20cm **Compression:** 150gr/5min | 3689 | 23.5 |
| 2017-04-25 | Control | 9036 | Outrigger | Yucatan | | 3589 | 25.0 |
| 2017-05-02 | Control | 9034 | Qianball | Yucatan | | 4207 | 23.5 |

| SX date | Group | ID# | Name | Species | Injury details | Force (kdyn) | Weight (kg) |
|---|---|---|---|---|---|---|---|
| 2017.04-03 | Duraplasty | 8996 | Javelin | Yucatan | **Contusion:** | 3581 | 21.51 |

| | | | | | | | |
|---|---|---|---|---|---|---|---|
| 2017-04-12 | Duraplasty | 9043 | Luge | Yucatan | 50gr/20cm **Compression**: 150gr/5min | 3637 | 19.5 |
| 2017-04-20 | Duraplasty | 8981 | Netball | Yucatan | | 3160 | 24.5 |

## Results:

Our data did not show an improvement in functional recovery after duraplasty surgery. No significant differences were seen in PTIBS score between the groups (**Figure 9**). Moreover, no major differences in %spared white matter and %spared gray matter were seen between the two groups. However, the duraplasty group had more spared gray matter in the more distal rostral and caudal regions compared to the control group (**Figure 10**).

The key problem, however, is that the adjustments that were made to the impactor device resulted in an increase in the impact force in these animals. These animals consistently had impact forces above 3000 kdyne, and in most cases, over 3500 kdyne. Such an impact force results in an extremely severe injury and therefore the likelihood of any degree of neuroprotection being afforded by the duraplasty is limited. The fact that the impact force is so high is reflected in the final PTIBS between 2 to 3 (Figure 9), where normally we would see animals at 3 to 4 with a 20 cm weight drop.

**Figure 9:** Behavioral recovery after SCI with or without duraplasty surgery as assessed with the Porcine Thoracic Behavior Scale. The duraplasty group reached on average a score of 3 by and was capable of some hindlimb stepping, while the control animals typically reached lower PTIBS scores (2). However, there is no visible difference between the two groups for PTIBS.

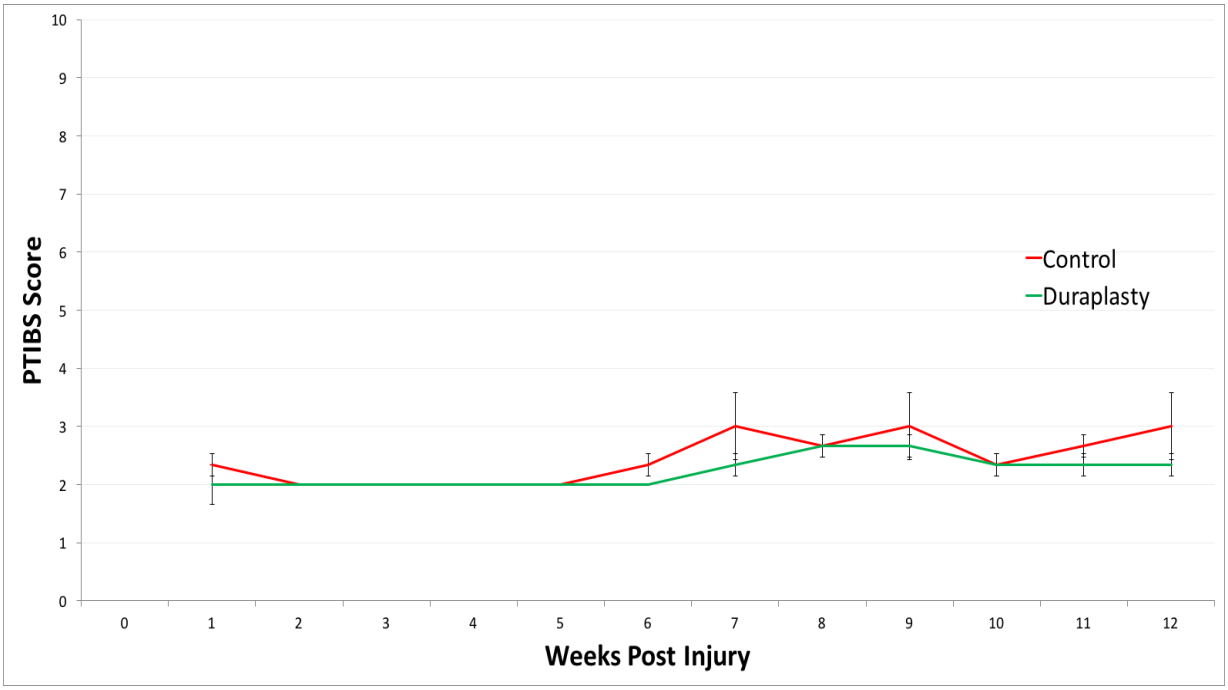

**Figure 10:** Percent spared white (A) and grey matter (B) of the spinal cords in the duraplasty and the control group. The epicenter is at the 0-mm position.

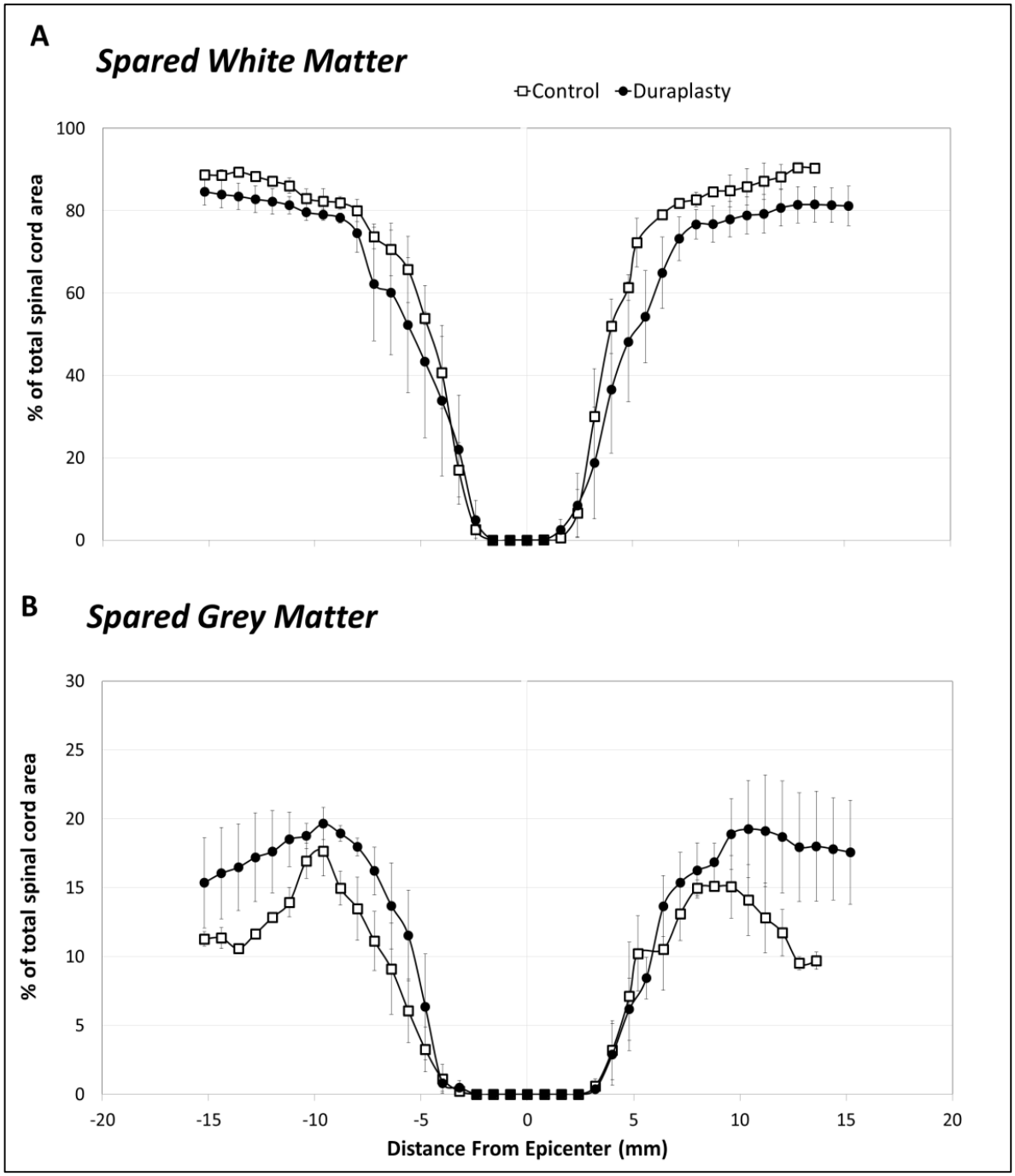

# 5 KEY RESEARCH ACCOMPLISHMENTS

- No significant differences were seen in PTIBS score between the groups
- No major differences in %spared white matter and %spared gray matter were seen between the two groups.
- The duraplasty group had more spared gray matter in the more distal rostral and caudal regions compared to the control group

# 6 CONCLUSION

In year 3 of our grant, we conducted series of experiments evaluating the consequence of duraplasty on intraparenchymal spinal cord oxygenation, blood flow, and pressure, downstream metabolic response, behavioral recovery as well as histological changes. We ended up repeating our 12-week behavioral recovery study because an earlier study that we performed showed a tremendous (and frankly, amazing) improvement in locomotor function in the duraplasty-treated animals. In our repeat experiment, we unfortunately did not see an improvement with duraplasty, although the injury severity was unexpectedly much more severe. We can conclude from this injury severity; a significant neuroprotective effect is not afforded by surgical duraplasty.

Ultrasound imaging, and Somatosensory-evoked potentials (SSEP) data evaluation, and evaluation of our PRx data is still on-going and will be completed in Year 4 (a no-cost 1-year extension has been requested). By using all these data, we shall be able to draw more definite conclusions on the impact of surgically opening the dura and expanding the subarachnoid space with a duraplasty.

# 7 PUBLICATIONS, ABSTRACTS AND PRESENTATIONS

1) Publication, submitted to Science Translational Medicine. **(full manuscript in appendix 1)**

**Sensorimotor Plasticity after Spinal Cord Injury: A Longitudinal Translational Study".**

Catherine R Jutzeler[1,2,3], Femke Streijger [2], Katelyn Shortt [2], Neda Manouchehri [1], Elena Okon [1], EMSCI Study Group [4], Markus Hupp [1], Armin Curt [1], Brian K Kwon [2], and John LK Kramer PhD [2,3]

[1]Spinal Cord Injury Center, University Hospital Balgrist, University of Zurich, Zurich, Switzerland
[2]ICORD, University of British Columbia, Vancouver, British Columbia, Canada
[3]School of Kinesiology, University of British Columbia, Vancouver, British Columbia, Canada
[4]European Multi-centre Study about Spinal Cord Injury (EMSCI) Study Group, University Hospital Balgrist, University of Zurich, Zurich 8008, Switzerland

**Abstract**

Introduction: Spinal cord injury prompts reorganization of the brain, including areas representing the intact body parts. Knowledge regarding underlying mechanisms has been gained largely from animal models of deafferentation.

Method: In order to refine our understanding of the human's brain response to spinal cord injury, in which deafferentation of the sensorimotor cortex occurs, 37 individuals with acute traumatic spinal cord injury were followed over time (1, 3, 6, and 12 months post injury) with repeated neurophysiological assessments. Somatosensory and motor evoked potentials were recorded in the upper extremities above the level of injury. In a reverse-translational approach, the same neurophysiological techniques were examined in a porcine model of thoracic spinal cord injury. Twelve Yucatan mini-pigs subjected to a contusive spinal cord injury at T10 underwent somatosensory and motor evoked potentials assessments in the fore- and hindlimbs pre- (baseline, post-laminectomy) and post injury (10min, 3hrs, 12 weeks).

Results: In both species, the sensory responses in the upper extremities/forelimbs progressively increased from immediately post injury to later time points. Motor responses in the forelimbs increased immediately after experimental injury in pigs, remaining elevated at 12 weeks. In humans, motor evoked potentials were significantly higher at 1-month (and remained so at 1 year) compared to normative values.

Interpretation: Despite notable differences between experimental models and the human condition, the brain's response to spinal cord injury is remarkably similar between humans and porcine species. Our findings further underscore the utility of this large animal model in translational spinal cord injury research.

2) Publication, J Neurotrauma. 2017 Sep 14. doi: 10.1089/neu.2017.5034, **(full manuscript in appendix 2)**

## CHANGES IN PRESSURE, HEMODYNAMICS, AND METABOLISM WITHIN THE SPINAL CORD DURING THE FIRST 7 DAYS AFTER INJURY USING A PORCINE MODEL

Femke Streijger,[1] Kitty So,[1] Neda Manouchehri,[1] Jae H.T. Lee,[1] Elena B. Okon,[1] Katelyn Shortt,[1] So-Eun Kim,[1] Kurt McInnes,[1,2] Peter Cripton,[1,2] and Brian K. Kwon[1,3]

[1]International Collaboration on Repair Discoveries (ICORD), University of British Columbia, Vancouver, British Columbia, Canada.
[2]Departments of Mechanical Engineering and Orthopedics, University of British Columbia, Vancouver, British Columbia, Canada.
[3]Vancouver Spine Surgery Institute, Department of Orthopedics, University of British Columbia, Vancouver, British Columbia, Canada.

### Abstract

Traumatic spinal cord injury (SCI) triggers many perturbations within the injured cord, such as decreased perfusion, reduced tissue oxygenation, increased hydrostatic pressure, and disrupted bioenergetics. While much attention is directed to neuroprotective interventions that might alleviate these early pathophysiologic responses to traumatic injury, the temporo-spatial characteristics of these responses within the injured cord are not well documented. In this study, we utilized our Yucatan mini-pig model of traumatic SCI to characterize intraparenchymal hemodynamic and metabolic changes within the spinal cord for 1 week post-injury. Animals were subjected to a contusion/compression SCI at T10. Prior to injury, probes for microdialysis and the measurement of spinal cord blood flow (SCBF), oxygenation (in partial pressure of oxygen; $PaPO_2$), and hydrostatic pressure were inserted into the spinal cord 0.2 and 2.2 cm from the injury site. Measurements occurred under anesthesia for 4 h post-injury, after which the animals were recovered and measurements continued for 7 days. Close to the lesion (0.2 cm), SCBF levels decreased immediately after SCI, followed by an increase in the subsequent days. Similarly, $PaPO_2$ plummeted, where levels remained diminished for up to 7 days post-injury. Lactate/pyruvate (L/P) ratio increased within minutes. Further away from the injury site (2.2 cm), L/P ratio also gradually increased. Hydrostatic pressure remained consistently elevated for days and negatively correlated with changes in SCBF. An imbalance between SCBF and tissue metabolism also was observed, resulting in metabolic stress and insufficient oxygen levels. Taken together, traumatic SCI resulted in an expanding area of ischemia/hypoxia, with ongoing physiological perturbations sustained out to 7 days post-injury. This suggests that our clinical practice of hemodynamically supporting patients out to 7 days post-injury may fail to address persistent ischemia within the injured cord. A detailed understanding of these pathophysiological mechanisms after SCI is essential to promote best practices for acute SCI patients.

3) Poster presentation, Society for Neuroscience 2017, Washington, D.C., Nov 11-15:

**THE EFFECT OF DURAPLASTY IN ACUTE TRAUMATIC SCI ON BEHAVIOURAL RECOVERY AND SPINAL CORD MORPHOLOGY, USING A PORCINE MODEL OF SCI**

Kitty So[1], Femke Streijger[1], Katelyn Shortt[1], Neda Manouchehri[1], Elena B. Okon[1], Brian K. Kwon[1,2]
[1]International Collaboration of Repair Discoveries (ICORD), University of British Columbia, Vancouver, BC, Canada; [2]Vancouver Spine Surgery Institute, Department of Orthopaedics, University of British Columbia, Vancouver, BC, Canada

**Abstract (max 2300 characters):**
Severe swelling of the human spinal cord is typically observed after a traumatic spinal cord injury (SCI). Intrinsic cord swelling within the pia mater, along with the swollen cord filling the subarachnoid space and pushing against the relatively stiff dura mater, may result in increased intraspinal pressure. Such cord constriction can lead to reduced blood flow, hypoxia and ischemia, leading to secondary damage. Using our porcine model of SCI, we examine the effects of an expansile duraplasty surgery on behavior, spinal cord morphology, and tissue sparing following an acute SCI. Female Yucatan mini-pigs received a T10 contusion SCI followed by 5-minutes of compression and were randomized into two groups: 1) SCI without dural expansion surgery (control group) or 2) SCI with dural expansion duraplasty with an artificial graft (Durepair, Medtronic; 1-cm width, 10-cm length) centered around the impact site (duraplasty group). Behavioral recovery was monitored weekly for 12 weeks and animals were scored using the Porcine Thoracic Injury Behaviour Scale (PTIBS). Ultrasound imaging at 7 days post-SCI was used to compare spinal cord morphology (dorsal-ventral height of the spinal cord and subarachnoid space) at various level of the spine between the two groups. At 12 weeks Oasis Helpdesk Leave OASIS Feedback Powered by cOASIS, The Online Abstract Submission and Invitation System SM © 1996 - 2017 CTI Meeting Technology All rights reserved. post-SCI, animals were euthanized and histological analysis was done on their spinal cords to quantify both grey and white matter sparing. At 7 days post-SCI, ultrasound analysis showed an enlargement of the subarachnoid space at the T9-T11 for the duraplasty group (T9-T11: 2.0 ± 0.4mm; 2.1 ± 0.3mm; 2.4 ± 0.2mm) compared to the controls (T9-T11: 1.1 ± 0.4mm; 0.5 ± 0.3mm; 0.5 ± 0.2mm) with an increased spinal cord height (duraplasty: 7.4 ± 0.2 mm; controls: 6.2 ± 0.2 mm). Throughout the 12- week recovery period, most control animals were only capable of hind limb dragging (PTIBS score of 1-3) after SCI, while most duraplasty animals showed weight-supported stepping (PTIBS ≥ 4). Histological analysis of the spinal cords demonstrated more spared white matter at the epicenter in the duraplasty group compared to the controls. No difference in the spare grey matter was demonstrated. In summary, our results demonstrated that, 7 days after SCI the swollen cord almost fills the subarachnoid space. Expansive duraplasty surgery in a porcine model of SCI, enlarged the subarachnoid space for days after SCI, and allowed for non-restrictive swelling of the spinal cord. This might have led to improve hind limb function and increased spared tissue at the site of injury as observed at 12 weeks post-SCI. This data supports the potential of improving neurologic outcome with expansile duraplasty.

Session Type: Poster
Session Title: Spinal cord: Animal models and human studies
Date and Time: Mon, Nov. 13, 2017, 8:00 AM - 9:00 AM
Location: Walter E. Washington Convention Center
Abstract Control Number: 2017-S-9710-SfN

## 8 INVENTIONS, PATENTS AND LICENSES

Nothing to report

## 9 REPORTABLE OUTCOMES

Nothing to report

## 10 OTHER ACHIEVEMENTS

Nothing to report

# 11 REFERENCES

Jones CF, Cripton PA, Kwon BK (2012) ***Gross morphological changes of the spinal cord immediately after surgical decompression in a large animal model of traumatic spinal cord injury.*** Spine (Phila Pa 1976); 37(15): E890-9. PMID: 22433504.

# 12 FINANCIAL HEALTH

| Date Range: 1 OCT 2016 - 30 SEP 2017 | | | |
|---|---|---|---|
| | Actual Expenditures | Commitments | Projected Actuals |
| | YTD | YTD | |
| Funding/Revenues | | | |
| Carry Forward Allocation | 390,829.83 | 0 | 390,829.83 |
| Expense Funding Allocation | 12,941.39 | 0 | 12,941.39 |
| Total Funding/Revenues | 403,771.22 | 0 | 403,771.22 |
| Expenses | | | |
| Salaries | | | |
| Student Salaries | 3,937.50 | 0.00 | 3,937.50 |
| Staff Salaries | 47,647.79 | 0.00 | 47,647.79 |
| Sessional Salaries | 8,000.00 | 0 | 8,000.00 |
| Total Salaries | 59,585.29 | 0.00 | 59,585.29 |
| Benefits | 10,530.26 | 0.00 | 10,530.26 |
| Supplies & Sundries | 241,650.29 | 0 | 241,650.29 |
| Travel | 2,141.55 | 0 | 2,141.55 |
| Professional Fees | 4,974.99 | 4265.1 | 9,240.09 |
| Total Expenses | 318,882.38 | 4,265.10 | 323,147.48 |
| Revenue Less Expenses | 84,888.84 | -4,265.10 | 80,623.74 |

# 13 APPENDICES

# Appendix 1

## Sensorimotor Plasticity after Spinal Cord Injury: A Longitudinal Study

**Authors:** Catherine R Jutzeler [1,2,3*], Femke Streijger [2], Katelyn Shortt[2], Neda Manouchehri[1], Elena Okon[1], EMSCI Study Group[4], Markus Hupp[1], Armin Curt[1], Brian K Kwon[2†], and John LK Kramer PhD[2,3†]

**Affiliations:**

[1]Spinal Cord Injury Center, University Hospital Balgrist, University of Zurich, Zurich, Switzerland

[2]ICORD, University of British Columbia, Vancouver, British Columbia, Canada

[3]School of Kinesiology, University of British Columbia, Vancouver, British Columbia, Canada

[4] European Multi-centre Study about Spinal Cord Injury (EMSCI) Study Group, University Hospital Balgrist, University of Zurich, Zurich 8008, Switzerland

[†]Shared senior authorship

***Corresponding author:**
Catherine R. Jutzeler
818 W 10th Ave
Vancouver, BC, Canada
V5Z 1M9
Phone: +1-604-675-8876
Catherine.Jutzeler@ubc.ca
URL: www.icord.org

**Running Title:** Cortical Plasticity after Spinal Trauma

**Abstract**

**Introduction:** Spinal cord injury prompts reorganization of the brain, including areas representing the intact body parts. Knowledge regarding underlying mechanisms has been gained largely from animal models of deafferentation.

**Method**: In order to refine our understanding of the human's brain response to spinal cord injury, in which deafferentation of the sensorimotor cortex occurs, 37 individuals with acute traumatic spinal cord injury were followed over time (1, 3, 6, and 12 months post injury) with repeated neurophysiological assessments. Somatosensory and motor evoked potentials were recorded in the upper extremities above the level of injury. In a reverse-translational approach, the same neurophysiological techniques were examined in a porcine model of thoracic spinal cord injury. Twelve Yucatan mini-pigs subjected to a contusive spinal cord injury at T10 underwent somatosensory and motor evoked potentials assessments in the fore- and hindlimbs pre- (baseline, post-laminectomy) and post injury (10min, 3hrs, 12 weeks).

**Results:** In both species, the sensory responses in the upper extremities/forelimbs progressively increased from immediately post injury to later time points. Motor responses in the forelimbs increased immediately after experimental injury in pigs, remaining elevated at 12 weeks. In humans, motor evoked potentials were significantly higher at 1-month (and remained so at 1 year) compared to normative values.

**Interpretation:** Despite notable differences between experimental models and the human condition, the brain's response to spinal cord injury is remarkably similar between humans and porcine species. Our findings further underscore the utility of this large animal model in translational spinal cord injury research.

## Introduction

Traumatic spinal cord injury is a devastating neurological event, characterized by varying severities of motor, sensory, and autonomic impairment[1]. In response to damage in the spinal cord, primary sensorimotor areas in the brain representing intact regions of the body (e.g., hand area following injury in the thoracic cord) undergo structural and functional reorganization[2–6]. Several theories have been proposed to explain the phenomenon of cortical reorganization, including changes in excitability due to increased use of the hands and altered intracortical connectivity[7].

Missing from our understanding of cortical reorganization after spinal cord injury is how changes in the brain evolve over time. This is complicated by several practical considerations, including the difficulty of performing detailed neurophysiological assessments in the very early stages of injury (<1 month). In experimental rodent models, both immediate and progressive changes in cortical activation to peripheral afferent stimuli delivered above the level of injury have been variably reported[8–15]. Immediate changes in the brain support the notion that spinal cord injury unmasks latent pathways[12,13,16–19], whereas progressive adaptions may reflect a form of functional reorganization[20,21].

Notable differences between rodent and human spinal cord injury have called into question the validity of existing small animal models and their relevance to the clinical condition [22]. By virtue of stark similarities with humans in terms of size, general systems physiology (e.g., cardiac), and genetic traits, larger animal models of spinal cord injury have been proposed to overcome some of the limitations inherent to rodents[23–26]. Of available models, pigs have emerged as a potential intermediate between humans and primates[23,25,27–29]. The extent to which pig models of spinal cord injury better represent changes in the CNS resulting from traumatic lesions in the spinal cord (e.g., changes in the brain) remains unknown.

The primary aim of this study was to investigate the progression of changes in the brain in response to spinal cord injury in humans from acute to chronic stages. Utilizing common neurophysiological techniques, observations in humans were then reverse translated in a pig model of thoracic spinal cord injury. The fundamental goal here was to determine if changes in the brain of pigs in response to spinal cord injury was similar to what has already been reported in animals (e.g., rodents and non-human primates)[12–14] and what we observed in humans.

## Materials and Methods

### Human data: Data source and selection

*Patient Data*

The European Multicenter Study about Spinal Cord Injury (EMSCI) was reviewed to identify individual with spinal cord injury eligible for our study. EMSCI is a longitudinal observational study comprising 19 participating trauma and rehabilitation centers from across Europe. A variety of neurological and functional outcomes are tracked at fixed time points over the first year of injury (i.e., 1, 3, 6, and 12 months). All individuals enrolled in EMSCI obtain standards of rehabilitation care. Further details on the EMSCI database can be found elsewhere (www.emsci.org, ClinicalTrials.gov Identifier: NCT01571531).

To be included in our analysis, individuals with spinal cord injury had to meet the following inclusion criteria: 1) spinal cord injury as a result of a single traumatic event, 2) the first neurophysiological assessment (i.e., somatosensory and motor evoked potentials) conducted within four weeks following injury, and 3) neurologic level of injury at or below C8. The rational for the selection of low cervical/high thoracic neurological level of injury arises from the study's objective to investigate the changes of brain areas representing intact body parts by performing electrophysiological measurements in the unaffected upper extremities. The ulnar nerve has spinal root entries at C8 and T1 **(Fig 1)**. Neurological levels of injury at and below C8 allow the assessment of intact upper limb sensory evoked potentials and motor evoked potentials. Exclusion criteria constituted other non-traumatic spinal cord injury (e.g., tumor), dementia or severe reduction of intelligence leading to reduced capabilities of cooperation or giving consent, polyneuropathy, and brain injury. Prior to the inclusion in the EMSCI, all individual with spinal cord injury gave their written informed consent. The study is in accordance with the Declaration of Helsinki and was approved by all responsible institutional review boards.

*Healthy Control Data*

The laboratory at the University Hospital Balgrist established a set of normative data for sensory evoked potentials and motor evoked potentials amplitudes and latencies in the upper and lower extremities. Derived from this in-house data set, a representative sample was used for statistical comparison to observations in the spinal cord injury cohort.

*Outcome measures*

Neurophysiological assessments (i.e., tibial and ulnar sensory evoked potentials, *abductor digit minimi* motor evoked potentials) were performed at four fixed time points: 1, 3, 6, and 12 months post injury (**Fig 2A)**. The N20 latency and N20-P25 amplitude of the ulnar sensory evoked potentials were the primary outcome variables, assessed separately at each of the four time points. All assessments were performed by trained examiners and in accordance with international standards [30,31]. Briefly, motor evoked potentials were recorded by applying single pulse transcranial magnetic stimulation (TMS) using a routine circular coil magnetic stimulator. For the adductor digiti minimi motor evoked potentials (hereafter referred as upper limb motor evoked potentials), the stimulation hot spot was determined by stepwise optimizing coil position to obtain a maximum motor evoked potentials response. Upper limb motor evoked potentials were recorded at 1.2 times active motor threshold. Three to five representative upper limb motor evoked potentials at the desired stimulus intensity were applied. Tibial and ulnar sensory evoked potentials were elicited by single 0.2 msec, repetitive, square wave electrical stimulation (3 Hz) using a Key Point electrophysiological stimulating and recording device (bandpass = 2 Hz to 2 kHz; Medtronic, Mississauga, Ontario, Canada). Standard clinical surface gel electrodes (10 mm) were positioned on the tibial nerve at the ankle and ulnar nerve at the wrist. sensory evoked potentials were collected at a stimulus intensity that adequately produced a consistent but tolerated muscle twitch[30,32,33].

## Animal Data: Study Design

**Figure 2B** illustrates the study design of the animal experiments. Briefly, the animals underwent behavioral training for five days. Subsequently, the baseline measurement was performed on the day before the surgery. Follow-up behavioral measurements were conducted weekly for 12 weeks starting within 7 days after the surgery to first allow the animals to recover from their initial surgery/injury. On the day of surgery, animals were anaesthetized and intubated. Baseline sensory evoked potentials and motor evoked potentials were recorded prior to initiating the surgical procedures, which included a dorsal exposure to the thoracic spine and laminectomy around T10. Following laminectomy, sensory evoked potentials and motor evoked potentials were recorded again in order to ensure that the spinal cord was not damaged. The

spinal cord injury was then induced by contusing and compressing the spinal cord. Specifically, a 50 gram weight was dropped from 20 cm height to the exposed spinal cord at the $10^{th}$ thoracic vertebrae. This was followed by five minutes of compression placing a 150g weight on the spinal cord. Sensory evoked potentials and motor evoked potentials were recorded immediately after the compression (approximately 10 minutes after the weight drop contusion injury). All animals underwent follow up assessments of sensory evoked potentials and motor evoked potentials at 3 hours and 12 weeks post injury. For all surgical and neurophysiological procedures, animals were anesthetized.

*Surgical procedures with animals*

Fourteen female Yucatan miniature pigs (Sinclair Bio-Resources, Columbia, MO) aged 125 to 142 days, weighing between 18.5-25 Kg, were housed, fed, and cared for in accordance with the Canadian Council for Animal Care regulations. The study was approved by our institution's animal care committee (University of British Columbia Animal Care Committee, Protocol Number A13-0013). Female animals were selected as the management of the bladder and urethra necessitated due to spinal cord injury is far less complicated in females compared to the male animals. Anesthesia was induced with propofol (1.6 - 7ml). Pigs were intubated, ventilated, and maintained with a combination of fentanyl (20 ± 2.8ug/kg/h), propofol (21.4 ± 6.1mg/kg/h), and ketamine (9.8 ± 1.7mg/kg/h). After the animal was anesthetized, the external jugular vein was catheterized (i.e., central line catheter) for the delivery of drugs and a rectal temperature probe was inserted to monitor the core temperature. The animals were covered with a surgical drape with a window above the surgical site.

*Screw placement for neurophysiological recordings*

For placement of the scalp electrodes, a 10-cm midline longitudinal incision was made at the level of the ears extending anteriorly towards the snout. Dissection was carried to the level of the bone until the sagittal and coronal sutures were visualized. A total of four electrodes were attached 1 cm lateral to the sagittal suture and 1 cm anterior and posterior to the coronal suture (**Fig. 2C**). To reduce the high impedance (i.e., due to the thickness of the pig's skull) and improve both motor cortex stimulation and signal recordings from the somatosensory cortex, screws were placed into the skull. The skull was carefully drilled bi-cortically to a standard depth

of 4 mm. Sterilized stainless steel screws (15 mm length, 1.1 mm diameter) were inserted and connected to alligator clips. To avoid complications such as infection, the electrode screws were removed at the end of neurophysiological recordings (i.e., 3h post-injury) and the skin was approximated with reverse cutting prolene suture. The electrode screws were reinserted at the same location for the 12-week follow-up measurement.

*Laminectomy*

Animals were placed in the prone position and a 15 cm dorsal midline incision was made between T6 and T14. The fascia was divided and the paraspinal musculature was stripped from the dorsal spinous processes, laminae, and transverse processes of T6 to T14 using electro-cautery (Surgitron Dual Frequency RF/120 Device; Ellman International, Oceanside, NY). Using anatomic landmarks, the T9, T10, and T11 pedicles were cannulated and instrumented with 4.5 · 35 mm screws (SelectTM Multi Axial Screw, Medtronic, Minneapolis, MN). The T10 segment was widened to ensure that a circular window was made measuring at least 1.2 cm in diameter to expose the dura and spinal cord.

*Induction of Spinal Cord Injury*

After the T10 laminectomy, the weight-drop device was rigidly secured to the pedicle screws and positioned so that the impactor (mass: 50 g) would fall directly on the exposed dura and spinal cord at vertebrae T10. The tip of the impactor (diameter: 9.53 mm) was instrumented with a load cell (LLB215, Futek Advanced Sensor Technology, Irvine, CA) to record the force at impact. Immediately following the contusion injury (drop height: 20 cm), compression was applied by placing a 100g mass on top of the impactor for five minutes. Subsequently, the weight-drop apparatus was removed.

*Somatosensory evoked potentials*

Somatosensory evoked potentials were recorded in response to the stimulation of the left and right tibial nerve (i.e., below the level of contusion) as well as the right median nerve (i.e., above the level of contusion). Electrical stimulation comprised repetitive square wave (0.5ms) pulses delivered at 3.1 Hz using sub-dermal needle electrodes (1.2 cm, 27 Gauge, Neuroline twisted pair, Ambu, Copenhagen, Denmark). Stimuli were delivered using a Keypoint electro-

diagnostic device (Medtronic, Mississauga, Ontario, Canada; bandpass = 2 Hz - 2 kHz). Stimuli were given at intensities four times the threshold required to visualize twitching in the muscles distal to the stimulation point. For each individual animal, the stimulation intensity was determined at baseline (i.e., control condition). The same intensity was applied for all testing sessions. Sensory evoked potentials were recorded from the skull screws of the cortex contralateral to the stimulated nerve.

*Motor evoked potentials*

Bilateral depolarization of the motor cortex was achieved by delivering stimulation trains through stainless steel alligator clips clamped to the electrode screws. Stimuli intensities ranged from 80 - 100mA in trains of 5 pulses (pulse duration = 0.5 ms, Interstimulus Interval = 0.5 ms) and were delivered by a Keypoint electro-diagnostic device (Medtronic, Mississauga, Ontario, Canada). Small bipolar needles (1.2 cm, 27 Gauge, Neuroline twisted pair, Ambu, Copenhagen, Denmark) were placed in the muscles of the right forelimb (*Extensor Carpi Radialis*) as well as left and right hindlimbs (*Tibialis Anterior*). Signal recorded from the muscles was amplified and then band-pass filtered at 30 Hz to 1 kHz, which is in accordance with set-up of human motor evoked potential recordings[30].

*Porcine Thoracic Injury Behavior Scale*

Upon four days of acclimatization and habituation to the large animal facility, animals were handled daily for five days (each day 15min) to become familiar with experimental handling. For the subsequent five days, animals were trained daily (each day 15min) to walk non-stop up and down a rubber mat (width 1.22m, length 5m).

Prior to the injury, animals were videotaped to establish the baseline hindlimb locomotor behavior score. Three high definition camcorders positioned behind the animals captured the movements of the hindlimbs and rump as they walked away from the cameras. Videotaping of locomotor recovery resumed one week post-injury and continued weekly for 12 weeks in total. The hindlimb function was analyzed and classified into 10 different categories according the Porcine Thoracic Injury Behavioral Scale[23]. This scale ranges from no active hindlimb movement (score = 1) to normal ambulation (score = 10). Specifically, Porcine Thoracic Injury Behavioral Scale scores of 1 – 3 are characterized by ‘hindlimb dragging’, scores of 4 – 6

represent varying degrees of 'stepping' ability, and scores of 7 – 10 reflect varying degrees of 'walking' ability.

*Spinal Cord Histology*

Twelve weeks post-injury all animals were euthanized and the spinal cord was harvested, post-fixed, and cryoprotected as described previously [29]. Subsequently, spinal cords were cut into 1 cm segments centered on the injury site, embedded in OCT blocks and frozen at -80$^{o}$ C before being cut into 20 μm thick cross cryosections. Sections were serially mounted onto adjacent silane-coated SuperFrost-Plus slides (Fisher Scientific, Pittsburgh, PA) such that sections on the same slide were obtained from tissue 400 micrometer apart and stored at -80C. For differentiating gray and white matter, Eriochrome Cyanine R histochemistry was performed. Neutral Red was used as a counterstain. ECR-stained sections were examined, and pictures (5x objective) were taken of sections at 800 lm intervals throughout the lesion site (Zeiss AxioImager M2 microscope, Carl Zeiss Canada Ltd., Toronto, ON, Canada). Images were analyzed using Zen Imaging Software (Carl Zeiss Canada Ltd., Toronto, ON, Canada), by manually tracing the spinal cord perimeter and spared tissue for each image captured. The spared white matter was defined as the areas that were stained for Eriochrome Cyanine R, whereas gray matter was considered spared when it was a stereotypic light gray color with a consistent neuropil texture. The percentages of white matter and gray matter were calculated by dividing the spared white or gray matter by the total area of the spinal cord on a given section.

**Statistical analyses**

All statistical procedures were performed using IBM`s Statistical Package for the SocialSciences (SPSS) version 23.0 (Armonk, New York, U.S.). For all analyses, $p < .05$ was considered as statistical significance. To take into account the longitudinal nature of the data (animal and human) and adjust for potential confounders, as well as to handle missing data, the primary analysis comprised a linear mixed effects model. Post-hoc analyses were performed and Bonferroni corrections were applied to adjust for multiple comparisons.

For the human data, the analysis focused on various primary dependent variables: Latencies and amplitudes of motor evoked potentials, tibial and ulnar sensory evoked potentials

(6 models). The time-points of assessment (i.e., 1, 3, 6, and 12 months), age at baseline, and lesion completeness (i.e., complete or incomplete) were included as independent variables. In a planned sub-analysis, the motor evoked potentials parameters of the individuals with spinal cord injury at all time points were compared to the healthy control cohort using a linear mixed model.

The primary outcomes of the animal study were motor evoked potentials and sensory evoked potentials latencies and amplitude (both hind- and forelimb) at pre-defined time-points: baseline, post-laminectomy, as well as 10 minutes, 3 hours, and 12 weeks post injury. In separate linear mixed models, latencies and amplitudes of sensory evoked potentials and motor evoked potentials were set as dependent variable, while time-points were included as independent variables. We further examined the amount of motor recovery following spinal cord injury employing a linear mixed model. In all models, subjects were included as random factor. Pearson correlation analyses were used to identify relationships between neurophysiological (motor evoked potentials and sensory evoked potentials), behavioral (Porcine Thoracic Injury Behavioral Scale Score), and immunohistochemistry outcomes (spared white and gray matter).

## Results

*HUMAN DATA*

Basic demographics and other characteristics of the study sample at all time-points after injury are summarized in **Table 1**. A total of 37 individuals with spinal cord injury from the EMSCI database were included in the analysis.

*Somatosensory and motor evoked potentials above the spinal cord injury level*

Ulnar sensory evoked potentials amplitude increased significantly over time ($F = 4.6$, df: 3, $p = 0.004$), while the sensory evoked potentials latency did not ($F = 1.0$, df: 3, $p = 0.392$). Pair-wise comparisons yielded an increase in amplitude at three and six months compared to the recordings at 1 month **(Fig 3A).** The average increase in amplitude was +33.0%, +47.8%, and +65.2% at three, six, and twelve months respectively. There was no main effect of injury completeness on ulnar sensory evoked potentials amplitude ($F = 1.3$, df: 1, $p = 0.256$) and latency ($F = 0.119$, df: 1, $p = 0.730$), suggesting independence from injury severity. There was also no interaction effect between injury completeness and time on amplitude ($F = 0.536$, df: 2, p

= 0.586) and latency (F = 0.129, df: 2, p = 0.879. This suggests that severity did not impact amplitude and latency as a function of time.

There was no main effect of time or injury completeness on the upper limb motor evoked potentials amplitude (Time: F = 1.571, df: 3, p = 0.200; Completeness: F = 2.400, df: 3, p = 0.124) or latency (Time: F = 0.536, df: 3, p = 0.155; Completeness: F = 0.915, df: 3, p = 0.549) (**Fig. 3B**). At the first assessment (1 month post-injury), the upper limb motor evoked potentials amplitudes were already significantly higher in individuals with spinal cord injury (mean = 2.3, SD = 0.8) than in healthy controls (mean = 1.4, SD = 0.6; Conditions t = 2.88 and p = 0.02). Over time during subsequent assessments there was no significant change. Motor evoked potentials latencies were not significantly different from healthy controls at 1 month post-injury (t = 0.891, p > 0.05) and also did not change significantly over time.

*Somatosensory evoked potentials below the spinal cord injury level*

We found a main effect of lesion completeness on tibial somatosensory evoked potential amplitude (F = 7.3, df: 1, p = 0.031), but not on the latency (Time: F = 0.8, df: 3, p = 0.506; Completeness: F = 0.22, df: 1, p = 0.882). Post-hoc analyses revealed a significant increase in amplitude at three, six, and twelve months compared to 1 month (**Fig 3C**). Individuals with spinal cord injury with sensory incomplete lesions (AIS B-D) exhibited an increase in tibial sensory evoked potentials amplitude, while the amplitude did not change over time in individuals with spinal cord injury with complete lesions (AIS A). This observation is in line with previous reports[32].

*ANIMAL DATA*

A total of 14 animals underwent experimental spinal cord injury. All animals received a contusion injury by dropping a 50 g mass from a 20 cm height at the T10 level of the spinal cord. The mean (standard deviation) impact force applied to the exposed spinal cord measured at the tip of the impactor was 2731 (514) kdynes. All animal characteristics are summarized in **Table 2**. Two animals had to be euthanized within the first 24 hours after surgery due to unexpected upper airway compromise and thus, were excluded from the data analysis. Complications related to the cortical stimulation procedures, such as damage due to screw placement or neurological deficits, were not observed upon postmortem examination. In order to prevent a drug-effect on

the neurophysiological outcomes, animals received the same anesthesia on both days (i.e., induction of SCI and follow-up at 12 weeks). Individual animal data is presented in supplementary table 1.

*Somatosensory and motor evoked potentials above the spinal cord injury level*

There was a significant main effect of time on ulnar sensory evoked potentials amplitude ($F = 5.7$, df: 4, $p = 0.001$, **Fig 4A**). Pair-wise comparisons yielded a significant increase (+64.3%) in amplitude at 12 weeks post injury compared to baseline ($p = 0.006$). The latency of ulnar sensory evoked potentials remained comparable over time ($F = 0.78$, df: 4, $p > 0.05$).

Immediately following the weight drop contusive spinal cord injury, the forelimb motor evoked potentials amplitude (i.e., *Extensor Carpi Radialis*) increased 365.7% ($p = 0.033$) compared to both pre-injury time-points (**Fig 4B**). The amplitude remained higher at all post-injury time-points (3hrs post spinal cord injury: +337%, $p = 0.049$, 12 weeks post spinal cord injury: +334%, $p = 0.046$). The linear mixed model confirmed that there was indeed a statistically significant main effect of time on forelimb motor evoked potentials amplitude ($F = 5.0$, df: 4, $p = 0.006$). No change in latency was observed at any time-point (all $p > 0.05$).

*Somatosensory evoked potentials below the spinal cord injury level*

Tibial sensory evoked potentials were abolished following spinal cord injury induction and did not recover, confirming the completeness of injury (**Fig 4C**). All animal latencies and amplitudes of medial and tibial sensory evoked potentials are summarized in **Table 2**.

*Motor recovery - Porcine Thoracic Injury Behavioral Score*

At baseline, all animals reached the highest PTIBS Score ($10 \pm 0$). One week after spinal cord injury, hindlimb motor function was severely impaired, resulting in a mean PTIBS Score of $2.0 \pm 0.9$. Motor recovery was observed in all animals over time ($F = 11.4$, df: 11, $p < 0.001$). The average recovery was $2 \pm 1.1$ points from 1 to 12 weeks post injury. The amount of motor recovery was not correlated with the observed changes in forelimb motor evoked potentials ($F = 11.4$, df: 11, $p =$) and sensory evoked potentials ($F = 11.4$, df: 11, $p =$).

*Immunohistochemical quantification of injury severity*

In order to quantify the extent of spared tissue at the lesion epicenter as well as the rostro-caudal spread of the injury, quantification of spared gray and white matter was performed on serial sections stained with Eriochrome cyanine R (**Fig 5A**). At week 12 post-spinal cord injury, both white and gray matter at the lesion epicenter was completely abolished and increased incrementally with distance from the epicenter (**Fig 5B**). We defined the lesion as all areas that were structurally not significantly different from the epicenter. There was no relationship between neurophysiological parameters and spared tissue (all comparisons $p > 0.05$).

## Discussion

The present study characterizes the brain's response to an acute spinal cord injury in humans and pigs. In both species, the amplitude of upper limb sensory evoked potentials (above the spinal cord injury level) progressively increased over time. In contrast, motor responses increased immediately after experimental injury in pigs and remained elevated out to 12 weeks. Along similar lines, motor evoked potentials were already significantly greater compared to the healthy control cohort at 1 month post injury. The observed changes in the sensory and motor areas in the brain occurred independently of the severity of injury. Despite many obvious differences between experimental models of spinal cord injury and the human condition, changes in neurophysiological measures of cortical function following damage in the spinal cord share remarkable similarities across species (i.e., porcine and humans).

The impact of peripheral and central deafferentation on the brain has been extensively investigated in various animal models[34–39]. In Wall and Egger's seminal publication in 1971, "functional reorganization" of the thalamus and sensory cortex was first reported in rats following a thoracic lesion[39]. Later studies demonstrated a similar capacity for neuroplasticity in primates, qualifying reorganization of the face into the deafferented hand area as "massive"[34,40]. A defining characteristic of the brain's response to spinal cord injury in primates is that sensory reorganization occurs progressively over time, consistent with a collateral sprouting hypothesis[36,41,42]. In rodents, however, immediate changes in the somatosensory cortex have been reported, occurring within seconds to minutes of experimental injury[12,13,19,43,44] (**Fig 6**).

In humans, changes in the brain have been primarily reported in chronic stages of injury, using cross-sectional neuroimaging[3,6,45–48] and neurophysiological techniques[2,49]. While consistently demonstrating that cortical reorganization occurs, knowledge regarding how these changes develop over time is limited. Our longitudinal study provides clear evidence that reorganization of the somatosensory cortex occurs in humans occurs over the initial months following spinal cord injury (**Fig 3**). Resembling the human profile, the reorganization of porcine somatosensory cortex was characterized by an increase in forelimb sensory evoked potentials amplitude from 1 to 3 months. To our knowledge, only one previous study examined changes in the brain to sensory stimulation above the level of injury. At 4-6 weeks post injury, median nerve sensory evoked potentials were normal, both in terms of amplitude and latency[50]. For a small cohort (n=5) that underwent a follow-up examination, 3 to 5 weeks later (i.e., 7-11 weeks post

injury), no change in sensory evoked potentials parameters was observed[50]. This finding is in agreement with our observations at early time-points (i.e., 1-month), in that sensory evoked potentials are still within normative values within the first weeks after injury. The progressive increase in sensory evoked potentials amplitudes (i.e., 12 weeks post injury) observed in later stages suggests the involvement of sensory sprouting[20,21] and the possible expansion of the active forelimb region into the adjacent deprived lower limb region within the sensorimotor cortex [51].

Interestingly, changes in the motor system appear to occur immediately after injury. The abrupt increase in motor evoked potentials amplitude in humans and pigs is in agreement with an immediate change reported in monkeys following T8/9 contusion injury[52], and in the acute phase of human spinal cord injury[53]. These immediate changes are similar to what has been reported in response to reversible ischemic nerve block[54]. Other studies in humans, however, have reported no change[55,56] or reduced amplitudes[57] (for review, please see[58]). Overall, the immediate nature of increases in motor evoked potentials amplitude that persist into chronic stages of injury suggest alternative mechanisms, potentially involving the unmasking of dormant neural synapses[13,16–18], or long-term intracortical disinhibition[54].

From a translational perspective, an understanding of mechanisms underlying neuroplasticity is fundamentally important to develop assessments to reveal and quantify even subtle changes as they may relate to recovery. To date, neuroplasticity has been widely studied in rodent models of spinal cord injury. Unfortunately, the translation of knowledge from preclinical rodent models of spinal cord injury to humans has, however, failed[1,59]. Among leading causes of failure are challenges modeling human spinal cord injury in rodents[22,60]. Our results demonstrate key differences in cortical reorganization after spinal cord injury in pigs and humans compared to that which has been reported in rodents[12,13,43,61] – namely that sensory reorganization occurs immediately in rats whereas it develops over time in humans and pigs. Pigs have emerged as potential intermediary large animal model of neurological disorders including spinal cord injury, stroke, and traumatic brain injury[23,25,27,62–64]. Our observations extend the advantages of the pig species as a translational pre-clinical model of neuroplasticity within the CNS after injury.

One limitation of this study relates to the measurement of cortical plasticity in humans after spinal cord injury. First, a relatively small number of individuals with neurological level of injury at or below C8 (n=37), in which upper limb sensory evoked potentials and motor evoked

potentials were recorded, were included in our analysis. These individuals were selected *a priori* because: a) lower thoracic injuries (e.g., T4 and below) are not routinely examined with upper limb sensory evoked potentials and motor evoked potentials, and b) according to International Standards[65], the C8 spinal segment is intact, thereby allowing for conduction of ascending and descending signals (i.e., sensory evoked potentials and motor evoked potentials, respectively). However, subclinical sensorimotor deficits in C8 (i.e., missed by muscle strength and sensory testing), and partial recovery in the adjacent T1 spinal segment may also have facilitated increased sensory evoked potentials and motor evoked potentials amplitudes. Additionally, sensory evoked potentials and motor evoked potentials were not examined in humans with spinal cord injury until 1-month. This is largely related to difficulties performing very early neurophysiological assessments in individual with spinal cord injury with acute, traumatic spinal cord injury. Consequently, increased motor evoked potentials amplitudes at 1-month post injury are relative to normal control values (i.e., not a within subject comparison, as was done for sensory evoked potentials). Although our animal study provided insights to what happens in immediately after SCI, future investigations are warranted to further consolidate our understanding of the mechanisms during the acute phase of injury (i.e., 1-3 months). Lastly, the technique used to elicit MEPs in the animals is different from the TMS pulses used in the patients. Thus, the observed corticospinal changes measured by MEP amplitude might reflect different underlying mechanisms.

In the present study, the progression of sensory and motor reorganization was characterized in humans and pigs following traumatic spinal cord injury. Findings derived from our reverse-translational approach suggest that the reorganization of the motor system (i.e., corticospinal tract) begins immediately after injury, while sensory reorganization occurs over time. Collectively, our findings highlight the importance of large animal species, such as the Yucatan mini-pigs, in translational research and development of spinal cord repair strategies to examine neuroplasticity.

**Acknowledgments:** The authors thank the very skilled and dedicated team of veterinarians and veterinarian technicians at the UBC Center for Comparative Medicine for their expertise in caring for the animals involved in these experiments.

**Funding**: The study was supported by the Clinical Research Priority Program in Neurorehabilitation of the University of Zurich, Switzerland (Armin Curt) and NSERC Discovery Grant (John Kramer). Catherine Jutzeler is supported by postdoctoral research fellowships from the International Foundation for Research in Paraplegia (IRP), the Swiss National Science Foundation, and the Craig H. Nielsen Foundation. Brian Kwon is the Canada Research Chair in Spinal Cord Injury. John Kramer is supported by a Michael Smith Foundation for Health Research and Rick Hansen Scholar Award.

**Author contributions**: CRJ contributed substantially to the conception and design of the study, the data acquisition, analysis, and interpretation. Furthermore, she drafted the research article. FS performed the surgeries and was involved in the data collection, data analysis, and revising the research article. KS was involved in the data collection, data analysis, and revising the research article. NM performed the surgeries, was involved in the data collection, and revised the manuscript. EO was involved in the data collection (immunohistochemistry) and revised the manuscript. MH was involved in the human data collection and revised the manuscript. AC made substantial contributions to study conception, design, and data collection as well as participated in revising the research article critically for important intellectual content. BK made substantial contributions to study conception and design as well as participated in revising the research article critically for important intellectual content. JLKK contributed substantially to study design, the data acquisition, analysis, and interpretation, and was involved in drafting the research article.

**Competing interests**: The authors have no conflicts of interest to declare.

**References:**

1. Ramer LM, Ramer MS, Bradbury EJ. Restoring function after spinal cord injury: Towards clinical translation of experimental strategies. The Lancet Neurology 2014;13(12):1241–1256.
2. Topka H, Cohen LG, Cole R a, Hallett M. Reorganization of corticospinal pathways following spinal cord injury. Neurology 1991;41(August):1276–1283.
3. Curt A, Alkadhi H, Crelier GR, et al. Changes of non-affected upper limb cortical representation in paraplegic patients as assessed by fMRI. Brain : a journal of neurology 2002;125(Pt 11):2567–2578.
4. Jutzeler CR, Huber E, Callaghan MF, et al. Association of pain and CNS structural changes after spinal cord injury. Scientific Reports 2016;6
5. Jutzeler CR, Curt A, Kramer JLK. Relationship between chronic pain and brain reorganization after deafferentation: A systematic review of functional MRI findings [Internet]. NeuroImage: Clinical

2015;9:599–606.Available from: http://dx.doi.org/10.1016/j.nicl.2015.09.018

6. Jutzeler CR, Freund P, Huber E, et al. Neuropathic pain and functional reorganization in the primary sensorimotor cortex after spinal cord injury [Internet]. The Journal of Pain 2015;16(12):1256–1267.Available from: http://www.sciencedirect.com/science/article/pii/S1526590015008421

7. Makin TR, Scholz J, Filippini N, et al. Phantom pain is associated with preserved structure and function in the former hand area. [Internet]. Nature communications 2013;4:1570.Available from: http://www.pubmedcentral.nih.gov/articlerender.fcgi?artid=3615341&tool=pmcentrez&rendertype=abstract

8. Merzenich MM, Nelson RJ, Stryker MP, et al. Somatosensory Cortical Map Changes Following Digit Amputation in Adult Monkeys. the Journal of Comparative Neurology 1984;224:591–605.

9. Florence SL, Taub HB, Kaas JH. Large-Scale Sprouting of Cortical Connections After Peripheral Injury in Adult Macaque Monkeys. Science 1998;282(5391):1117–1121.

10. Jain N, Qi H-X, Collins CE, Kaas JH. Large-scale reorganization in the somatosensory cortex and thalamus after sensory loss in macaque monkeys. The Journal of neuroscience : the official journal of the Society for Neuroscience 2008;28(43):11042–11060.

11. Garraghty PE, Kaas JH. Large-scale functional reorganization in adult monkey cortex after peripheral nerve injury. Proceedings of the National Academy of Sciences of the United States of America 1991;88(August):6976–6980.

12. Alonso-Calviño E, Martínez-Camero I, Fernández-López E, et al. Increased responses in the somatosensory thalamus immediately after spinal cord injury [Internet]. Neurobiology of Disease 2016;87:39–49.Available from: http://dx.doi.org/10.1016/j.nbd.2015.12.003

13. Aguilar J, Alonso-calvin E, Yague G, et al. Spinal Cord Injury Immediately Changes the State of the Brain and Guglielmo Foffani. 2010;30(22):7528–7537.

14. Wu CW, Kaas JH. Reorganization in primary motor cortex of primates with long-standing therapeutic amputations. The Journal of neuroscience : the official journal of the Society for Neuroscience 1999;19(17):7679–97.

15. Qi H-X, Stepniewska I, Kaas JH. Reorganization of Primary Motor Cortex in Adult Macaque Monkeys with Long-standing Amputations. Journal of Neurophysiology 2000;84(July):2133–2147.

16. Jacobs, KM; Donoghue J, Jacobs KM, Donoghue JP. Reshaping the Cortical Motor Map by Unmasking Latent Intracortical Connections [Internet]. Science 1991;251(4996):944–947.Available from: http://www.sciencemag.org/content/251/4996/944.short%5Cnhttp://www.ncbi.nlm.nih.gov/pubmed/2000496

17. Sanes JN, Suner S, Lando JF, Donoghue JP. Rapid reorganization of adult rat motor cortex somatic representation patterns after motor nerve injury. [Internet]. Proceedings of the National Academy of Sciences of the United States of America 1988;85(6):2003–7.Available from: http://www.pubmedcentral.nih.gov/articlerender.fcgi?artid=279910&tool=pmcentrez&rendertype=abstract

18. Donoghue JP, Sanes JN. Organization of adult motor cortex representation patterns following neonatal forelimb nerve injury in rats. The Journal of neuroscience : the official journal of the Society for Neuroscience 1988;8(9):3221–3232.

19. Humanes-Valera D, Foffani G, Alonso-Calviño E, et al. Dual Cortical Plasticity After Spinal Cord Injury [Internet]. Cerebral Cortex 2016;(May 2016):bhw142.Available from: http://www.cercor.oxfordjournals.org/lookup/doi/10.1093/cercor/bhw142

20. Carmichael ST. Cellular and molecular mechanisms of neural repair after stroke: Making waves. Annals of Neurology 2006;59(5):735–742.

21. Nudo RJ. Recovery after brain injury: mechanisms and principles. [Internet]. Frontiers in human neuroscience 2013;7:887.Available from: http://www.ncbi.nlm.nih.gov/pubmed/24399951%5Cnhttp://www.pubmedcentral.nih.gov/articlerender.fcgi?artid=PMC3870954

22. Friedli L, Rosenzweig ES, Barraud Q, et al. Pronounced species divergence in corticospinal tract reorganization and functional recovery after lateralized spinal cord injury favors primates. Science translational medicine 2015;7(302):302ra134.

23. Lee JHT, Jones CF, Okon EB, et al. A novel porcine model of traumatic thoracic spinal cord injury. [Internet]. Journal of neurotrauma 2013;30(3):142–59.Available from: http://www.ncbi.nlm.nih.gov/pubmed/23316955

24. Schomberg DT, Miranpuri GS, Chopra A, et al. Translational Relevance of Swine Models of Spinal Cord Injury [Internet]. Journal of Neurotrauma 2016;11:[Epub ahead of print].Available from: http://online.liebertpub.com/doi/10.1089/neu.2016.4567

25. Benavides FD, Santamaria AJ, Bodoukhin N, et al. Characterization of Motor and Somatosensory Evoked Potentials in the Yucatan Micropig. 2016;14:1–14.

26. Kwon BK, Streijger F, Hill CE, et al. Large animal and primate models of spinal cord injury for the testing of novel therapies. Experimental Neurology 2015;269

27. Leonard AV, Menendez JY, Pat BM, et al. Localization of the corticospinal tract within the porcine spinal cord: Implications for experimental modeling of traumatic spinal cord injury [Internet]. Neuroscience Letters 2017;648:1–7.Available from: http://linkinghub.elsevier.com/retrieve/pii/S0304394017302306

28. Streijger F, Lee JHT, Manouchehri N, et al. The Evaluation of Magnesium Chloride within a Polyethylene Glycol Formulation in a Porcine Model of Acute Spinal Cord Injury. [Internet]. Journal of neurotrauma 2016;15:1–49.Available from: http://www.ncbi.nlm.nih.gov/pubmed/27125815

29. Streijger F, Lee JH, Chak J, et al. The Effect of Whole-Body Resonance Vibration in a Porcine Model of Spinal Cord Injury [Internet]. J Neurotrauma 2015;921:908–921.Available from: http://www.ncbi.nlm.nih.gov/pubmed/25567669%5Cnhttp://online.liebertpub.com/doi/pdfplus/10.1089/neu.2014.3707

30. Petersen J a., Spiess M, Curt a., et al. Spinal Cord Injury: One-Year Evolution of Motor-Evoked Potentials and Recovery of Leg Motor Function in 255 Patients. Neurorehabilitation and Neural Repair 2012;26(8):939–948.

31. Kramer JLK, Moss AJ, Taylor P, Curt A. Assessment of posterior spinal cord function with electrical perception threshold in spinal cord injury. Journal of neurotrauma 2008;25(8):1019–1026.

32. Kuhn F, Halder P, Spiess MR, Schubert M. One-year evolution of ulnar somatosensory potentials after trauma in 365 tetraplegic patients: early prediction of potential upper limb function. Journal of neurotrauma 2012;29(10):1829–37.

33. Spiess M, Schubert M, Kliesch U, Halder P. Evolution of tibial SSEP after traumatic spinal cord injury: Baseline for clinical trials. Clinical Neurophysiology 2008;119(5):1051–1061.

34. Pons TP, Garraghty PE, Ommaya AK, et al. Massive cortical reorganization after sensory deafferentation in adult macaques. Science (New York, NY) 1991;252(5014):1857–60.

35. Onifer SM, Smith GM, Fouad K. Plasticity After Spinal Cord Injury: Relevance to Recovery and Approaches to Facilitate It. Neurotherapeutics 2011;8(2):283–293.

36. Endo T, Spenger C, Tominaga T, et al. Cortical sensory map rearrangement after spinal cord injury: fMRI responses linked to Nogo signalling. Brain 2007;130(11):2951–2961.

37. Rao J-S, Manxiu M, Zhao C, et al. Atrophy and primary somatosensory cortical reorganization after unilateral thoracic spinal cord injury: a longitudinal functional magnetic resonance imaging study. [Internet]. BioMed research international 2013;2013:753061.Available from: http://www.pubmedcentral.nih.gov/articlerender.fcgi?artid=3891744&tool=pmcentrez&rendertype=abstract

38. Yang P-F, Qi H-X, Kaas JH, Chen LM. Parallel functional reorganizations of somatosensory areas 3b and 1, and S2 following spinal cord injury in squirrel monkeys. [Internet]. The Journal of neuroscience : the official journal of the Society for Neuroscience 2014;34(28):9351–63.Available from: http://www.pubmedcentral.nih.gov/articlerender.fcgi?artid=4087212&tool=pmcentrez&rendertype=abstract

39. Wall PD, Egger MD. Formation of New Connexions in Adult Rat Brains after Partial Deafferentation [Internet]. Nature 1971;232(5312):542–545.Available from: http://www.scopus.com/inward/record.url?eid=2-s2.0-0015233953&partnerID=tZOtx3y1

40. Jain N, Catania KC, Kaas JH. Deactivation and reactivation of somatosensory cortex after dorsal spinal cord injury. Nature 1997;386(6624):495–498.

41. Ghosh A, Haiss F, Sydekum E, et al. Rewiring of hindlimb corticospinal neurons after spinal cord injury. [Internet]. Nature neuroscience 2010;13(1):97–104.Available from: http://www.ncbi.nlm.nih.gov/pubmed/20010824

42. Vipin Ashwati, Thow XY, Mir H, et al. Natural Progression of Spinal Cord Transection Injury and Reorganization of Neural Pathways. Journal of Neurotrauma 2016;33:1–11.

43. Humanes-Valera D, Aguilar J, Foffani G. Reorganization of the Intact Somatosensory Cortex Immediately after Spinal Cord Injury. PLoS ONE 2013;8(7):1–14.

44. Yague JG, Humanes-Valera D, Aguilar J, Foffani G. Functional reorganization of the forepaw cortical representation immediately after thoracic spinal cord hemisection in rats [Internet]. Experimental Neurology 2014;257:19–24.Available from: http://dx.doi.org/10.1016/j.expneurol.2014.03.015

45. Bruehlmeier M, Dietz V, Leenders KL, et al. How does the human brain deal with a spinal cord injury? The European journal of neuroscience 1998;10(12):3918–3922.

46. Green JB, Sora E, Bialy Y, et al. Cortical sensorimotor reorganization after spinal cord injury: an electroencephalographic study. Neurology 1998;50(4):1115–1121.

47. Turner J a, Lee JS, Schandler SL, Cohen MJ. An fMRI investigation of hand representation in paraplegic humans. Neurorehabilitation and neural repair 2003;17:37–47.

48. Mikulis DJ, Jurkiewicz MT, McIlroy WE, et al. Adaptation in the motor cortex following cervical spinal cord injury. [Internet]. Neurology 2002;58(5):794–801.Available from: http://www.ncbi.nlm.nih.gov/pubmed/11889245

49. Levy WJ, Amassian VE, Traad M, Cadwell J. Focal magnetic coil stimulation reveals motor cortical system reorganized in humans after traumatic quadriplegia. Brain Research 1990;510(1):130–134.

50. Kaplan PE, Rosen JS. SOMATOSENSORY EVOKED POTENTIALS IN SPINAL CORD INJURED PATIENTS. 1981;19:118–122.

51. Jones E. CORTICAL AND SUBCORTICAL CONTRIBUTIONS TO ACTIVITY-DEPENDENT PLASTICITY IN PRIMATE SOMATOSENSORY CORTEX [Internet]. Annual Review of Neuroscience 2002;31(1):45–67.Available from: http://www.annualreviews.org/doi/abs/10.1146/annurev.anthro.31.040202.105553

52. Ye J. Evaluation of the neural function of nonhuman primates with spinal cord injury using an evoked potential-based scoring system [Internet]. European Journal of Neuroscience 2013;(August):1–13.Available from: http://dx.doi.org/10.1038/srep33243

53. Streletz. Transcranial magnetic stimulation: cortical motor maps in acute spinal cord injury. Brain topography 1995;7(3):245–250.

54. Brasil-Neto JP, Valls-Solè J, Pascual-Leone A, et al. Rapid modulation of human cortical motor outputs following ischaemic nerve block. Brain 1993;116(3):511–525.

55. Laubis-Herrmann U, Dichgans J, Billow H, Topka H. Motor Reorganization after Spinal Cord Injury: Evidence of adaptive changes in remote muscles. Restorative Neurology and Neuroscience 2000;1–8.

56. Der-Sheng H, Chih-Ming L, Chein-Wei C. REORGANIZATION OF THE CORTICO-SPINAL PATHWAY IN PATIENTS WITH CHRONIC COMPLETE THORACIC SPINAL CORD INJURY: A STUDY OF MOTOR EVOKED POTENTIALS. J Rehabil Med 2013;0(18):488–497.

57. Lotze M, Laubis-Herrmann U, Topka H. Combination of TMS and fMRI reveals a specific pattern of reorganization in M1 in patients after complete spinal cord injury. Restorative neurology and neuroscience

2006;24(2):97–107.

58. Moxon KA, Oliviero A, Aguilar J, Foffani G. Cortical reorganization after spinal cord injury: Always for good? [Internet]. Neuroscience 2014;283:78–94.Available from: http://dx.doi.org/10.1016/j.neuroscience.2014.06.056

59. Kwon BK, Soril LJJ, Bacon M, et al. Demonstrating efficacy in preclinical studies of cellular therapies for spinal cord injury - How much is enough? Experimental Neurology 2013;248:30–44.

60. Courtine G, Bunge MB, Fawcett JW, et al. Can experiments in nonhuman primates expedite the translation of treatments for spinal cord injury in humans? Nature Medicine 2007;13(5):561–566.

61. Humanes-Valera D, Foffani G, Aguilar J. Increased cortical responses to forepaw stimuli immediately after peripheral deafferentation of hindpaw inputs. [Internet]. Scientific reports 2014;4(2):7278.Available from: http://www.ncbi.nlm.nih.gov/pubmed/25451619

62. Donati G, Kapetanios A, Dubois-Dauphin M, Pournaras CJ. Caspase-related apoptosis in chronic ischaemic microangiopathy following experimental vein occlusion in mini-pigs. Acta Ophthalmologica 2008;86(3):302–306.

63. Mordasini P, Frabetti N, Gralla J, et al. In vivo evaluation of the first dedicated combined flow-restoration and mechanical thrombectomy device in a swine model of acute vessel occlusion. American Journal of Neuroradiology 2011;32(2):294–300.

64. Browne KD, Chen X-H, Meaney DF, Smith DH. Mild traumatic brain injury and diffuse axonal injury in swine. Journal of neurotrauma 2011;28(9):1747–55.

65. Kirshblum SC, Burns SP, Biering-Sorensen F, et al. International standards for neurological classification of spinal cord injury (Revised 2011). J Spinal Cord Med 2011;34(6):535–546.

## FIGURE LEGENDS

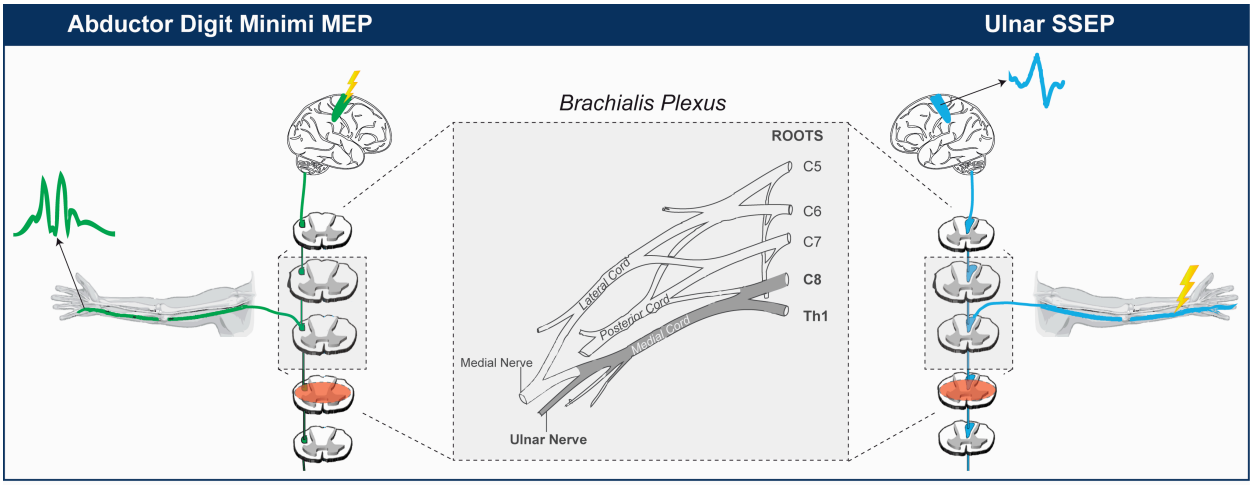


**Fig. 1: Brachial Plexus Anatomy and Assessments Of Sensorimotor Evoked Potentials**

The ulnar nerve originates from the C8-T1 nerve roots forming, in part, the medial cord of the brachial plexus. It also innervates the Abductor Digit Minimi. In response to electrical stimulation, evoked potentials are generated by the transmission of the afferent (somatosensory evoked potentials [SSEP]) or efferent (motor evoked potentials [MEP]) volleys between the periphery and the cortex. Thus, SSEPs and MEPs provide unique indices of the integrity of the afferent and efferent volley in spinal, brain-stem and thalamocortical pathways, as well as primary sensorimotor cortical regions. By virtue of the anatomical arrangement of the ulnar nerve, damage to the spinal cord at or above C8 will result in impaired SSEPs and MEPs. However, damage below C8 facilitates the recording of normal ulnar SSEPs and MEPs (i.e., intact pathways).

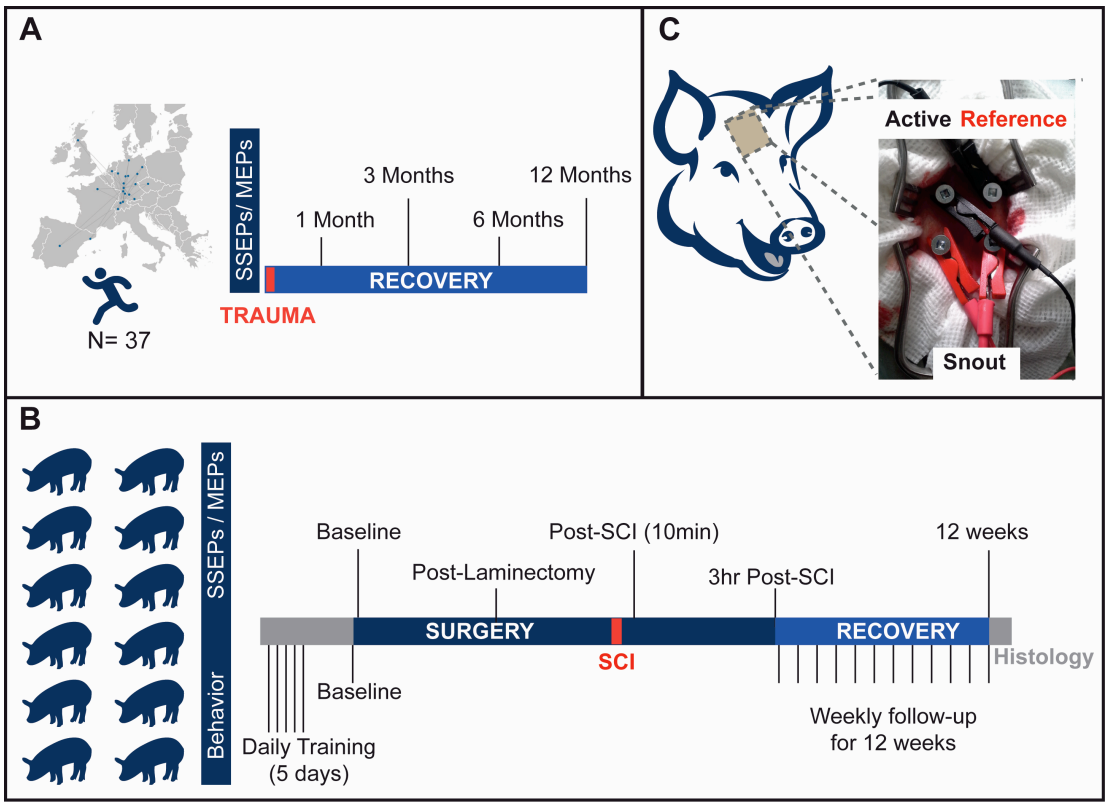


**Fig. 2: Design of Human and Animal Study**

**(A)** A total of 37 patients with spinal cord injury were enrolled in the study and meticulously followed for a year. Neurophysiological (SSEPs and MEPs) and behavioral assessments (sensory and motor score) were performed 1, 3, 6, and 12 months post-injury.

**(B)** Twelve female Yucatan miniature pigs underwent behavioral training for five days. Subsequently, the baseline measurement was conducted on the day before the surgery. Follow-up measurements were conducted weekly for 12 weeks starting seven days after the surgery allowing the animals to recover. On the day of surgery, animals were anaesthetized and intubated. Prior to the surgical procedures baseline SSEPs and MEPs were recorded. Following laminectomy, SSEPs and MEPs were recorded again in order to ensure that the spinal cord was not damaged. The spinal cord injury was then induced by contusing and compressing the spinal cord. SSEPs and MEPs were recorded immediately after the compression. All animals underwent follow up assessments of SSEPs and MEPs at 3 hours and 12 weeks post injury.

**(C)** Experimental set-up of the neurophysiological assessment in pigs. Four screws served as recording and stimulation electrodes (black = active, red = reference).To reduce the high impedance (i.e., due to the thickness of the pig's skull) the screws were drilled in to skull.

*SSEP: Somatosensory evoked potentials, MEP: Motor evoked potentials*

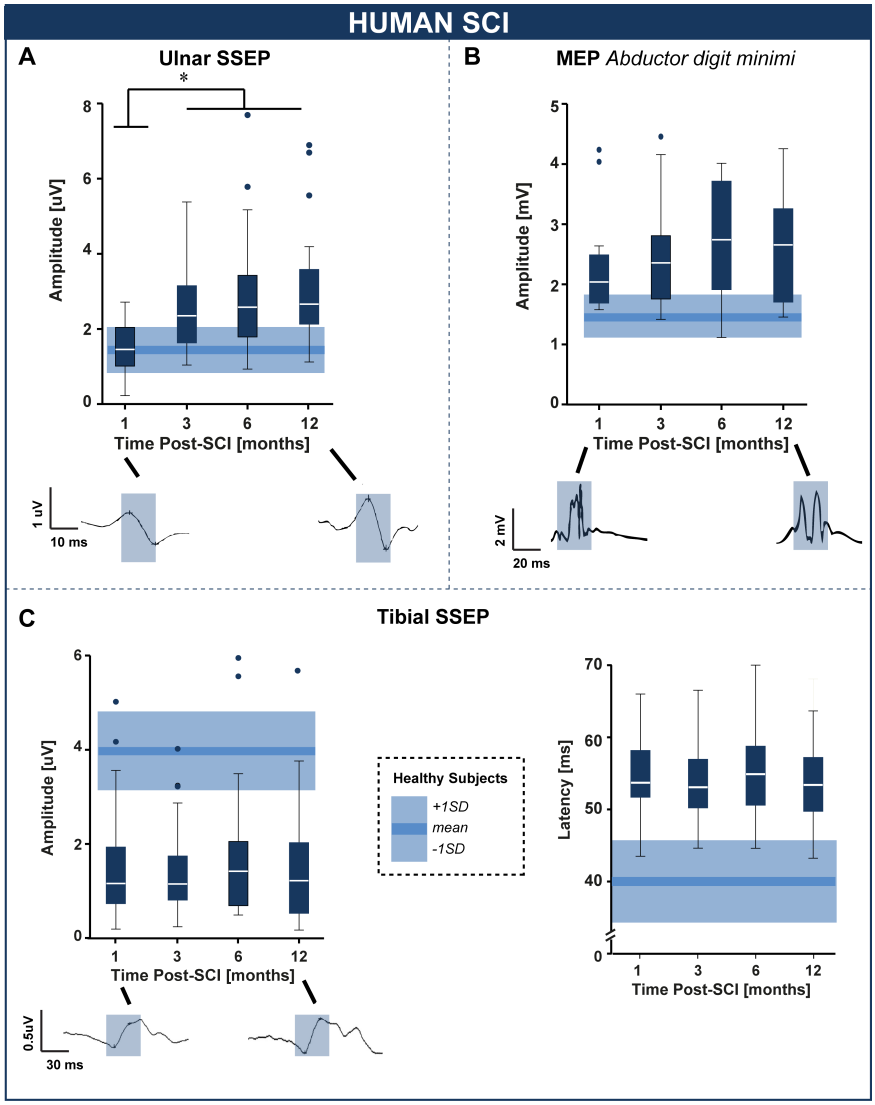


**Fig. 3: Neurophysiological Assessments in Human Patients**

**(A)** Human ulnar SSEPs amplitude increased over time independent of the injury severity.

**(B)** Motor evoked potentials (MEP) remained stable independent of the injury severity. In comparison to healthy controls, the MEP amplitude in patients was elevated

**(C)** Temporal progression tibial somatosensory evoked potentials (SSEP) in patients with spinal cord injuries. In comparison to healthy controls, the tibial SSEP remained impaired over time. Specifically, smaller amplitudes and prolonged latencies hallmarked the patient population.

*AIS Scale: A – no motor or sensory function preserved below the level of lesion, B –sensory but not motor function is preserved, C and D - Motor and sensory function is preserved, but impaired to variable degree* [65].

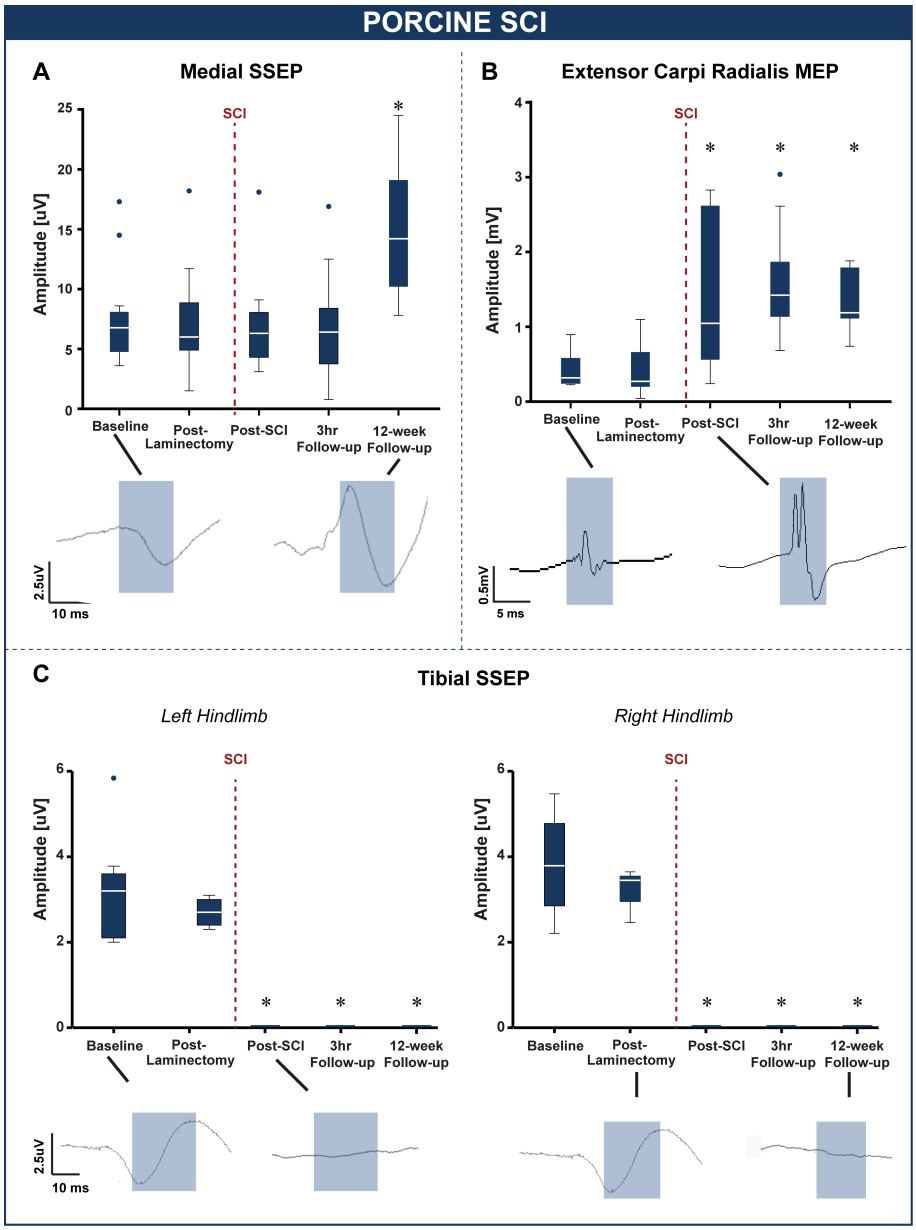


**Fig. 4: Neurophysiological Assessments in Yucatan Miniature Pigs**

**(A)** The medial SSEPs were not affected by the laminectomy and spinal cord injury and remained stable up to 3 hours post injury. An increase in amplitude was evident 12 weeks post injury alluding to potential reorganization of the sensory cortex.

**(B)** Motor evoked potentials (MEP) were unaffected by the laminectomy. However, the spinal cord injury induced a massive increase in MEP amplitude likely due to an increase in cortical excitability. The MEPs remained elevated over the follow-up period (12 weeks).

**(C)** Temporal progression of left and right tibial somatosensory evoked potentials (SSEP). The SSEPs remained stable after laminectomy confirming that the surgical procedure did not harm the spinal cord. Following the contusion, the SSEPs were abolished and did not recover over a period of 12 weeks reflecting the severity of the injury.

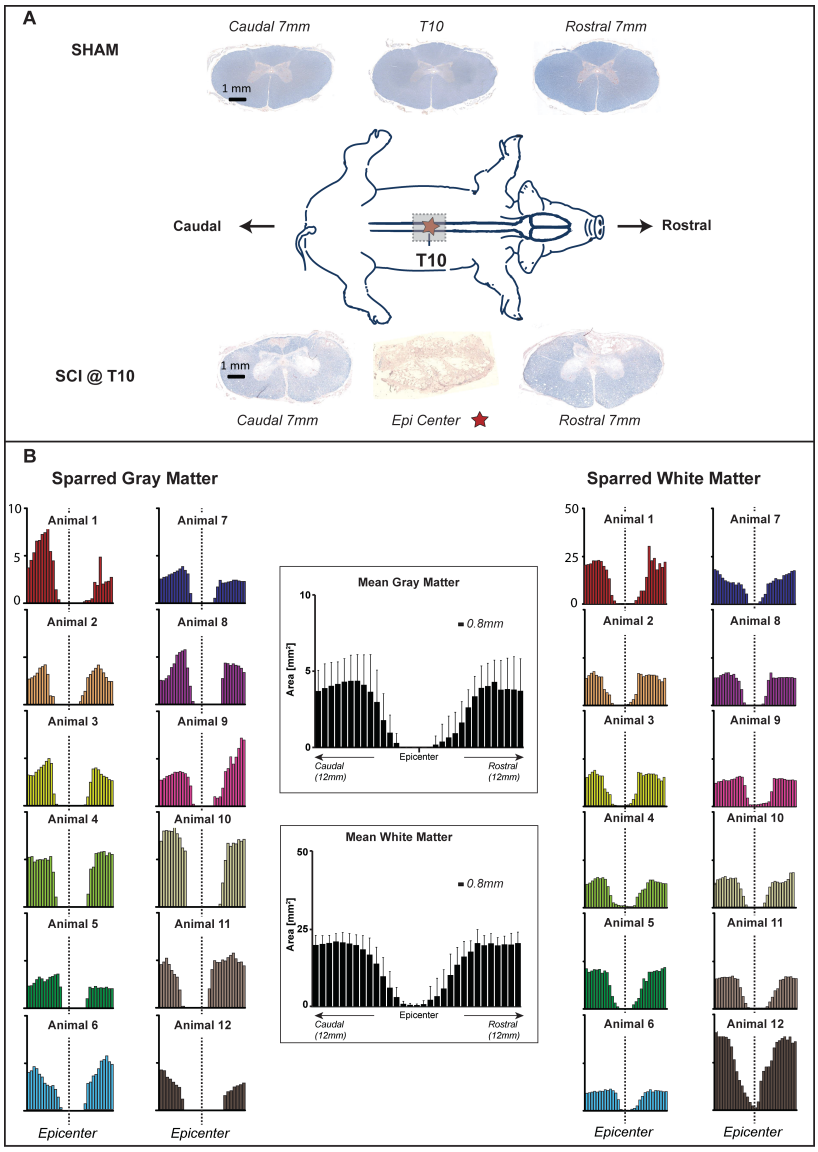


**Fig. 5: Immunohistochemistry Findings**

**(A)** Representative Eriochrome cyanine R–stained images of axially sectioned spinal cords. Cross-sectional sections of spinal cord tissue, at 12 weeks post-injury, stained with Eriochrome cyanine R to detect tightly packed myelin in SHAM (top row) and spinal-cord–injured pigs (bottom row). Scale bar = 1mm. SCI results in the loss of myelin, large cavitation and tissue disorganization extending away from the lesion epicenter.

**(B)** Total spared gray matter (left panel) and spared white matter (right panel) determined by area measurements taken from axial sections of spinal cord tissue 800 μm apart in all spinal cord injured animals.

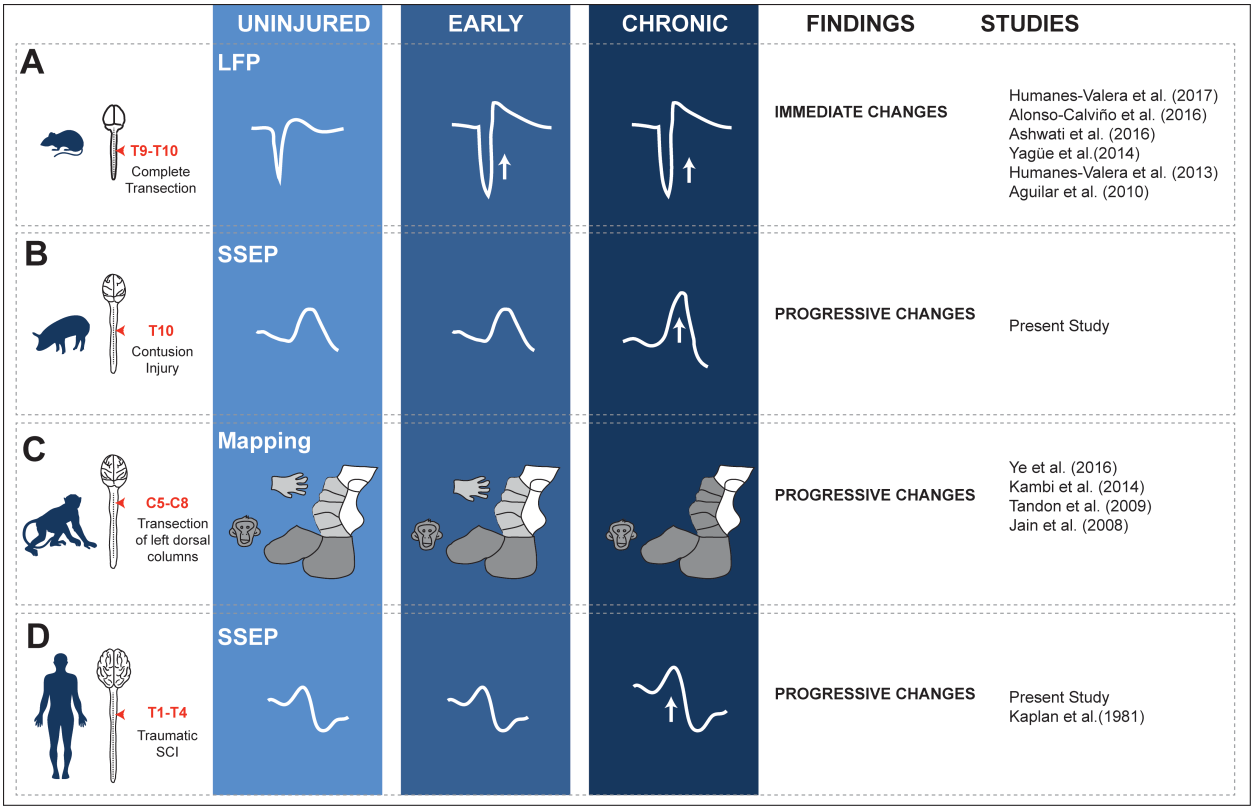


**Fig. 6: Cortical Reorganization across Species**

Reorganization of the sensory cortex occurs across species. **(A)** In rodents, alterations to the sensory cortex occur immediately after injury and remain unchanged over time. **(B)** Pigs, **(C)** monkeys, and **(D)** humans are characterized by progressive cortical reorganization. Apparent in the chronic phase of injury, cortical reorganization is characterized as increase in SSEP amplitude (i.e., in pigs and humans) as well as enlargement of cortical areas representing the intact body parts (monkey).

*LFP: Local field potential, SSEP: somatosensory evoked potentials, Mapping: Microelectrode mapping of cortical areas*

**Table 1: Demographics and neurophysiological data of all individuals with spinal cord injury**

| **Characteristics** | | |
|---|---|---|
| Total | | 37 |
| Sex, n(%) | | |
| Male | | 28 (75.7) |
| Female | | 9 (24.3) |
| Age at Injury | | |
| Mean (SD) | | 51.8 (18.9) |
| AIS at Baseline* | | |
| A | | 6 (16.2) |
| B | | 5 (13.5) |
| C | | 4 (10.8) |
| D | | 22 (59.5) |
| Neurological Level of Injury at Baseline | | |
| C8 | | 26 (70.3) |
| T1 | | 8 (21.6) |
| T2 | | 2 (5.4) |
| T3 | | 1 (2.7) |
| Neurophysiological Data | Mean (SD) | Mean (SD) |
| Motor evoked potentials (ADM) | *Amplitude [mV]* | *Latency [ms]* |
| 1 Month | 2.3 (0.8) | 23.6 (6.6) |
| 3 Months | 2.4 (1.3) | 22.9 (4.1) |
| 6 Months | 2.8 (0.4) | 24.0 (5.0) |
| 12 Months | 2.7 (0.6) | 22.6 (2.3) |
| Sensory evoked potentials (Tibial ) | *Amplitude [uV]* | *Latency [ms]* |
| 1 Month | 1.0 (1.3) | 54.9 (1.0) |
| 3 Months | 1.0 (0.9) | 55.1 (0.9) |
| 6 Months | 1.4 (1.2) | 55.5 (1.4) |
| 12 Months | 1.2 (1.1) | 54.2 (1.3) |
| Sensory evoked potentials (Ulnar) | | |
| 1 Month | 1.7 (0.8) | 26.2 (3.6) |
| 3 Months | 2.2 (0.9) | 26.6 (3.3) |
| 6 Months | 2.6 (0.8) | 26.1 (3.0) |
| 12 Months | 2.7 (0.9) | 26.3 (4.7) |

* = American Spinal Injury Association Impairment Scale: A, no sensory or motor function is preserved; B, sensory function is preserved below the level of the injury, but there is no motor function; C, motor function is preserved below the neurological level, and more than half of the key muscles below the neurological level have a muscle grade of < 3; D, motor function is preserved below the neurological level, and at least half of the key muscles below the neurological level have a muscle grade of ≥ 3.

ADM: abductor digit minimi

**Table 2:** Animal Characteristics, behavioral and neurophysiological outcomes

| Characteristics | | |
|---|---|---|
| **Total, n** | | 12 |
| Weight, kg | | |
| Range | | 18.5-25 |
| Age, days | | |
| Range | | 125 -142 |
| Anaesthesia (SCI induction), mean (SD) | | |
| Hydromorphone (mg/kg/hr) | | 0.1 (0) |
| Propofol (mg/kg/hr) | | 19.5 (1.4) |
| Ketamine (mg/kg/hr) | | 9.8(1.7) |
| Fentanyl (ug/kg/hr) | | 20.0 (2.8) |
| Anaesthesia (Follow-up), mean (SD) | | |
| Hydromorphone (mg/kg/hr) | | 0.1 (0) |
| Propofol (mg/kg/hr) | | 21.7 (5.5) |
| Ketamine (mg/kg/hr) | | 9.8 (1.6) |
| Fentanyl (ug/kg/hr) | | 19.8 (2.7) |
| Force applied for SCI [Kdynes] | | |
| Mean (SD) | | 2731 (514) |
| PTIBS, mean (SD) | | |
| Baseline | | 10 (0) |
| Follow – up: 1 Week | | 1.9 (1.0) |
| Follow – up: 2 Week | | 2.8 (1.2) |
| Follow – up: 3 Week | | 2.8 (1.1) |
| Follow – up: 4 Week | | 3.0 (0.9) |
| Follow – up: 5 Week | | 3.3 (0.7) |
| Follow – up: 6 Week | | 3.5 (1.4) |
| Follow – up: 7 Week | | 3.6 (1.2) |
| Follow – up: 8 Week | | 3.5 (1.2) |
| Follow – up: 9 Week | | 3.6 (1.2) |
| Follow – up: 10 Week | | 3.8 (1.2) |
| Follow – up: 11 Week | | 3.8 (1.0) |
| Follow – up: 12 Week | | 3.8 (1.0) |
| Motor evoked potentials *(Extensor Carpi Radialis)* | *Amplitude [uV], mean (SD)* | *Latency [ms], mean (SD)* |
| Baseline | 385 (249) | 21.4 (2.0) |
| Laminectomy | 474 (588) | 21.2 (2.4) |
| Post-SCI | 1108 (980) | 20.0 (1.3) |
| 3hr Follow-up | 1400 (916) | 20.8 (2.2) |
| 12 Weeks Follow-up | 1296(894) | 20.9 (2.1) |
| Sensory evoked potentials (Median right) | | |
| Baseline | 7.6 (4.2) | 17.6 (2.5) |
| Laminectomy | 7.2 (4.7) | 18.2 (2.5) |
| Post-SCI | 7.0 (4.2) | 17.6 (1.9) |
| 3hr Follow-up | 6.9 (4.7) | 17.8 (2.3) |
| 12 Weeks Follow-up | 14.7 (5.3) | 17.8 (1.2) |

| | | |
|---|---|---|
| Sensory evoked potentials (Tibial right) | | |
| Baseline | 3.8 (1.6) | 27.9 (2.0) |
| Laminectomy | 3.5 (0.7) | 26.0 (2.4) |
| Post-SCI | 0 (0) | 0 (0) |
| 3hr Follow-up | 0 (0) | 0 (0) |
| 12 Weeks Follow-up | 0 (0) | 0 (0) |
| Sensory evoked potentials (Tibial left) | | |
| Baseline | 3.4 (1.7) | 26.7 (1.6) |
| Laminectomy | 2.7 (0.4) | 25.7 (1.8) |
| Post-SCI | 0 (0) | 0 (0) |
| 3hr Follow-up | 0 (0) | 0 (0) |
| 12 Weeks Follow-up | 0 (0) | 0 (0) |

PTIBS: Porcine Thoracic Injury Behavioral Scale

Appendix 2

Original Article

# Changes in Pressure, Hemodynamics, and Metabolism within the Spinal Cord during the First 7 Days after Injury Using a Porcine Model

Femke Streijger,[1] Kitty So,[1] Neda Manouchehri,[1] Jae H.T. Lee,[1] Elena B. Okon,[1] Katelyn Shortt,[1] So-Eun Kim,[1] Kurt McInnes,[1,2] Peter Cripton,[1,2] and Brian K. Kwon[1,3]



## Abstract

Traumatic spinal cord injury (SCI) triggers many perturbations within the injured cord, such as decreased perfusion, reduced tissue oxygenation, increased hydrostatic pressure, and disrupted bioenergetics. While much attention is directed to neuroprotective interventions that might alleviate these early pathophysiologic responses to traumatic injury, the temporo-spatial characteristics of these responses within the injured cord are not well documented. In this study, we utilized our Yucatan mini-pig model of traumatic SCI to characterize intraparenchymal hemodynamic and metabolic changes within the spinal cord for 1 week post-injury. Animals were subjected to a contusion/compression SCI at T10. Prior to injury, probes for microdialysis and the measurement of spinal cord blood flow (SCBF), oxygenation (in partial pressure of oxygen; $PaPO_2$), and hydrostatic pressure were inserted into the spinal cord 0.2 and 2.2 cm from the injury site. Measurements occurred under anesthesia for 4 h post-injury, after which the animals were recovered and measurements continued for 7 days. Close to the lesion (0.2 cm), SCBF levels decreased immediately after SCI, followed by an increase in the subsequent days. Similarly, $PaPO_2$ plummeted, where levels remained diminished for up to 7 days post-injury. Lactate/pyruvate (L/P) ratio increased within minutes. Further away from the injury site (2.2 cm), L/P ratio also gradually increased. Hydrostatic pressure remained consistently elevated for days and negatively correlated with changes in SCBF. An imbalance between SCBF and tissue metabolism also was observed, resulting in metabolic stress and insufficient oxygen levels. Taken together, traumatic SCI resulted in an expanding area of ischemia/hypoxia, with ongoing physiological perturbations sustained out to 7 days post-injury. This suggests that our clinical practice of hemodynamically supporting patients out to 7 days post-injury may fail to address persistent ischemia within the injured cord. A detailed understanding of these pathophysiological mechanisms after SCI is essential to promote best practices for acute SCI patients.

**Keywords:** blood flow; L/P ratio; microdialysis; oxygenation; porcine model; pressure; spinal cord injury

## Introduction

Acute trauma to the spinal cord can result in devastating neurologic impairment for which there currently remains few treatment options that can be offered to improve neurologic function. While the primary damage to the spinal cord occurs at the time of mechanical impact (e.g., from a motor vehicle accident, fall from height), early treatment approaches for the acutely injured patient aim to mitigate the secondary pathophysiologic processes that are triggered within the injured cord. These include vascular disruption, intraparenchymal hemorrhage, vasospasm, impaired autoregulation, and vasogenic edema as a consequence of blood–spinal cord barrier breakdown.[1] These combined responses can lead to impaired spinal cord perfusion with resultant ischemia, hypoxia, and energy dysfunction, of which all can negatively impact spared neural tissue at and around the injury site.[2] Therefore, current clinical practice guidelines encourage aggressive hemodynamic resuscitation and elevation of mean arterial blood pressure (MAP) to 85–90 mm Hg for the first 7 days post-injury.[3–6] Recent clinical evidence suggests that the elevation of MAP and the avoidance of hypotension are indeed beneficial for neurologic recovery in acute spinal cord injury (SCI) patients.[7]

Given that the hemodynamic management of acute SCI appears to represent an opportunity to influence neurologic outcome, an understanding of the post-traumatic alterations in spinal cord perfusion and the downstream metabolic consequences is essential. Our current understanding of the spatial and temporal dynamics of the changes in perfusion within the acutely injured spinal cord is

[1]International Collaboration on Repair Discoveries (ICORD), [2]Departments of Mechanical Engineering and Orthopedics, [3]Vancouver Spine Surgery Institute, Department of Orthopedics, University of British Columbia, Vancouver, British Columbia, Canada.

limited. There is a considerable body of pre-clinical literature that has provided fundamental insights into the changes in spinal cord blood flow (SCBF) after traumatic injury.[2,8–12] However, most of these studies employ rodent models and induce injury to the spinal cord with extradural clip compression for 1 min up to 40 min, at most.[10–13] Extrapolating these data to the human condition is therefore challenging where the spinal cord is much larger, compression can be sustained for many hours, and the typical period of hemodynamic support extends for a full week post-injury.

Further, while much of the pre-clinical literature has focused on alterations in SCBF, it is ultimately desirable to understand the subsequent downstream metabolic consequences of these changes within the areas of potentially vulnerable spinal cord tissue. As the balance between SCBF and metabolic demand for oxygen influences whether the tissue is hypoxic or not, monitoring SCBF alone may not provide a complete assessment of the metabolic insult within the injury penumbra. As such, simultaneously measuring spinal cord oxygenation and downstream metabolic changes in addition to SCBF would allow for a more comprehensive assessment of the tissue hemodynamics. To our knowledge, such a combined approach of directly measuring SCBF, oxygenation, pressure, and metabolites from the spinal cord parenchyma continuously for days after injury has not been previously reported.

In previous work, we used intraparenchymal spinal cord microdialysis in our porcine model of SCI to measure the extent to which energy-related substrates such as lactate, pyruvate, and glucose were affected for the first 4 h post-injury.[14] Our data reveal significant and prolonged tissue ischemia and hypoxia at the injury site after contusion-compression SCI, marked by a dramatic increase in lactate/pyruvate (L/P) ratio (> 700% of pre-injury levels), with a concurrent fall in glucose levels (< 50%) within the first 20 min post-injury.[14] It also was evident that the observed metabolic changes had not plateaued or normalized at the conclusion of the experiment 4 h post-injury. Therefore, in the present study, we extend these observations by continuing these intraparenchymal microdialysis measurements for a full 7 days post-injury, while also measuring SCBF, oxygenation (in partial pressure of oxygenation; $PaPO_2$), and hydrostatic pressure to investigate the relationship between these important physiologic variables.

## Methods

All animal protocols and procedures employed in this study were approved by the Animal Care Committee of the University of British Columbia and were compliant with the policies of the Canadian Council of Animal Care.

### *Animals and housing*

Female miniature Yucatan pigs (Sinclair Bio-resources, Columbia, MO) were transported to our animal facility 5 weeks before surgery. Upon arrival, the animals were housed in groups of four in an indoor pen bedded with sawdust and toys (chains, balls) with access to an adjoining outdoor pen. Animals were given water *ad libitum* and fed 1.5% of their body weight twice a day (Mazuri Mini-Pig Youth; PMI Nutrition International, Brentwood MO). Each pig was individually handled for at least 15 min daily to improve the comfort level with human contact.

### *Porcine model of SCI*

Prior to the day of surgery, animals were fasted for 12 h. Tracheal intubation and mechanical ventilation was performed as described previously.[15,16] Anesthesia was maintained with a combination of isoflurane (0.5% in 100% $O_2$) and propofol (8–20 mg/kg/h; Baxter, Allison, Ontario). All animals received ketoprofen (3 mg/kg) via intravenous administration and fentanyl (15–30 $\mu$g/kg/h; Sandoz Canada, Boucherville, Quebec) delivered via continuous rate infusion. After a surgical plane of anesthesia was reached, a skin incision was made along the dorsal midline of the thoracic region of each animal. Using electro-cautery (Surgitron Dual Frequency RF/120 Device; Ellman International, Oceanside, NY), the semispinalis, multifidus, and longissimus lumborum muscles were separated from the dorsal spinous processes and laminae. A T9 to T13 laminectomy was performed and widened to expose the dura and spinal cord with sufficient clearance for sensor insertion and weight-drop injury.

The SCI was delivered by a weight drop impactor device, which was securely fixed to the spine using an articulating arm (660; Starrett, Athol, MA) mounted via bilaterally inserted T6 and T8 pedicle screws. This arm enabled the guide-rail to be precisely positioned and aligned, allowing for the impactor to fall straight vertically onto the exposed dura and cord at T10. The tip of the impactor (diameter, 0.953 cm) was outfitted with a load cell (LLB215; Futek Advanced Sensor Technology, Irvine, CA) to record the force at impact. The guide rail was equipped with a Balluff Micropulse linear position sensor (BTL6-G500-M0102-PF-S115; Balluff Canada Inc., Mississauga, Ontario) to record the impactor position from 10 cm above the impact (for calculation of impact velocity and cord displacement). A custom controller was used to operate the device and filter the force and position data was collected with the simultaneous USB DAQ module (DT9816-S; Data Translation Inc., Marlboro, MA). A LabVIEW (National Instruments, Austin, TX) program enabled remote operation of the device and real-time data collection feedback.

Immediately after the weight-drop contusion injury (weight, 50 g; height, 50 cm), sustained compression was maintained on the contused spinal cord for 1 h by placing an additional 100 g weight onto the impactor (150 g total). The weight of the impactor (50 g), height of the weight drop (50 cm), and duration of compression with the additional 100 g weight (1 h) were chosen so as to replicate the injury parameters of our previous study in which we performed similar intraparenchymal microdialysis measurements for 4 h post-SCI.[14] Our current experiment was intended to extend the findings of this previous study.

### *Insertion of the intraparenchymal blood flow/$O_2$, pressure, and microdialysis probes*

To consistently insert the monitoring probes into a desired location within the spinal cord and to maintain their position for the duration of the experiment, a custom-made sensor holder was created (Fig. 1). The sensor holder was attached rigidly to the spine via bilateral T9, T11, T12, and T14 pedicle screws (Select Multi Axial Screw; Medtronic, Minneapolis, MN) and 3.5 mm titanium rods (Medtronic). The location of the sensor holder was locked in place by sliding the device over the rod and adjusting the height of the pedicle screws. Additional transverse connecting bridges were fixed between two polyaxial pedicle screws to produce a stable, rigid construct. Six custom-made introducers with a lumen wide enough to fit one sensor/probe were inserted through precision-drilled holes in the sensor-holder (holes were drilled at a 45-degree angle relative to the holder; Fig. 1), entering the dura at approximately 1.2 and 3.2 cm from the center of the intended impact. Subsequently, the sensors were guided through the introducers and advanced another 0.2 cm, placing the sensors in the ventral aspects of the white matter (Fig. 2). The distance between adjacent tip locations was 0.5–1.0 mm. The final location of the tip of the sensors were situated approximately 0.2 cm and 2.2 cm away from the edge of intended impact location. Ultrasound imaging (L14-5/38, 38 mm linear array probe, Ultrasonix RP; BK Ultrasound, Richmond, British Columbia) was utilized to verify accurate positioning of sensors and probes into the cord (Fig. 2). To prevent

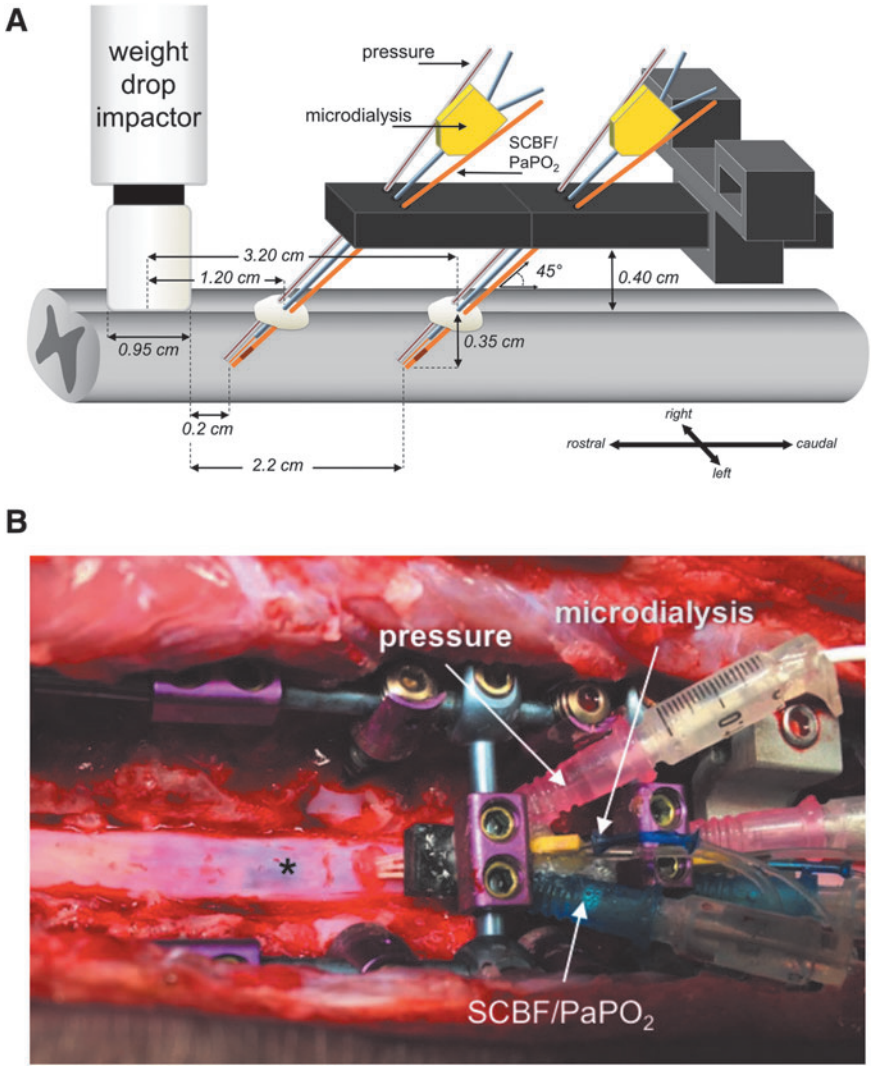


**FIG. 1.** Intraparenchymal monitoring set-up for inserting and securing SCBF/$PaPO_2$, pressure, and microdialysis probes within the spinal cord. This figure illustrates the fixation device, which is secured rigidly via the pedicle screw/rod construct to the spinal column. The device has three independently drilled channels through which the SCBF/$PaPO_2$ (left), pressure (right), and microdialysis (middle) probes are inserted. The probes penetrate the dura 1.2 cm and 3.2 cm caudal from the anticipated epicenter of the contusion impact and are advanced approximately 14 mm at a 45° angle. As the impactor is 0.95 cm in diameter, the final location of the sensor tips are approximately 0.2 cm and 2.2 cm away from the edge of the impactor. *Spinal cord injury hemorrhage. SCBF, spinal cord blood flow; $PaPO_2$, partial pressure of oxygen. Color image is available online at www.liebertpub.com/neu

cerebrospinal fluid (CSF) leakage, cyanoacrylate glue was applied to the dural surface where the catheters entered. After sensor insertion, a 2-h period was given to allow ''stabilization'' before recording the ''baseline'' samples for a period of 60 min prior to SCI.

### *Measure of intraparenchymal blood flow and $PaPO_2$*

For measurement of blood flow and oxygen, we utilized a single multi-parameter probe that at the tip contains both a sensor for measuring flow and another for measuring $PaPO_2$. This probe with a tip diameter of 450 $\mu$m (NX-BF/OF/E; Oxford Optronix, Oxford, UK) was connected to the OxyLab/OxyFlo combined channel monitor (OxyLab: Oxford Optronix) with LabChart Pro software for interpretation (ADInstruments, Colorado Springs, Colorado,). $PaPO_2$ was measured by a fluorescence quenching technique, which monitors the mean time between photon absorption and emission of the oxygen-sensitive fluorescent ruthenium lumiphor dye after being excited by a short pulse of light (luminescence lifetime). In the presence of oxygen, the fluorescence lifetime is quenched proportionally to the oxygen concentration. The OxyLab system measures the reduced lifetime of luminescence of the reflected signal and displays a value for $PaPO_2$ in mm Hg. Since the luminescence-based oxygen sensing technique is sensitive to temperature changes, a thermocouple transducer is incorporated into the sensor to correct for temperature variations within its operating range of 30–44°C. Blood flow is determined via laser-Doppler flowmetry (LDF) where light from the probe tip is projected into the tissue, scattered, then reabsorbed by a sensor. Only the laser light backscattered from moving cells undergoes a Doppler shift, which creates Doppler frequencies at the detectors to produce a voltage output that can be interpreted as blood flow by the OxyFlo monitor (in arbitrary perfusion units, BPU). The numeric calculation of LDF is dependent on the relative concentration of local red blood cells in the tissue and the velocity.

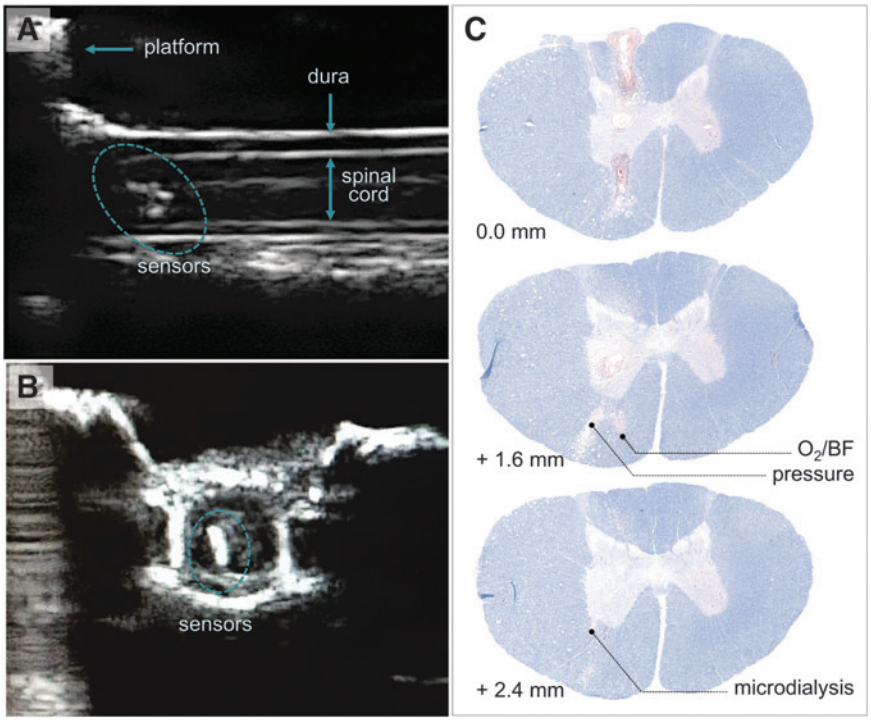


**FIG. 2.** Evaluation of intraparenchymal probe position with ultrasound and histologic methods. Representative ultrasound images in both **(A)** midsagittal and **(B)** axial planes showing the location of the probes within the parenchyma of the spinal cord at the time of surgery. Each probe was advanced through the spinal cord at a 45° angle. The dorso-ventral diameter of the porcine spinal cord was ~5.5 mm at this level (T10); the diameter of the subarachnoid space was ~9 mm. **(C)** Eriochrome Cyanine R–stained spinal cord section from 7-day post-injury revealed that the final locations of the probe tips were in the ventral aspects of the white matter. In this example, the tips of the SCBF/$PaPO_2$ and pressure probes were situated +1.6 mm from the initial point of entry (0.0 mm); the tip of the microdialysis probe was situated +2.4 mm rostral from the initial point of entry. In all animals studied, the anterior-posterior distance between adjacent tip locations ranged between 0.5 and 1.0 mm. SCBF, spinal cord blood flow; $PaPO_2$, partial pressure of oxygen. Color image is available online at www.liebertpub.com/neu

### *Intraparenchymal pressure measurement*

Spinal cord pressure was characterized using custom-manufactured fiber optic pressure transducers (FOP-LS-NS-1006A; FISO Technologies Inc., Harvard Apparatus, Quebec) with a sensor tip diameter of 333 $\mu$m. This technology has been used in previous studies to measure CSF pressure *in vivo* in spinal cord injured pigs,[17] intracranial pressure during blast and shock waves in rats[18,19] and pigs,[20] pressure in the nucleus of the intervertebral discs,[21] and was recently evaluated for monitoring pressure in spinal cord tissue.[22]

The sensor tip is comprised of two parallel reflecting mirrors on either side of an optical cavity. The first mirror is semi-reflective and the second is a flexible membrane. As pressure is applied, the membrane deflects, reducing the cavity length. The reduced cavity lengths cause phase shifts in the reflected light, which are distinguished by a detector. Transducers are calibrated in such way that each cavity length corresponds to a specific pressure value, with the transducers being capable of measuring pressure changes of ±300 mm Hg, with a resolution of ±0.3 mm Hg. Transducers were connected to a chassis-mounted signal conditioner module (EVO-SD-5/FPI-LS-10; FISO Technologies Inc., Harvard Apparatus) with internal atmospheric pressure compensation, which is particularly valuable for long-term animal studies. The data was acquired digitally through the Evolution software (FISO Technologies Inc., Harvard Apparatus) at a frequency of 1 Hz.

### *Microdialysis*

Microdialysis probes (CMA11, CMA Microdialysis; Harvard Apparatus) with an outer diameter of 380 $\mu$m, 2 mm membrane length, and a 6-kDa cutoff were used to sample the extracellular fluid for energy related metabolites. Probes were continuously perfused with artificial CSF (Perfusion Fluid CNS, CMA Microdialysis; Harvard Apparatus) using a subcutaneous implantable micro-pump at a flow rate of 0.5 $\mu$l/min (SMP-200, IPrecio, Alzet Osmotic Pumps; Durect Corporation, Cupertino, CA). Dialysates were collected every 15 min in micro tubes, capped, and frozen on dry ice from the beginning of the baseline period to 6 h post-injury, and then every 12 h, providing a sample volume of 7.5 $\mu$L sufficient for the exploration of five metabolites (lactate, pyruvate, glucose, glutamate, and glycerol). Samples were analyzed within a week of collection using the ISCUSflex Microdialysis Analyzer (M Dialysis, Stockholm, Sweden). Measured sample concentrations below the manufacturer's indicated linear range of the assays were replaced with the minimum linear range value.

### *Post-operative recovery and continuous monitoring*

Anesthesia and mechanical ventilation with 100% oxygen were stopped at 4 h after SCI and the animal was extubated on room air. Between animals there was a 5–10-min variability in anesthesia duration. Subsequently within 2 h (i.e., between 4–6 h post-injury), animals were returned to their respective recovery enclosures for 7 days.

Post-surgical pain control was managed with fentanyl via constant rate infusion (2–12 mcg/kg/h intravenously) for the first 7 days after surgery. Animals were given tramadol (1–2 mg/kg; orally), and received enrofloxacin (5mg/kg; subcutaneously) daily for at least 3 days as an antibiotic, and ketoprofen (3 mg/kg;

intramuscularly) once a day for 3 days as an anti-inflammatory agent. Urinary catheters remained in place until the animals were able to reflexively empty their bladders, usually within 7–10 days. If fecal production was low and the animals appeared to be experiencing stasis in the gastrointestinal tract, a constant rate infusion of metaclopramide (5 mg/mL at 0.01–0.02 mg/kg/h) and lactulose (5 mL) was administered. Sucralfate (5 mL) was given if an animal experienced anorexia and/or bloating.

Sensor cables were kept away from the animal's reach using a custom-designed counter-balanced lever system, and the microdialysis collection lines and tubes were securely placed into a harness worn by the animal (Fig. 3). This set-up allowed for continuous recording and sampling over 7 days without the need to disconnect and reconnect the monitoring wires.

### *Eriochrome Cyanine R staining*

Spinal cord segments were fixed in 4% PFA and cryoprotected using graded concentrations of sucrose (6, 12, 24% sucrose in 0.1 M Phosphate Buffer each for 48 h). Tissue was then transversely cut in 20-$\mu$m sections and stained with Eriochrome Cyanine R as described previously.[15,16,23] The distribution of spared white and grey matter was mapped using digital color images taken at 800-$\mu$m intervals throughout the lesion site (Zeiss AxioImager M2 microscope) and analyzed using Zen Imaging Software (Carl Zeiss Canada Ltd., Toronto, Ontario). The extent of spared white matter and gray matter were calculated as the percentage of total area of the spinal cord (i.e., area within the tracing of spinal cord perimeter), with lesion epicenter located centrally.

### *Data analysis*

SCBF and $PaPO_2$ were recorded continuously at a sampling rate of 10 and 1 Hz respectively during baseline recording and for 3 h after SCI. Thereafter, the sampling rate for $PaPO_2$ was reduced to 1/60 Hz, as the sensor carries only a limited supply of the ruthenium lumiphor. To mitigate movement artifacts in the oxygenation and blood flow data, a post-processing filter was applied (smoothing type, median filter; window width, 601 samples/1 min of sampling). For SCBF, $PaPO_2$, and pressure data, values were averaged over 15-min intervals for the first 24 h and into 60-min bins after the first 24 h. Microdialysis samples were collected every 15 min from the beginning of the baseline period to 6 h post-injury. After 6 h, dialysates were taken in duplicate at 15-min intervals every 12 h. These duplicate values were averaged for each time-point. The delay from microdialysis catheter tip to collecting vial was 12 mins, and this was accounted for when analyzing the results. The lactate to pyruvate (L/P) ratio was calculated from the measured values of lactate and pyruvate concentrations. To account for absolute differences in the baseline recordings, all values were expressed as a percentage change from baseline (% from baseline) as a function of time (min). Results are expressed as mean values (± standard error of the mean), with correlations between parameters determined using Spearman correlation coefficients with Bonferroni correction (GraphPad Prism 6).

## Results

### *Injury parameters*

Eight animals received a contusion SCI by dropping a 50 g weight from a 50 cm height at the T10 level of the spinal cord followed by 1 h of compression (150 g total weight). The maximum impact force applied to the exposed spinal cord measured at the tip of the impactor was on average 5443 ± 438 kdynes (Table 1). The impactor tip traveled 6.36 ± 0.30 mm from initial contact with the exposed dura with a velocity of 2736 ± 102 mm/sec at impact. Such contusion-compression injury resulted in a compete loss of gray and white matter at center of the impact (T10), with loss of white and gray matter at distances up to 10–13 mm from the epicenter in both rostral and caudal directions (Fig. 4).

### *Post-injury changes in intraparenchymal pressure, blood flow, $PaPO_2$, and pressure*

At the 0.2-cm position (i.e., the more proximal of the two sensor insertion points), intraparenchymal spinal cord pressure, which started at 10.4 ± 1.0 mm Hg drastically increased ~370% (an absolute difference of about 35 mm Hg) of baseline values and remained elevated while residual compression remained on the cord (Fig. 5A). Following decompression, the pressure immediately dropped back to slightly above baseline values. After this transient fall, the pressure gradually increased once again to reach a maximum of ~220% of baseline (an absolute difference of about 14 mm Hg) at 4.5 h post-SCI. After 15 h, a slight decrease in pressure was observed, although values remained above baseline levels for the 7 days of observation (~150%; an absolute difference of about 5 mm Hg).

SCBF and $PaPO_2$ levels fell rapidly below baseline levels following SCI and while the spinal cord remained compressed (Fig. 5B, 5C). Following decompression, both SCBF and $PaPO_2$

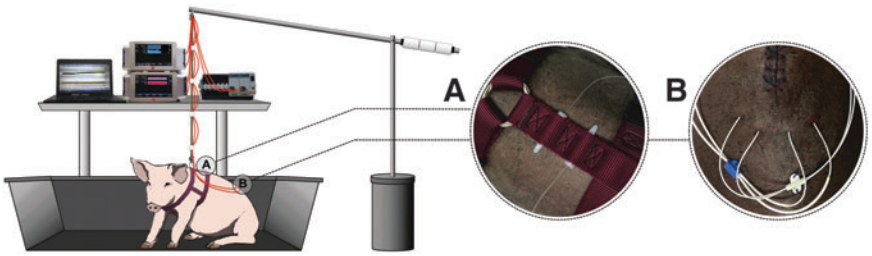


**FIG. 3.** Post-operative set-up for continuous microdialysis sampling and monitoring of SCBF/$PaPO_2$ and pressure for a total of 7-days after SCI. SCBF/$PaPO_2$, pressure, and microdialysis probes were inserted into the spinal cord 0.2 and 2.2 cm away from the edge of the initial impact **(A)** To achieve microdialysis samples over 7 days, we used a miniature infusion pump (iPRECIO) for dialysate inflow that was implanted and left within the animal. The outflow tubing for each microdialysis catheter was tunneled percutaneously out to a collection vial (*) and secured via a harness to the upper thoracic region of the animal. **(B)** The SCBF/$PaPO_2$ and pressure probes were also tunneled percutaneously and attached to a lead, connecting the harness to the counter-balance lever system that was positioned above the center of the pen. The lever system with counterweights ensured the sensor wires were held out of the animals' reach at all times so that they could not be chewed on or otherwise disrupted, yet still allowed free movement of the animals within the enclosure. SCBF, spinal cord blood flow; SCI, spinal cord injury; $PaPO_2$: partial pressure of oxygen. Color image is available online at www.liebertpub.com/neu

Table 1. Measures of Age, Body Weight, and Injury

| *Age (months) [Average ± SEM]* | *Body weight (kg) [Average ± SEM]* | *Max force (kdynes) [Average ± SEM]* | *Displacement (mm) [Average ± SEM]* | *Impact velocity (mm/sec) [Average ± SEM]* |
|---|---|---|---|---|
| 4.57 | 23.0 | 6004 | 6.75 | 2935 |
| 4.77 | 23.0 | 5310 | 6.11 | 2835 |
| 5.23 | 24.0 | 5128 | 5.63 | 2542 |
| 4.40 | 24.5 | 5048 | 7.33 | 2911 |
| 3.83 | 22.5 | 5227 | 6.93 | 2826 |
| 4.00 | 23.5 | 8075 | 6.92 | 2917 |
| 4.00 | 23.5 | 3712 | 4.73 | 2091 |
| 4.47 | 20.0 | 5039 | 6.47 | 2838 |
| **[4.4 ± 0.2]** | **[23.0 ± 0.5]** | **[5443 ± 438]** | **[6.36 ± 0.30]** | **[2736 ± 102]** |

SEM, standard error of the mean.



recovered slightly in the first few minutes, but remained below baseline levels for the next 3 h (~25% of baseline for $PaPO_2$ and ~60% of baseline for SCBF). Thereafter, SCBF showed a modest but continuous increase with time to about 150% of the baseline value. At around 4–6 h post-injury, the anesthesia and mechanical ventilation with 100% oxygen were stopped, and the animal was extubated on room air. This coincided with increased spinal cord perfusion and a dramatic drop in $PaPO_2$ levels to ~8% of baseline. Starting at around 24 h post-injury, the SCBF steadily increased to about 200% of baseline at the 7-day post-injury time-point. Despite this increase in SCBF, the $PaPO_2$ levels stayed fairly constant and remained at 8–10% of baseline values until the end of the study.

At the 2.2-cm position (i.e., the more distal of the two sensor positions), only modest changes in SCBF, $PaPO_2$, and pressure were observed following traumatic contusion, during sustained compression, and after decompression (Fig. 6). Notably, $PaPO_2$ dropped drastically after anesthesia and mechanical ventilation were discontinued (~4 h post-SCI). Thereafter, $PaPO_2$ continued to decrease for up to 48 h post-injury, after which it leveled off and remained low (Fig. 6). There was also a slight increase in intraparenchymal pressure at 4 h post-injury and remained elevated (albeit very slightly) for the duration of the experiment.

### *Post-injury changes in microdialysis markers*

Time-dependent post-injury changes in microdialysis markers of excitotoxicity and membrane damage (glutamate and glycerol) and energy metabolism (glucose, lactate, and pyruvate) are summarized in Figure 7 and Figure 8, respectively.

At the 0.2-cm position, a sharp increase in glutamate levels was detected, reaching a peak increase of ~6000% within 15 min after contusion (Fig.7A; solid circles) and rapidly declined thereafter. This decreasing trend continued for another 2–3 h after decompression when glutamate reached high steady-state levels of

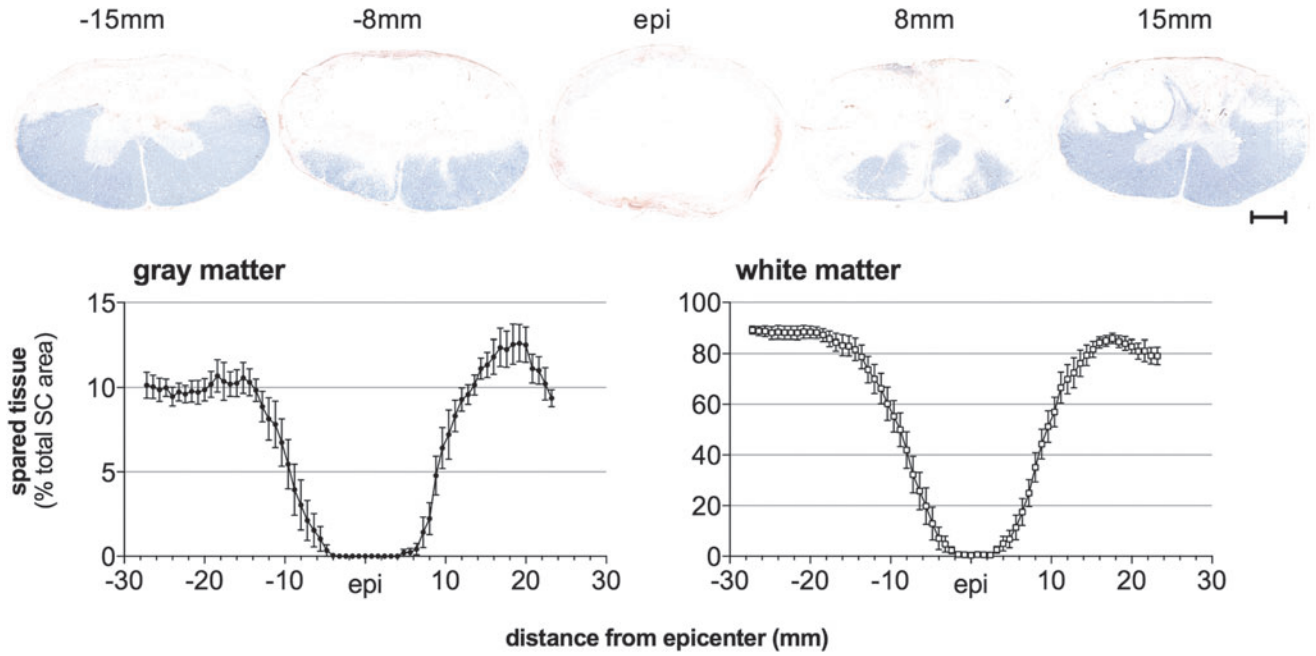


**FIG. 4.** Spared tissue analyses of Eriochrome Cyanine R–stained spinal cords. Spared gray and white matter determined by area measurements taken from axial sections of porcine spinal cord tissue 800 $\mu$m apart. Our T10 50-g/50-cm contusion injury model followed by 1 h of compression resulted in significant tissue damage extending 10–13 mm away from the lesion epicenter (''epi'') in both rostral-caudal directions. The values are means ± standard error of the mean. Scale bar: 1 mm. Color image is available online at www.liebertpub.com/neu

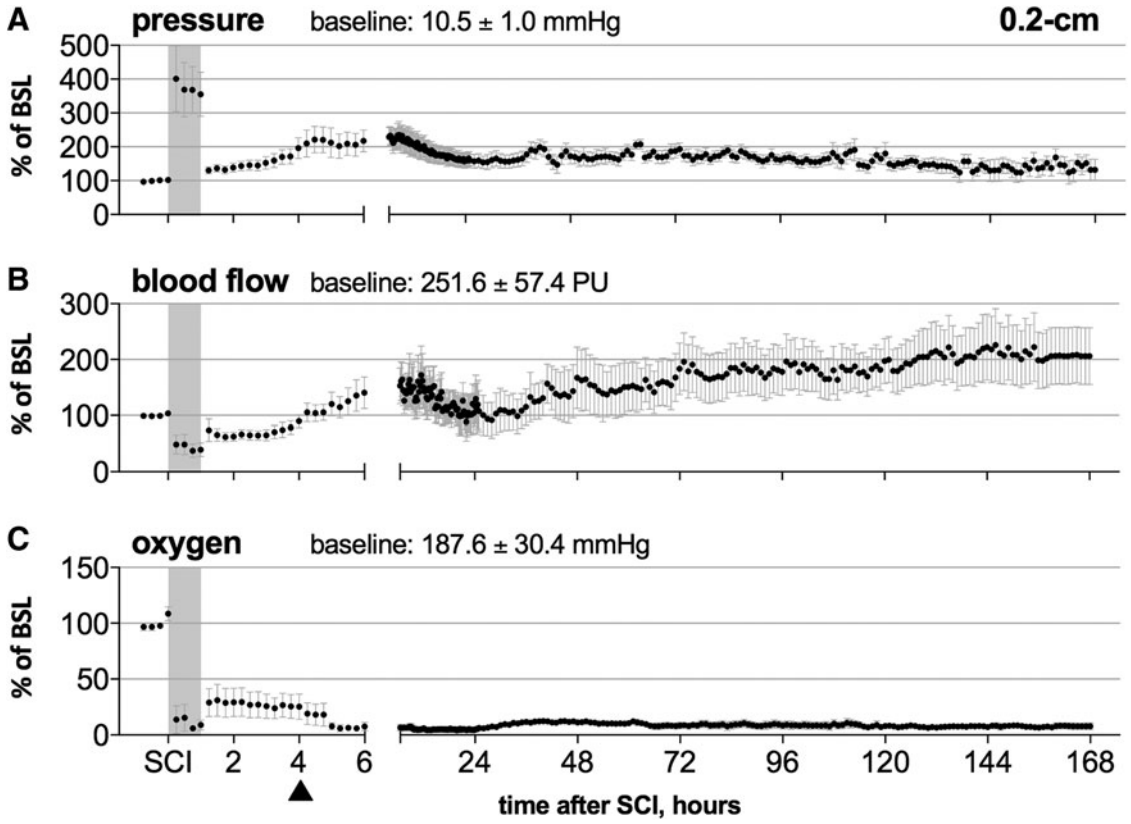


**FIG. 5.** Dynamic changes (%Δ) of blood flow, partial pressure of oxygen and pressure in the penumbra (0.2 cm) of the traumatic spinal cord injury site. The percentage change (%Δ) is calculated using an average of 60 min of baseline before SCI. **(A)** Intraparenchymal spinal cord pressure, **(B)** spinal cord blood flow (SCBF), **(C)** and partial pressure of oxygen ($PaPO_2$) responses before, during and after 1 h spinal cord contusion/compression (gray shading). SCI resulted in a prompt increase in cord pressure and a loss of SCBF with a critical reduction in $PaPO_2$. Following decompression, spinal cord pressure decreased sharply; however, it increased again within hours and remained consistently elevated for days. Within hours of decompression, SCBF restored to within baseline levels and continued to increase up to 200% above baseline levels by Day 7. Decompression only partially restored $PaPO_2$ and throughout the 7-day monitoring period seemed entirely unaffected. The dashed line at the 4 h post-SCI mark (▲) represents the discontinuation of anesthesia and ventilation at the end of the surgical procedure. BSL, baseline; SCI, spinal cord injury.

~1400% that persisted for several days. Glycerol levels exhibited a peak value of 272% ± 48.2 within 30 min after contusion and remained around this level throughout the compression period (Fig. 7B). Immediately after decompression, levels increased again and remained high at around 325% for a period of 12 h. This was followed by a gradual decline to almost 60% of baseline values as of Day 2.

At the 0.2-cm position, glucose levels declined rapidly during the 60-min sustained compression period to a value as low as 60% of baseline (Fig. 8A). Decompression was not associated with an increase in glucose, and levels remained well below baseline (~65%) for up to 5 h after decompression. Subsequently, glucose levels returned nearly to baseline values within 24 h of SCI. Elevated lactate and decreasing pyruvate levels were observed during SCI (Fig. 8B, 8C), resulting in a marked rise in L/P ratio to above 700% within 60 min of sustained compression (Fig. 8D). After decompression, both lactate and pyruvate levels steadily increased up to 24 h after injury but proceeded to decrease after that point. As lactate levels did not change in direct proportion to pyruvate, the L/P ratio declined within the first 24 h followed by a gradual progressive rise until the end of the experiment (reaching nearly 350% at end of experiment). Throughout the entire post-injury period, the L/P ratio remained above baseline values.

At the 2.2-cm position, glutamate levels showed a similar pattern to the 0.2 cm probe, although far less pronounced (reaching close to 850%; Fig. 7A; open squares). After SCI, glycerol levels were elevated to about 225% from baseline but then declined, although they remained elevated above baseline for the first 4 h after injury (Fig. 7B).

A modest increase in glucose levels was observed acutely after SCI to around 140% at the 2.2-cm location, which quickly returned to baseline levels within minutes (Fig. 8A). Cessation of anesthesia and mechanical ventilation also coincided with a slight and transient increase above baseline. Lactate levels steadily increased to just above 150% during the first 24 h, followed by a decrease (Fig. 8B). Acutely after SCI, pyruvate levels also rose to about 150% before levels dropped to within or below baseline values (Fig. 8C). A steady rise in L/P ratio was detected after SCI, resulting in an increase in L/P ratio similar to the 0.2-cm probe, reaching a value of about 300% at Day 7 (Fig. 8D).

### *Relationships between tissue hemodynamics, hydrostatic pressure, and metabolic responses*

Changes in SCBF, $PaPO_2$, and pressure during and after SCI were compared with changes in microdialysis data to define the

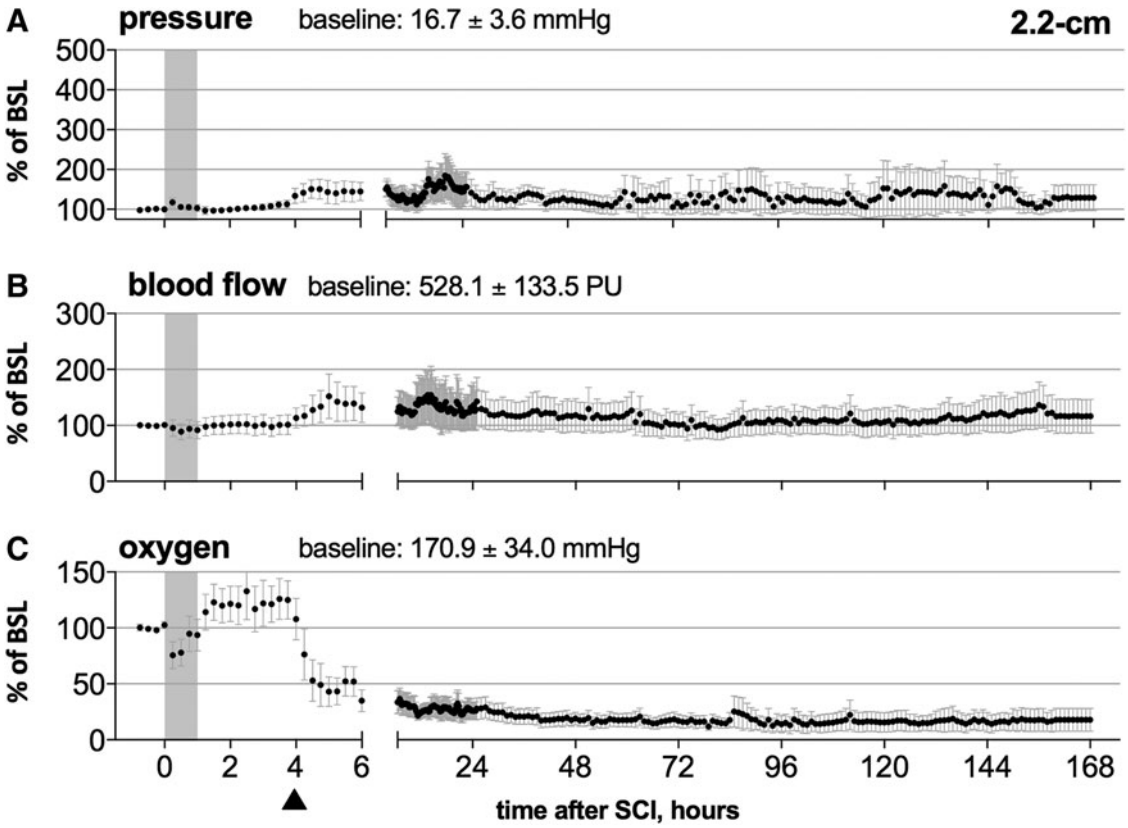


**FIG. 6.** Dynamic changes (%Δ) of blood flow, partial pressure of oxygen ($PaPO_2$), and pressure distal (2.2 cm) to the traumatic spinal cord injury site. The percentage change (%Δ) is calculated using an average of 60 min of baseline before SCI. **(A)** Intraparenchymal spinal cord pressure, **(B)** spinal cord blood flow (SCBF), and **(C)** $PaPO_2$ responses before, during and after 1 h spinal cord contusion/compression (gray shading). Following SCI a gradual increase in intraparenchymal pressure was observed during the first 24 h after which levels dropped back to baseline levels. SCBF seemed rather stable throughout the experiment. We observed a slow progressive decrease in $PaPO_2$ over time. The dashed line at the 4 h post-SCI mark (▲) represents the discontinuation of anesthesia and ventilation at the end of the surgical procedure. BSL, baseline; SCI, spinal cord injury.



relationship between these parameters. Spearman correlation coefficients are presented in Supplementary Tables 1 and 2 (see online supplementary material at www.liebertpub.com). We divided the entire dataset into three different time-points after injury based on the metabolic response defined by the L/P ratio (marker of hypoxia) as follows: 0–1 h post-SCI (the first hour immediately following the initial impact, which includes compression of the spinal cord marked by a dramatic increase in L/P ratio); 2) 1–24 h post-SCI (the early 24 h ''acute'' phase after decompression/reperfusion, marked by a continual decrease in L/P ratio); and 3) 25–156 h after SCI (the ''sub-acute'' phase after decompression/reperfusion, marked by a secondary increase in L/P ratio). The Bonferroni correction for alpha with 36 comparisons is $p < 0.001$

Following SCI and during compression of the spinal cord, changes in SCBF at the 0.2-cm location positively correlated with changes in pyruvate ($r = 0.967$; $p < 0.001$), and $PaPO_2$ ($r = 0.967$; $p < 0.001$). Though not maintaining statistical significance after correction for multiple comparisons, there was a trend towards a positive relationship between SCBF and glucose ($r = 0.867$; $p = 0.005$) and a negative relationship between SCBF and the L/P ratio ($r = -0.833$; $p < 0.008$). Similarly, a strong negative correlation was observed between changes in glucose and an increase in L/P ratio ($r = -0.933$; $p < 0.001$). No significant relation was found between $PaPO_2$ and L/P ratio after correction for multiple comparisons ($r = -0.783$; $p = 0.017$). Notably, the magnitude of spinal cord pressure changes positively correlated with glutamate release ($r = 0.833$; $p = 0.008$).

Following the first 24 h after decompression, strong relationships between SCBF, glucose, and L/P ratio also were observed, akin to the early (0–1 h) SCI phase. SCBF positively correlated with change in glucose ($r = 0.785$; $p < 0.001$) and pyruvate levels ($r = 0.886$; $p < 0.001$), and negatively correlated with changes in L/P ratio ($r = -0.858$; $p < 0.001$) and glycerol levels ($r = -0.765$; $p < 0.001$). Glucose levels also correlated with increased pyruvate levels ($r = 0.765$; $p < 0.001$) levels and decreased L/P ratio ($r = -0.719$; $p < 0.001$). Additionally, changes in spinal cord pressure positively correlated with changes in SCBF ($r = 0.813$; $p < 0.001$).

During the later days after decompression (Days 1–7), a decrease in spinal cord pressure was associated with enhanced SCBF ($r = -0.551$; $p < 0.001$). Further, a negative correlation was found between $PaPO_2$ and L/P ratio ($r = -0.900$; $p < 0.001$). Contrary to the results of the prior two phases, SCBF correlated negatively with $PaPO_2$ ($r = -0.465$; $p < 0.001$) and positively with L/P ratio ($r = 0.845$; $p = 0.002$) during the late decompression phase. This apparent uncoupling of SCBF and $PaPO_2$ during this late phase was not observed at the 2.2-cm location.

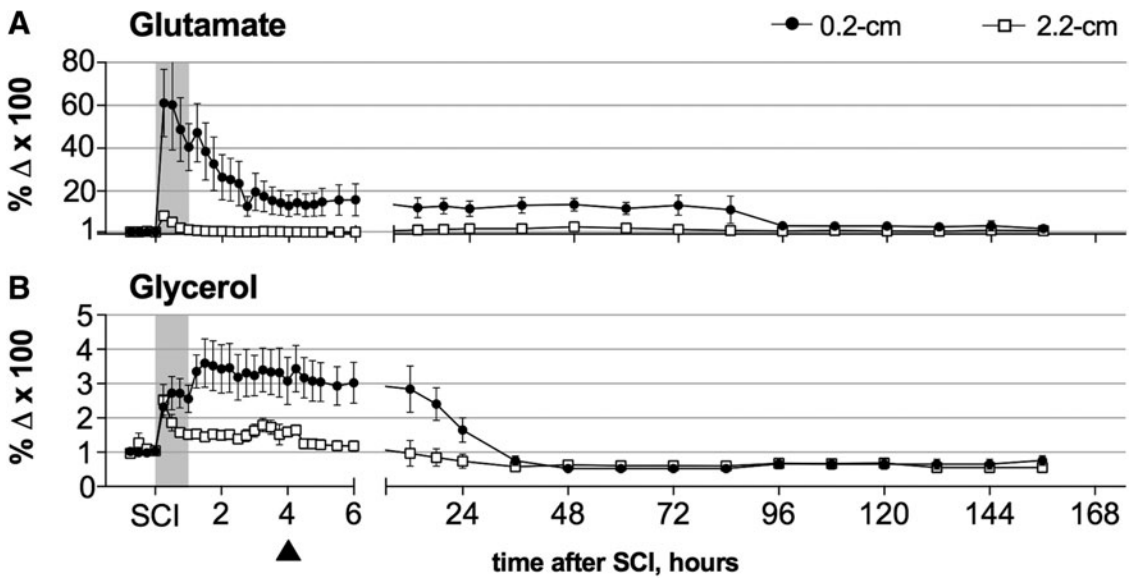


**FIG. 7.** Microdialysis measurements of intraparenchymal glutamate and glycerol changes (%Δ) in response to SCI at 0.2 and 2.2 cm from injury. The percentage change (%Δ) is calculated using the average of measurements obtained through 60 min of baseline recordings just prior to the SCI. **(A)** glutamate and **(B)** glycerol responses before, during and after 1 h spinal cord contusion/compression (gray shading). At the 0.2-cm position (●), an increase in glutamate and glycerol levels was observed upon SCI. The slope of glycerol increase was not as steep as that of glutamate and peaked later, but the increase was more sustained. Additionally, glycerol levels increased after decompression while glutamate levels remained unchanged. At the 2.2-cm position (□), a similar SCI-pattern for glutamate and glycerol was observed, although the responses were modest compared to the responses within the penumbra (0.2 cm). The dashed line at the 4 h post-SCI mark (▲) represents the discontinuation of anesthesia and ventilation at the end of the surgical procedure. SCI, spinal cord injury.



## Discussion

Pre-clinical studies by Tator and Fehings[2] and others[8–12] have revealed that vascular disruption and inadequate perfusion are key factors contributing to the development of secondary ischemic damage to the traumatically injured spinal cord. Intraparenchymal hemorrhage, vasospasm, impaired autoregulation, and vasogenic edema contribute to spinal ischemia, hypoxia, and energy dysfunction, of which all have a significant impact on tissue and functional recovery. Clinical treatment options to mitigate the effect of these responses are limited to early surgical decompression and aggressive hemodynamic support to improve spinal cord perfusion.[3,4] Given that aggressive hemodynamic support with the augmentation of MAP to 85–90 mm Hg may improve neurologic recovery in acute human SCI,[7] having an understanding of the post-traumatic alterations in SCBF and downstream consequences is central to the management of SCI patients.

Here, spatial and temporal dynamics of local SCBF, tissue oxygenation, pressure, and metabolism were investigated in the ''penumbra'' surrounding a traumatic SCI using a porcine model. This was achieved by simultaneously collecting data with laser Doppler/oxygen probes, pressure sensors, and microdialysis probes positioned in close proximity to one another within the spinal cord for 7 days post-injury. To our knowledge, this represents the first description of combined and continuous intraparenchymal physiologic and metabolic measures (perfusion, oxygenation, pressure, and microdialysis) over the first 7 days after traumatic spinal cord contusion/compression injury. We divided the entire dataset into three different time-points after injury: 1) 0–1 h post-SCI—the first hour immediately following the initial impact, which includes compression of the spinal cord; 2) 1–24 h post-SCI—the early 24 h ''acute'' phase after decompression/reperfusion; and 3) 25–156 h after SCI—the ''sub-acute'' phase after decompression/reperfusion.

First, during the initial 1 h of compression following contusive impact, tissue pressure markedly increased and was accompanied by a severe reduction in SCBF, low $PaPO_2$ levels, and a dramatic increase in L/P ratio, as well as in glutamate and glycerol levels. Second, during the first day (~24 h) following decompression, SCBF increased towards pre-injury baseline levels and then surpassed it. This is accompanied by a significant reduction in the L/P ratio, but only a limited and incomplete recovery of $PaPO_2$. Finally, between post-injury Days 1 and 7, SCBF increased to about 200% of baseline levels and underwent a transition from being positively correlated with $PaPO_2$ to being negatively correlated. During this late phase of apparent uncoupling of SCBF and $PaPO_2$, L/P ratio values increased consistently throughout the 7-day period. Further from the injury site (at the 2.2 cm probe position), the perturbations in SCBF, $PaPO_2$, and cord pressure were modest, with only a subtle increase in cord pressure over 7 days. This was nevertheless accompanied by a continuous increase in the L/P ratio. Various articles have demonstrated that probe insertion results in ''probe encapsulation'' and initiates an inflammatory response around the probe that can affect the recovery of small molecules, such as glucose.[24,25] These changes usually begin 24–36 h after probe implantation.[26] Because of the 7-day duration of our experiments, it is certainly possible that such probe encapsulation might occur. We acknowledge that this complicates the interpretation of our results, and hence the physiologic responses to traumatic SCI measured in the latter days of our study might be an underestimation of what is actually occurring.

While there are many published animal studies that have characterized the effect of traumatic injury on SCBF, most have utilized

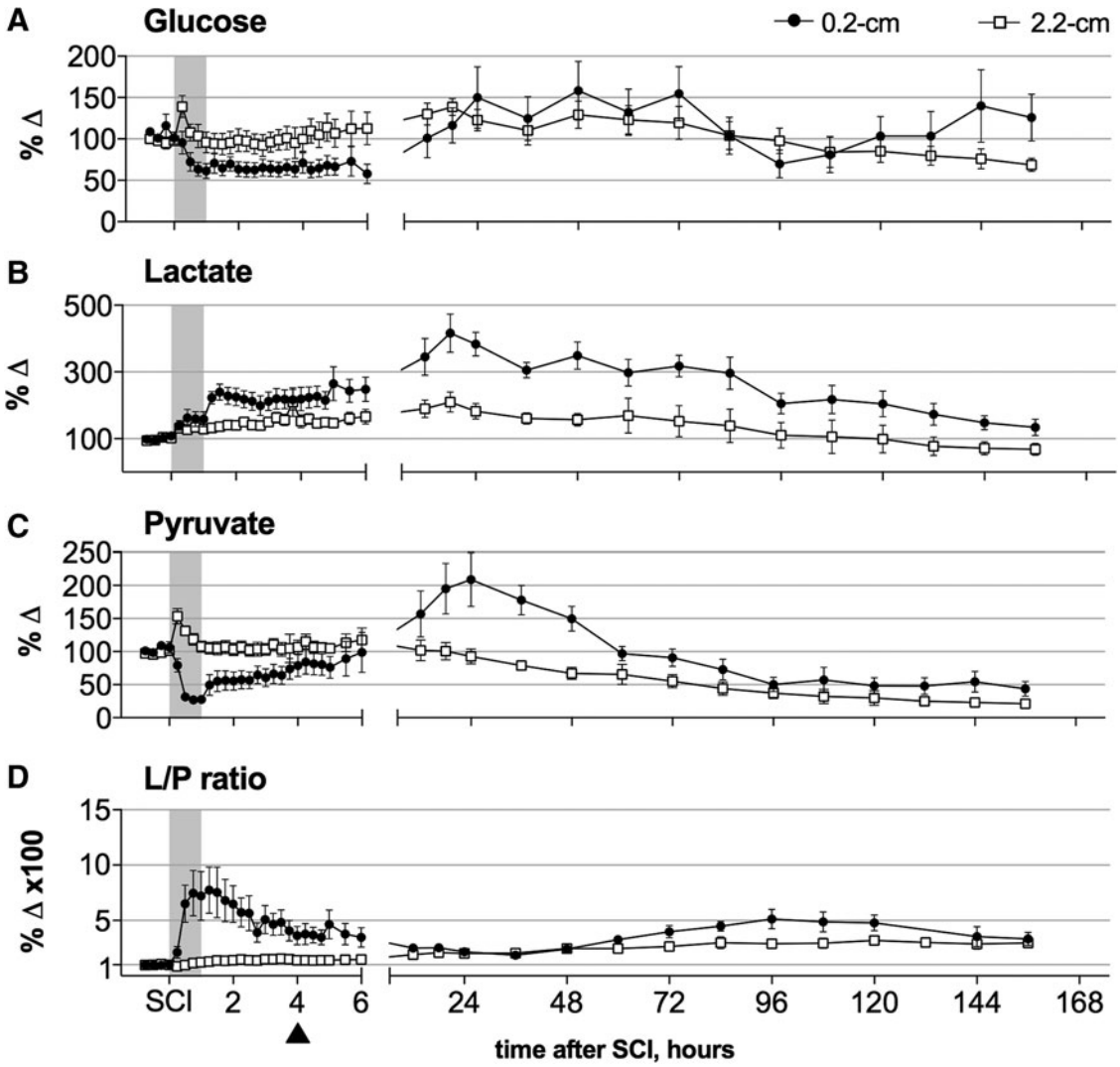


**FIG. 8.** Microdialysis measurements of intraparenchymal glucose, lactate, and pyruvate (%Δ) in response to SCI at 0.2 and 2.2 cm from injury. The percentage change (%Δ) is calculated using the average of measurements obtained through 60 min of baseline recordings just prior to the SCI. **(A)** Glucose, **(B)** lactate, **(C)** pyruvate, and **(D)** lactate to pyruvate (L/P) ratio responses before, during, and after 1 h spinal cord contusion/compression (gray shading). At the 0.2-cm position (•), glucose values decreased significantly upon SCI, and subsequently returned to baseline by Day 1. Within minutes after SCI, we observed an increase in lactate, a decrease in pyruvate, and a resulting increase in L/P ratio. After decompression, glucose, pyruvate and lactate increased while L/P ratio declined to 200% above baseline at 24 h. Thereafter, both lactate and pyruvate levels decreased again, although pyruvate fell proportionately more, resulting in a subsequent rise in L/P ratio till the end of the experiment (500% above baseline). At the 2.2-cm position (□), a slight increase in glucose levels was observed within the first 24 h after SCI; however, levels retuned to baseline thereafter. Within hours after SCI, we observed a slow but steady rise in lactate while pyruvate levels remained unchanged, producing an increase in L/P ratio. After 24 h, we observed a drop in lactate and a simultaneous and disproportionately greater drop in pyruvate, resulting in a continuous increase in L/P ratio to 500% above baseline at Day 7. The dashed line at the 4 h post-SCI mark (▲) represents the discontinuation of anesthesia and ventilation at the end of the surgical procedure. SCI, spinal cord injury.

rodent models with SCI induced by extradural clip compression for relatively short durations (1 min up to 40 min).[10–13] A few investigators have employed ongoing compression for 3 h up to 3 days using a metal rod placed on the dorsal dura of the spinal cord or by inserting a water-absorbing urethane polymer under the lamina.[27,28] Although different injury models and techniques of assessing blood flow were used (laser Doppler flowmetry, hydrogen clearance, microspheres) these compressive SCI models generally have reported acute decreases in SCBF in white and gray matter at and around the injury site, although Kobrine and colleagues have reported hyperemia during compression.[29] The latter is generally observed with lesser severities of injury. Further, it has been shown that functional recovery is dependent on the return of blood flow, which is in turn proportionate to the duration and severity of the compression.[30–32] In animal studies that have employed a contusive injury mechanism[9,33–39] the effect on SCBF is not as consistent. However, it is important to remember that traumatic human SCI is typically caused by a sudden, high-velocity contusive injury followed by periods of sustained compression (often for many hours to days). Besides our study, only a few other articles have evaluated SCBF in a combined contusion/compression model of SCI.[40,41] Kubota and colleagues[40] found a significant reduction in SCBF

during spinal cord compression following an initial contusion injury of the cord, which is consistent with our findings. Conversely, Sjovold[41] showed an elevated SCBF that steadily increased over 60 min of compression; however, Sjovold does state that the SCBF response varied considerably across individual animals. Nonetheless, while focusing on post-traumatic changes in SCBF can provide important insights, most studies only largely extend for the duration of the surgery and knowledge of the long-term monitoring of SCBF after SCI is limited.

Additionally, it is ultimately desirable to understand the subsequent downstream metabolic consequences of these changes within the areas of potentially vulnerable spinal cord tissue. As the balance between SCBF and metabolic rate of oxygen influences whether the tissue is hypoxic or not, monitoring SCBF alone may not provide a complete picture of the metabolic insult within the injury penumbra. For these reasons, we concurrently evaluated post-traumatic changes in SCBF and $PaPO_2$, as well as metabolic responses in a large animal model of contusion/compression SCI.

Adjacent to the impact site (represented by our 0.2 mm probe position), our data revealed a significant reduction in SCBF and $PaPO_2$ immediately following SCI while the cord remained compressed, reflecting severe compression-induced hypoperfusion. The rapid drop in glucose can be attributed to impaired blood flow as well as rapid conversion of local glucose into pyruvate, as supported by the close correlations between these parameters. In accordance with our previous study,[14] the increased lactate and decreased pyruvate resulting in an elevated L/P ratio is indicative of anaerobic glycolysis due to ischemia/hypoxia within the spinal cord. Glutamate increased immediately and remained elevated for days, indicating cellular release and/or lack of re-uptake, which is hampered by lack of adenosine triphosphate (ATP) and breakdown of membrane potentials in both neurons and glial cells. Cellular release of glutamate, as observed in several other studies, is mainly due to release of metabolic pools from neuronal and glial cell bodies, while the transmitter pool of glutamate contributes only a small fraction of early release.[42] In the present experiments, the increase of glycerol is likely a reflection of cellular membrane damage and breakdown of glycerol-containing phospholipids. A small fraction of glycerol also can be potentially generated as a byproduct of the glycolytic pathway in the post-traumatic scenario.[43–45] However, during profound ischemia, ATP deficiency would favor pyruvate and lactate instead of glycerol production. Further, glucose levels approached zero in microdialysate samples, which makes *de novo* synthesis of glycerol from glucose unlikely during this time period immediately after SCI while the cord remains compressed.

Immediately following the decompression, we observed SCBF and glucose to recover only partially ($\sim$25%), most likely due to the proximity to the injury and structural damage of microvasculature. $PaPO_2$ changed in proportion to blood flow, as one would expect if oxygen delivery were limited by SCBF. The drop in pyruvate observed during the immediate phase after SCI was gradually restored following partial return of blood flow and glucose. Accumulation of lactate with the L/P ratio remaining above baseline levels suggests ongoing anaerobic glycolysis in the ischemia/hypoxic lesion area. The strong negative correlation between $PaPO_2$ levels and the L/P ratio (i.e., low $PaPO_2$ is related to high L/P ratio) indicates that the persistent poor oxygenation might be the driving force for the continual increase in L/P ratio, as the increase in oxygen consumption exceeds oxygen availability.

For glycerol, there was a further increase at decompression followed by a reduction 1 day after the primary SCI, which may indicate reperfusion injury associated with reestablishing the blood supply. The interpretation of what is driving the glycerol levels is rather complicated by the existence of other sources of glycerol, transferred from the bloodstream into CSF and central nervous system compartments when the blood–brain and blood–spinal cord barriers are damaged. However, available data after brain injury (both traumatic and subarachnoid hemorrhage) suggest that this process might not make a significant contribution to interstitial glycerol concentrations.[44,46] We therefore believe that the rise in glycerol reflects actual structural damage of cell membranes, rather than extrinsic delivery through a disrupted blood–spinal cord barrier.

Contrary to the positive correlation between SCBF and $PaPO_2$ observed during the immediate phase after SCI, a modest but statistically significant negative correlation was seen in the late phase after SCI (1–7 days). SCBF levels started to rise above baseline values at 48 h after SCI and continued to increase until the end of the experiment at 7 days. Comparable changes in blood flow have been observed after traumatic brain injury (TBI), with most TBI patients showing reduced cerebral blood flow during the first 12 h after injury, followed by hyperperfusion (and in some patients vasospasms) before blood flow eventually normalizes.[47] The rise in SCBF during this time may be attributed to hypoxia, which is known to cause vasodilation either by direct (inadequate $O_2$ to sustain smooth muscle contraction) or indirect (production of vasodilator metabolites) actions on cerebral microvasculature. In our experiment, however, the rise in SCBF during days 1 through 7 post-injury did not confer a measurable improvement in $PaPO_2$. This observation is consistent with that of Gupta and colleagues,[48] who also reported the lack of a direct correlation between cerebral blood flow and oxygenation in TBI patients. This suggests that mechanisms other than a sheer reduction in blood perfusion are responsible for the tissue hypoxia in the latter stages after acute SCI. Importantly, our findings also highlight that the degree of hypoxia in the injured spinal cord may be underestimated if we rely solely on measures of blood perfusion in the post-injury period.

One explanation for the persistently low $PaPO_2$ during Days 1 through 7 is the imbalance between oxygen delivery and oxygen consumption. The later could be due to mitochondrial dysfunction and ineffective ATP production during oxidation, observed in ischemic brain tissue and in spinal cord after injury.[49,50] Delivery also may be compromised by impaired intraparenchymal oxygen diffusion, leading to decreased proportion of oxygen extracted from the blood during capillary passage through the spinal cord tissue (oxygen extraction fraction; OEF). Microvascular edema might cause increased barriers for oxygen diffusion with reduction of cellular oxygen delivery, despite the observation of blood flow remaining above what would be considered to be ''ischemic'' levels. Irregular microvascular collapse could result in significant increases in tissue path lengths for oxygen, with perivascular edema contributing to further increases in diffusion barriers for oxygen delivery. Recent work by Østergaard and colleagues[47] has proposed that changes in capillary flow patterns may have substantial influence on the relationship between CBF, tissue oxygen tension, and OEF after TBI. Their model predicts that severely disturbed capillary flow patterns could cause a parallel reduction in tissue oxygen tension and OEF even when gross perfusion is maintained.

To our knowledge, the first experimental SCI study to directly quantify spinal cord edema and intraparenchymal cord pressure after traumatic SCI was reported by Saadoun and colleagues in 2008.[51] Using a Millar pressure-monitoring microcatheter (SPR-1000) 2 days post-injury, they reported mean cord pressures around

27 mm Hg in the wild-type mice, which were significantly higher than in sham-operated animals (with pressures less than 10 mm Hg). Subsequent clinical studies by this same group have reported similar pressure increases in traumatic human SCI, in which intraspinal pressure (ISP) has been measured with a Codman pressure monitoring catheter placed into the intrathecal space directly at the site of spinal cord injury. Werndle and colleagues first reported in a series of 18 patients an increase in ISP to a mean of approximately 20 mm Hg over the first 9 days post-injury.[52] Such intraspinal pressures were found to be decreased with expansion duraplasty in a prospective series of 10 patients treated with duraplasty and laminectomy versus 11 patients with laminectomy alone.[53] An interesting case report of one patient from this series revealed that the intraspinal pressure as measured by the intrathecal pressure probe placed at the site of injury were correlated very closely to measurements determined by a pressure probe placed directly into the spinal cord.[54] This suggests that as long as the cord swells to fill the intrathecal space and presses up against the dura, the subdural pressure recordings reflect the intraparenchymal recordings. More recently, the Papadopoulos group also has reported on the use of microdialysis catheters (CMA61; CMA Microdialysis AB, Solna, Sweden) inserted under the arachnoid on the spinal cord surface in SCI patients.[55,56] They also documented metabolic derangements such as elevated glutamate, glycerol, and lactate/pyruvate ratio, with the latter being elevated even a week post-injury.

Our findings in the large animal model of SCI followed over 7 days reveal many similarities with the novel findings of the Papadopoulos group in human SCI. In our large animal model, we, too, observed a considerable increase in intraparenchymal pressure near the site of injury, doubling to $\sim$20 mm Hg in the first 48 h. Our intraparenchymal microdialysis monitoring revealed similar derangements in the metabolic responses, with increased glycerol and glutamate early post-injury and an elevated L/P ratio that was sustained out to 7 days post-injury. As expected, the hemodynamic and metabolic abnormalities were most pronounced near the site of injury and less so 2 cm farther from the injury site. However, we noted that the L/P ratio in our animals did continue to rise over Days 2–7 even at the more distal measurement site, suggesting a rostrocaudal expansion of potential ischemia over the 7 days. Combined, our results reveal a translational relevance of our experimental animal paradigm in studying these important hemodynamic and metabolic responses to acute SCI. Additionally, they support the recent contention from Saadoun and Papadopoulos that local monitoring of the injured spinal cord can provide novel insights into the pathophysiology of acute SCI that can be acted upon by clinicians with standard hemodynamic management strategies.[57] We recognize that there are many aspects of the pathophysiology of secondary cord edema that we have not studied, including, for example, the role that prostaglandin E2 (PGE2) may play. Of interest, PGE2 is thought to be a principle mediator vascular permeability and promoting local blood flow associated with edema seen during acute inflammation.[58] Its release has been reported after SCI in both CSF and spinal cord tissue,[59,60] and pursuing such downstream mediators would be a logical goal of further studies using our model.

The experimental paradigm we employed is extremely complex and demanding, and discussion of the limitations is warranted. Our experiments utilized the pig as a large animal model of SCI. While many fundamental insights into the local hemodynamic responses to SCI have been derived from rodent models, we contend that the porcine model represents a reasonable alternative, particularly for these types of acute studies of hemodynamic physiology. Relevant to this line of inquiry, the spinal cord macro- and micro-vasculature of the pig shares many similarities to humans,[61–63] making it a routinely utilized animal species for the modeling of ischemic thoracic SCI in the context of thoraco-abdominal aortic aneurysm repair.[64,65] These vascular similarities also would make the pig a useful species to study acute physiological responses in traumatic thoracic SCI. Despite this, we understand that our experimental paradigm still has important differences with the human SCI condition. While we simulated the contusive nature of human SCI, the latter is often accompanied by compression that may be sustained for hours to days before being surgically relieved, if at all. This was recently illustrated in the landmark 313 patient Surgical Trial of Acute Spinal Cord Injury Study,[66] where the average time of ''early decompression'' was $14.2 \pm 5.4$ h and that of ''late decompression'' was $48.3 \pm 29.3$ h. Our experimental paradigm utilized 1 h of compression, far exceeding the 1 min of compression typically utilized in the rodent clip compression model. While it would be interesting to continue the experiment with persistent compression beyond 1 h, there are some physiologic limitations for the animal, which under the current protocol undergoes almost 12 h of anesthesia, with ongoing blood loss from the large posterior exposure and extensive laminectomy. We would acknowledge, however, that prolonging the duration of compression and severity of contusion would provide additional insights into the heterogeneity of human SCI.

As mentioned earlier, there are numerous ways by which investigators have measured SCBF in animal models of SCI. LDF has been shown to be a valid method for assessing microvascular blood flow in tissues such as the spinal cord[67] and has been employed in various pre-clinical studies to quantitatively measure hemodynamic responses by using small probes placed over the dura at the spinal segment of interest.[13,36,41,68–73] While LDF cannot provide the absolute blood flow rates as the hydrogen clearance or the microsphere technique, LDF has been shown to be highly correlated with both.[67,74,75] One of our main considerations in the use of LDF for SCBF monitoring in our experimental paradigm was that it could be used post-operatively to continuously monitor SCBF over several days without requiring an anesthetic and endotracheal intubation for precise hydrogen delivery, as is required for the hydrogen clearance technique. Since motion artifact has been a recognized problem with LDF,[76] considerable effort was extended to rigidly stabilize the spinal cord column and the LDF probes.

From a translational perspective, our observations point to the potential importance of being able to monitor local tissue hemodynamics in the acutely injured spinal cord, as emphasized by work of Papadopoulos and colleagues. While we have taken advantage of the ability in an animal model to invasively monitor the spinal cord to derive direct intra-parenchymal measures of blood flow, oxygenation, pressure, and metabolic responses, application in humans would require a less invasive approach. We are nonetheless intrigued by the observation in our model of persistent ischemia around the injury site even at 7 days post-injury, which is the time at which current clinical practice guidelines suggest to stop aggressive MAP augmentation in patients with acute SCI. We also find that the measurement of SCBF alone does not paint the complete picture of what is occurring at a metabolic level within the spinal cord. This advocates for the application of multi-modal monitoring of the spinal cord, as is done in TBI. Given that we currently have few treatment options for acute SCI patients, such measures to monitor local tissue hemodynamics within the injured spinal cord are justified to optimize our treatment protocols in the acute post-

injury phase—a period where growing evidence points to an opportunity to improve neurologic recovery in human SCI.

## Acknowledgments

The authors gratefully acknowledge the funding support of the United States Department of Defense, Spinal Cord Injury Research Program and also the ICORD Spinal Cord Equipment Fund. Dr. Kwon holds the Canada Research Chair in Spinal Cord Injury. The authors also acknowledge the tremendous support, commitment, and expertise of many individuals at the University of British Columbia Center for Comparative Medicine (CCM). These include Dr. Ian Welch (Director), Gordon Gray (Facilities Manager), the clinical veterinarians Dr. Cathy Schuppli, Dr. Shelly McErlane, Dr. Laura Mobrey, Dr. Tamara Godbey, and Dr. Po-Yan Chen, and the amazing team of veterinarian technicians, including Micky Burgess, Kate Cooper, Shanna Dumontier, Kris Gillespie, Rhonda Hildebrandt, Mark Huang, Nicole Jackson, Tina Jorgensen, Stephanie Laprise, Ava McHugh, Kayla Reich, and Belinda To. Only through the skills and dedication of the entire CCM team is it possible to conduct these complex and demanding SCI experiments.

## Author Disclosure Statement

No competing financial interests exist.

## References

1. Mautes, A.E., Weinzierl, M.R., Donovan, F., and Noble, L.J. (2000). Vascular events after spinal cord injury: contribution to secondary pathogenesis. Phys. Ther. 80, 673–687.
2. Tator, C.H. and Fehlings, M.G. (1991). Review of the secondary injury theory of acute spinal cord trauma with emphasis on vascular mechanisms. J. Neurosurg. 75, 15–26.
3. Ryken, T.C., Hurlbert, R.J., Hadley, M.N., Aarabi, B., Dhall, S.S., Gelb, D.E., Rozzelle, C.J., Theodore, N., and Walters, B.C. (2013). The acute cardiopulmonary management of patients with cervical spinal cord injuries. Neurosurgery 72 Suppl 2, 84–92.
4. Furlan, J.C., Noonan, V., Cadotte, D.W., and Fehlings, M.G. (2011). Timing of decompressive surgery of spinal cord after traumatic spinal cord injury: an evidence-based examination of pre-clinical and clinical studies. J. Neurotrauma 28, 1371–1399.
5. Casha, S. and Christie, S. (2011). A systematic review of intensive cardiopulmonary management after spinal cord injury. J. Neurotrauma 28, 1479–1495.
6. Consortium for Spinal Cord Medicine. (2008). Early acute management in adults with spinal cord injury: a clinical practice guideline for health-care professionals. J. Spinal. Cord Med. 31, 403–479.
7. Hawryluk, G., Whetstone, W., Saigal, R., Ferguson, A., Talbott, J., Bresnahan, J., Dhall, S., Pan, J., Beattie, M., and Manley, G. (2015). Mean arterial blood pressure correlates with neurological recovery after human spinal cord injury: analysis of high frequency physiologic data. J. Neurotrauma 32, 1958–1967.
8. Sandler, A.N. and Tator, C.H. (1976). Review of the effect of spinal cord trauma on the vessels and blood flow in the spinal cord. J. Neurosurg. 45, 638–646.
9. Sandler, A.N. and Tator, C.H. (1976). Effect of acute spinal cord compression injury on regional spinal cord blood flow in primates. J. Neurosurg. 45, 660–676.
10. Kang, C.E., Clarkson, R., Tator, C.H., Yeung, I.W.T., and Shoichet, M.S. (2010). Spinal cord blood flow and blood vessel permeability measured by dynamic computed tomography imaging in rats after localized delivery of fibroblast growth factor. J. Neurotrauma 27, 2041–2053.
11. Rivlin, A.S. and Tator, C.H. (1978). Regional spinal cord blood flow in rats after severe cord trauma. J. Neurosurg. 49, 844–853.
12. Guha, A., Tator, C.H., and Rochon, J. (1989). Spinal cord blood flow and systemic blood pressure after experimental spinal cord injury in rats. Stroke 20, 372–377.
13. Hamamoto, Y., Ogata, T., Morino, T., Hino, M., and Yamamoto, H. (2007). Real-time direct measurement of spinal cord blood flow at the site of compression: relationship between blood flow recovery and motor deficiency in spinal cord injury. Spine (Phila. Pa. 1976) 32, 1955–1962.
14. Okon, E.B., Streijger, F., Lee, J.H.T., Anderson, L.M., Russell, A.K., and Kwon, B.K. (2013). Intraparenchymal microdialysis after acute spinal cord injury reveals differential metabolic responses to contusive versus compressive mechanisms of injury. J. Neurotrauma 30, 1564–1576.
15. Streijger, F., Lee, J.H.T., Manouchehri, N., Melnyk, A.D., Chak, J., Tigchelaar, S., So, K., Okon, E.B., Jiang, S., Kinsler, R., Barazanji, K., Cripton, P.A., and Kwon, B.K. (2016). Responses of the acutely injured spinal cord to vibration that simulates transport in helicopters or mine-resistant ambush-protected vehicles. J. Neurotrauma 33, 2217–2226.
16. Streijger, F., Lee, J.H.T., Chak, J., Dressler, D., Manouchehri, N., Okon, E.B., Anderson, L.M., Melnyk, A.D., Cripton, P.A., and Kwon, B.K. (2015). The effect of whole-body resonance vibration in a porcine model of spinal cord injury. J. Neurotrauma 32, 908–921.
17. Jones, C.F., Cripton, P.A., and Kwon, B.K. (2012). Gross morphological changes of the spinal cord immediately after surgical decompression in a large animal model of traumatic spinal cord injury. Spine (Phila. Pa. 1976) 37, E890–E899.
18. Chavko, M., Koller, W.A., Prusaczyk, W.K., and McCarron, R.M. (2007). Measurement of blast wave by a miniature fiber optic pressure transducer in the rat brain. J. Neurosci. Methods 159, 277–281.
19. Leonardi, A.D.C., Bir, C.A., Ritzel, D.V., and VandeVord, P.J. (2011). Intracranial pressure increases during exposure to a shock wave. J. Neurotrauma 28, 85–94.
20. Bauman, R.A., Ling, G., Tong, L., Januszkiewicz, A., Agoston, D., Delanerolle, N., Kim, Y., Ritzel, D., Bell, R., Ecklund, J., Armonda, R., Bandak, F., and Parks, S. (2009). An introductory characterization of a combat-casualty-care relevant swine model of closed head injury resulting from exposure to explosive blast. J. Neurotrauma 26, 841–860.
21. Dennison, C.R., Wild, P.M., Byrnes, P.W.G., Saari, A., Itshayek, E., Wilson, D.C., Zhu, Q.A., Dvorak, M.F.S., Cripton, P.A., and Wilson, D.R. (2008). Ex vivo measurement of lumbar intervertebral disc pressure using fibre-Bragg gratings. J. Biomech. 41, 221–225.
22. Soicher J. (2015). Evaluating the feasibility of quantifying spinal cord swelling as a function of pressure using fiber optic pressure sensors. Electronic Theses and Dissertations (ETDs) 2008+. University of British Columbia. Available at: https://open.library.ubc.ca/cIRcle/collections/24/items/1.0167187. Accessed August 10, 2017.
23. Streijger, F., Lee, J.H.T., Manouchehri, N., Okon, E.B., Tigchelaar, S., Anderson, L.M., Dekaban, G.A., Rudko, D.A., Menon, R.S., Iaci, J.F., Button, D.C., Vecchione, A.M., Konovalov, A., Sarmiere, P.D., Ung, C., Caggiano, A.O., and Kwon, B.K. (2016). The evaluation of magnesium chloride within a polyethylene glycol formulation in a porcine model of acute spinal cord injury. J. Neurotrauma 33, 2202–2216.
24. Wisniewski, N., Rajamand, N., Adamsson, U., Lins, P.E., Reichert, W.M., Klitzman, B., and Ungerstedt, U. (2002). Analyte flux through chronically implanted subcutaneous polyamide membranes differs in humans and rats. Am. J. Physiol. Endocrinol. Metab. 282, E1316–E1323.
25. Wisniewski, N., Klitzman, B., Miller, B., and Reichert, W.M. (2001). Decreased analyte transport through implanted membranes: differentiation of biofouling from tissue effects. J. Biomed. Mater. Res. 57, 513–521.
26. Cirrito, J.R., May, P.C., O'Dell, M.A., Taylor, J.W., Parsadanian, M., Cramer, J.W., Audia, J.E., Nissen, J.S., Bales, K.R., Paul, S.M., DeMattos, R.B., and Holtzman, D.M. (2003). In vivo assessment of brain interstitial fluid with microdialysis reveals plaque-associated changes in amyloid-beta metabolism and half-life. J. Neurosci. 23, 8844–8853.
27. Mautes, A.E., Schröck, H., Nacimiento, A.C., and Paschen, W. (2000). Regional spinal cord blood flow and energy metabolism in rats after laminectomy and acute compression injury. European. J. Trauma 26, 122–130.
28. Kurokawa, R., Murata, H., Ogino, M., Ueki, K., and Kim, P. (2011). Altered blood flow distribution in the rat spinal cord under chronic compression. Spine (Phila. Pa. 1976) 36, 1006–1009.

29. Kobrine, A.I., Evans, D.E., and Rizzoli, H. (1978). Correlation of spinal cord blood flow and function in experimental compression. Surg. Neurol. 10, 54–59.
30. Carlson, G.D., Gorden, C.D., Nakazowa, S., Wada, E., Warden, K., and LaManna, J.C. (2000). Perfusion-limited recovery of evoked potential function after spinal cord injury. Spine (Phila. Pa. 1976) 25, 1218–1226.
31. Carlson, G.D., Warden, K.E., Barbeau, J.M., Bahniuk, E., Kutina-Nelson, K.L., Biro, C.L., Bohlman, H.H., and LaManna, J.C. (1997). Viscoelastic relaxation and regional blood flow response to spinal cord compression and decompression. Spine (Phila. Pa. 1976) 22, 1285–1291.
32. Carlson, G.D., Minato, Y., Okada, A., Gorden, C.D., Warden, K.E., Barbeau, J.M., Biro, C.L., Bahnuik, E., Bohlman, H.H., and Lamanna, J.C. (1997). Early time-dependent decompression for spinal cord injury: vascular mechanisms of recovery. J. Neurotrauma 14, 951–962.
33. Chehrazi, B.B., Scremin, O., and Decima, E.E. (1989). Effect of regional spinal cord blood flow and central control in recovery from spinal cord injury. J. Neurosurg. 71, 747–753.
34. Wu, X.H., Yang, S.H., Duan, D.Y., Cheng, H.H., Bao, Y.T., and Zhang, Y. (2007). Anti-apoptotic effect of insulin in the control of cell death and neurologic deficit after acute spinal cord injury in rats. J. Neurotrauma 24, 1502–1512.
35. Soubeyrand, M., Laemmel, E., Dubory, A., Vicaut, E., Court, C., and Duranteau, J. (2012). Real-time and spatial quantification using contrast-enhanced ultrasonography of spinal cord perfusion during experimental spinal cord injury. Spine (Phila. Pa. 1976) 37, E1376–E1382.
36. Soubeyrand, M., Laemmel, E., Court, C., Dubory, A., Vicaut, E., and Duranteau, J. (2013). Rat model of spinal cord injury preserving dura mater integrity and allowing measurements of cerebrospinal fluid pressure and spinal cord blood flow. Eur. Spine. J. 22, 1810–1819.
37. Cawthon, D.F., Senter, H.J., and Stewart, W.B. (1980). Comparison of hydrogen clearance and 14C-antipyrine autoradiography in the measurement of spinal cord blood flow after severe impact injury. J. Neurosurg. 52, 801–807.
38. Yeo, J.D., Hales, J.R., Stabback, S., Bradley, S., Fawcett, A.A., and Kearns, R. (1984). Effects of a contusion injury on spinal cord blood flow in the sheep. Spine (Phila. Pa. 1976) 9, 676–680.
39. Huang, L., Lin, X., Tang, Y., Yang, R., Li, A.H., Ye, J.C., Chen, K., Wang, P., and Shen, H.Y. (2013). Quantitative assessment of spinal cord perfusion by using contrast-enhanced ultrasound in a porcine model with acute spinal cord contusion. Spinal Cord 51, 196–201.
40. Kubota, K., Saiwai, H., Kumamaru, H., Kobayakawa, K., Maeda, T., Matsumoto, Y., Harimaya, K., Iwamoto, Y., and Okada, S. (2012). Neurological recovery is impaired by concurrent but not by asymptomatic pre-existing spinal cord compression after traumatic spinal cord injury. Spine (Phila. Pa. 1976) 37, 1448–1455.
41. Sjovold, S.G. (2006). Spinal cord tissue changes due to residual compression in a novel rat contusion model. Electronic Theses and Dissertations (ETDs) 2008+. University of British Columbia. Available at: https://open.library.ubc.ca/cIRcle/collections/24/items/1.0080765. Accessed August 20, 2017.
42. Danbolt, N.C. (2001). Glutamate uptake. Prog. Neurobiol. 65, 1–105.
43. Merenda, A., Gugliotta, M., Holloway, R., Levasseur, J.E., Alessandri, B., Sun, D., and Bullock, M.R. (2008). Validation of brain extracellular glycerol as an indicator of cellular membrane damage due to free radical activity after traumatic brain injury. J. Neurotrauma 25, 527–537.
44. Marklund, N., Salci, K., Lewén, A., and Hillered, L. (1997). Glycerol as a marker for post-traumatic membrane phospholipid degradation in rat brain. Neuroreport 8, 1457–1461.
45. Clausen, F., Hillered, L., and Gustafsson, J. (2011). Cerebral glucose metabolism after traumatic brain injury in the rat studied by 13C-glucose and microdialysis. Acta Neurochir. (Wien) 153, 653–658.
46. Hillered, L., Valtysson, J., Enblad, P., and Persson, L. (1998). Interstitial glycerol as a marker for membrane phospholipid degradation in the acutely injured human brain. J. Neurol. Neurosurg. Psychiatry 64, 486–491.
47. Østergaard, L., Engedal, T.S., Aamand, R., Mikkelsen, R., Iversen, N.K., Anzabi, M., Næss-Schmidt, E.T., Drasbek, K.R., Bay, V., Blicher, J.U., Tietze, A., Mikkelsen, I.K., Hansen, B., Jespersen, S.N., Juul, N., Sørensen, J.C.H., and Rasmussen, M. (2014). Capillary transit time heterogeneity and flow-metabolism coupling after traumatic brain injury. J. Cereb. Blood. Flow Metab. 34, 1585–1598.
48. Gupta, A.K., Hutchinson, P.J., Fryer, T., Al-Rawi, P.G., Parry, D.A., Minhas, P.S., Kett-White, R., Kirkpatrick, P.J., Mathews, J.C., Downey, S., Aigbirhio, F., Clark, J., Pickard, J.D., and Menon, D.K. (2002). Measurement of brain tissue oxygenation performed using positron emission tomography scanning to validate a novel monitoring method. J. Neurosurg. 96, 263–268.
49. Jia, Z.Q., Li, G., Zhang, Z.Y., Li, H.T., Wang, J.Q., Fan, Z.K., and Lv, G. (2016). Time representation of mitochondrial morphology and function after acute spinal cord injury. Neural. Regen. Res. 11, 137–143.
50. McEwen, M.L., Sullivan, P.G., Rabchevsky, A.G., and Springer, J.E. (2011). Targeting mitochondrial function for the treatment of acute spinal cord injury. Neurotherapeutics 8, 168–179.
51. Saadoun, S., Bell, B.A., Verkman, A.S., and Papadopoulos, M.C. (2008). Greatly improved neurological outcome after spinal cord compression injury in AQP4-deficient mice. Brain 131, 1087–1098.
52. Werndle, M.C., Saadoun, S., Phang, I., Czosnyka, M., Varsos, G.V., Czosnyka, Z.H., Smielewski, P., Jamous, A., Bell, B.A., Zoumprouli, A., and Papadopoulos, M.C. (2014). Monitoring of spinal cord perfusion pressure in acute spinal cord injury: initial findings of the injured spinal cord pressure evaluation study*. Crit. Care Med. 42, 646–655.
53. Phang, I., Werndle, M.C., Saadoun, S., Varsos, G., Czosnyka, M., Zoumprouli, A., and Papadopoulos, M.C. (2015). Expansion duroplasty improves intraspinal pressure, spinal cord perfusion pressure, and vascular pressure reactivity index in patients with traumatic spinal cord injury: injured spinal cord pressure evaluation study. J. Neurotrauma 32, 865–874.
54. Phang, I. and Papadopoulos, M.C. (2015). Intraspinal pressure monitoring in a patient with spinal cord injury reveals different intradural compartments: Injured Spinal Cord Pressure Evaluation (ISCoPE) Study. Neurocrit. Care 23, 414–418.
55. Phang, I., Zoumprouli, A., Papadopoulos, M.C., and Saadoun, S. (2016). Microdialysis to optimize cord perfusion and drug delivery in spinal cord injury. Ann. Neurol. 80, 522–531.
56. Chen, S., Phang, I., Zoumprouli, A., Papadopoulos, M.C., and Saadoun, S. (2016). Metabolic profile of injured human spinal cord determined using surface microdialysis. J. Neurochem. 139, 700–705.
57. Saadoun, S. and Papadopoulos, M.C. (2016). Spinal cord injury: is monitoring from the injury site the future? Crit. Care 20, 308.
58. Davies, P., Bailey, P.J., Goldenberg, M.M., and Ford-Hutchinson, A.W. (1984). The role of arachidonic acid oxygenation products in pain and inflammation. Annu. Rev. Immunol. 2, 335–357.
59. Marsala, M., Malmberg, A.B., and Yaksh, T.L. (1995). The spinal loop dialysis catheter: characterization of use in the unanesthetized rat. J. Neurosci. Methods 62, 43–53.
60. Bernards, C.M. and Akers, T. (2006). Effect of postinjury intravenous or intrathecal methylprednisolone on spinal cord excitatory amino-acid release, nitric oxide generation, PGE2 synthesis, and myeloperoxidase content in a pig model of acute spinal cord injury. Spinal Cord 44, 594–604.
61. Strauch, J.T., Lauten, A., Zhang, N., Wahlers, T., and Griepp, R.B. (2007). Anatomy of spinal cord blood supply in the pig. Ann. Thorac. Surg. 83, 2130–2134.
62. Etz, C.D., Kari, F.A., Mueller, C.S., Silovitz, D., Brenner, R.M., Lin, H.M., and Griepp, R.B. (2011). The collateral network concept: a reassessment of the anatomy of spinal cord perfusion. J. Thorac. Cardiovasc. Surg. 141, 1020–1028.
63. Christiansson, L., Ulus, A.T., Hellberg, A., Bergqvist, D., Wiklund, L., and Karacagil, S. (2001). Aspects of the spinal cord circulation as assessed by intrathecal oxygen tension monitoring during various arterial interruptions in the pig. J. Thorac. Cardiovasc. Surg. 121, 762–772.
64. Geisbüsch, S., Stefanovic, A., Koruth, J.S., Lin, H.M., Morgello, S., Weisz, D.J., Griepp, R.B., and Di Luozzo, G. (2014). Endovascular coil embolization of segmental arteries prevents paraplegia after subsequent thoracoabdominal aneurysm repair: an experimental model. J. Thorac. Cardiovasc. Surg. 147, 220–226.
65. Saether, O.D., Bäckström, T., Aadahl, P., Myhre, H.O., Norgren, L., and Ungerstedt, U. (2000). Microdialysis of the spinal cord during thoracic aortic cross-clamping in a porcine model. Spinal Cord 38, 153–157.
66. Fehlings, M.G., Vaccaro, A., Wilson, J.R., Singh, A., W Cadotte, D., Harrop, J.S., Aarabi, B., Shaffrey, C., Dvorak, M., Fisher, C., Arnold, P., Massicotte, E.M., Lewis, S., and Rampersaud, R. (2012). Early

versus delayed decompression for traumatic cervical spinal cord injury: results of the Surgical Timing in Acute Spinal Cord Injury Study (STASCIS). PLoS One 7, e32037.
67. Lindsberg, P.J., O'Neill, J.T., Paakkari, I.A., Hallenbeck, J.M., and Feuerstein, G. (1989). Validation of laser-Doppler flowmetry in measurement of spinal cord blood flow. Am. J. Physiol. 257, H674–H680.
68. Phillips, J.P., Cibert-Goton, V., Langford, R.M., and Shortland, P.J. (2013). Perfusion assessment in rat spinal cord tissue using photoplethysmography and laser Doppler flux measurements. J. Biomed. Opt. 18, 037005.
69. Lindsberg, P.J., Jacobs, T.P., Frerichs, K.U., Hallenbeck, J.M., and Feuerstein, G.Z. (1992). Laser-Doppler flowmetry in monitoring regulation of rapid microcirculatory changes in spinal cord. Am. J. Physiol. 263, H285–H292.
70. Yamada, T., Morimoto, T., Nakase, H., Hirabayashi, H., Hiramatsu, K., and Sakaki, T. (1998). Spinal cord blood flow and pathophysiological changes after transient spinal cord ischemia in cats. Neurosurgery 42, 626–634.
71. Westergren, H., Farooque, M., Olsson, Y., and Holtz, A. (2001). Spinal cord blood flow changes following systemic hypothermia and spinal cord compression injury: an experimental study in the rat using Laser-Doppler flowmetry. Spinal Cord 39, 74–84.
72. Martirosyan, N.L., Kalani, M.Y.S., Bichard, W.D., Baaj, A.A., Gonzalez, L.F., Preul, M.C., and Theodore, N. (2015). Cerebrospinal fluid drainage and induced hypertension improve spinal cord perfusion after acute spinal cord injury in pigs. Neurosurgery 76, 461–468.
73. Marsala, M., Sorkin, L.S. and Yaksh, T.L. (1994). Transient spinal ischemia in rat: characterization of spinal cord blood flow, extracellular amino acid release, and concurrent histopathological damage. J. Cereb. Blood Flow Metab. 14, 604–614.
74. Kramer, M.S., Vinall, P.E., Katolik, L.I., and Simeone, F.A. (1996). Comparison of cerebral blood flow measured by laser-Doppler flowmetry and hydrogen clearance in cats after cerebral insult and hypervolemic hemodilution. Neurosurgery 38, 355–361.
75. Skarphedinsson, J.O., Hårding, H., and Thorén, P. (1988). Repeated measurements of cerebral blood flow in rats. Comparisons between the hydrogen clearance method and laser Doppler flowmetry. Acta. Physiol. Scand. 134, 133–142.
76. Oberg, P.A. (1999). Tissue motion—a disturbance in the laser-Doppler blood flow signal? Technol. Health Care 7, 185–192.

Address correspondence to:
*Brian K. Kwon, MD, PhD, FRCSC*
*Department of Orthopedics*
*University of British Columbia*
*6th Floor, Blusson Spinal Cord Center*
*Vancouver General Hospital*
*818 West 10th Avenue*
*Vancouver, British Columbia, Canada V5Z 1M9*

*E-mail:* brian.kwon@ubc.ca

# Spinal Cord Swelling and Alterations in Hydrostatic Pressure After Acute Injury

SC130008 Investigator Initiated Research Award
W81XWH-14-1-0619

**PI:** Dr. Brian K. Kwon **Org:** University of British Columbia, ICORD **Award Amount:** $630,109

## Approach

After acute spinal cord injury (SCI) the spinal cord is frequently found to have swollen dramatically, particularly after it has been surgically decompressed. In traumatic brain injury (TBI), brain swelling and increases in intraparenchymal pressure are routinely considered in both the surgical and hemodynamic management of such patients. However, this swelling has largely been neglected in SCI, despite being consistently observed. Even after surgical decompression, such swelling may result in the cord being subjected to significant pressure, either due to constriction by the pia mater, the dura mater, or both. The physiologic consequences of this are poorly understood, and many fundamental questions remain about its impact on intraparenchymal pressure, spinal cord perfusion, and downstream metabolic responses. Determining the physiologic/biologic consequences of this swelling and how they can be mitigated to reduce secondary injury will guide the optimal clinical management of acute SCI. As an example of how swelling, increased intraparenchymal pressure, and its effects on perfusion are factored into clinical decision-making, TBI investigators have established the Pressure Reactivity Index (PRx) to identify where autoregulation remains intact and to guide optimal perfusion support based on that. The PRx has not been investigated in SCI, but given that the cord also swells and has impaired autoregulation, it is likely applicable here as well. This promising approach opens the possibility that we could individualize and optimize the hemodynamic support of acute SCI patients in order to support perfusion without exacerbating deleterious increases in intraparenchymal pressure.

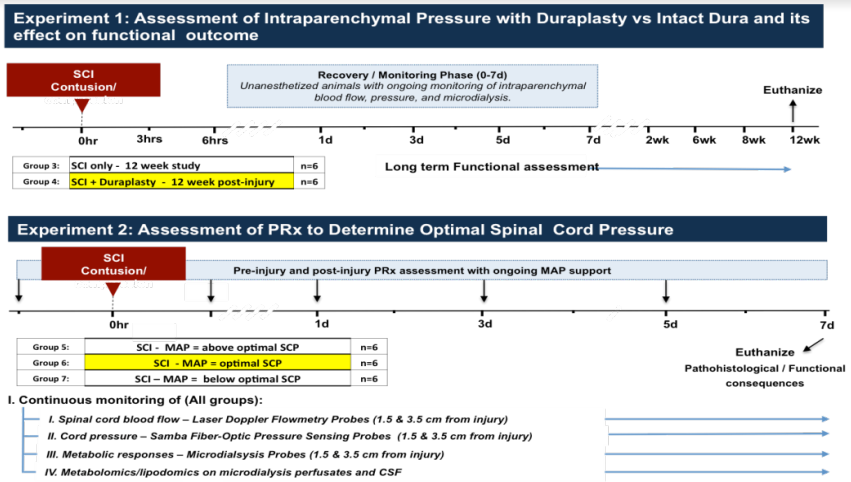


**Update:** In **Year 3, Quarter 1**, we have finished analyzing the microdialsysis data of 8 animals as part of Aim 2. Data thus far show that although pyruvate and lactate are higher in duraplasty group; there are no clear differences in L/P ratio between two groups close to the injury site. Also no visible differences for glutamate and glycerol at 0.2 cm from injury was observed. Interestingly, higher glucose was observed in duraplasty group over 6-hours post-injury compared to control group. Notably, this study is still in its early days, and it is too preliminary to draw any firm conclusions from these limited data.

## Timeline and Cost

**Updated:** (Jun 2017)

| Major Aims (As Described in the SOW) | 2014 | 2015 | 2016 | 2017 |
|---|---|---|---|---|
| Specific Aim 1: Evaluate if compression by the surrounding dura produces increased intraparenchymal pressure within the injured, swollen cord. | | | | |
| Specific Aim 2: To evaluate if dural compression contribute to progressive deficit in blood perfusion and contribute to the pathophysiology of secondary damage after traumatic SCI | | | | |
| Specific Aim 3. Determine if MAP support during the decompression phase of SCI results in worse long-term functional outcome | | | | |
| Specific Aim 4. Evaluate if a moving correlation index exists between mean arterial blood pressure and CSF/cord pressure (pressure reactivity index; PRx) | | | | |
| Estimated Budget (in thousands) | 0 | $203 | $213 | $214 |

## Goals/Milestones

**Goal 1** – evaluation of duraplasty

- ✓ ACURO approval
- ✓ Assessment of behavioral and functional consequence of SCI with or without duraplasty
- ❑ Assessment of histological consequence of SCI with or without duraplasty

**Goal 2** – Evaluation of PRx-based MAP support

- ✓ Quantification of relationship between Mean Arterial Pressure, spinal cord blood flow, and intraparenchymal pressure
- ☐ Determination of efficacy of PRx-based MAP support

**Budget Expenditure to Date**

Approved expenditure granting period: $630,109
Actual Expenditure Year 3: $318,882.38